DEVELOPMENT OF A SCREENING MODEL FOR THE CYCLIC STEAM INJECTION (CSI) PROCESS

A THESIS SUBMITTED TO
THE GRADUATE SCHOOL OF NATURAL AND APPLIED SCIENCES
OF
MIDDLE EAST TECHNICAL UNIVERSITY

BY

GAMZE YALGIN

IN PARTIAL FULFILLMENT OF THE REQUIREMENTS
FOR
THE DEGREE OF MASTER OF SCIENCE
IN
PETROLEUM AND NATURAL GAS ENGINEERING

JANUARY 2018

Approval of the thesis:

DEVELOPMENT OF A SCREENING MODEL FOR THE CYCLIC STEAM INJECTION (CSI) PROCESS

submitted by **GAMZE YALGIN** in partial fulfillment of the requirements for the degree of **Master of Science in Petroleum and Natural Gas Engineering Department, Middle East Technical University** by,

Prof. Dr. Gülbin Dural Ünver _____
Dean, **Graduate School of Natural and Applied Sciences**

Prof. Dr. Serhat Akın _____
Head of Department, **Petr. and Nat. Gas Eng.**

Prof. Dr. Mustafa Verşan Kök _____
Supervisor, **Petr. and Nat. Gas Eng., METU**

Assoc. Prof. Dr. Emre Artun _____
Co-Supervisor, **Petr. and Nat. Gas Eng., METU NCC**

Examining Committee Members:

Prof. Dr. Serhat Akın _____
Petroleum and Natural Gas Engineering Dept., METU

Prof. Dr. Mustafa Verşan Kök _____
Petroleum and Natural Gas Engineering Dept., METU

Assoc. Prof. Dr. Emre Artun _____
Petroleum and Natural Gas Engineering Dept., METU NCC

Asst. Prof. Dr. İsmail Durgut _____
Petroleum and Natural Gas Engineering Dept., METU

Assoc. Prof. Dr. Çağlar Sınayuç _____
Petroleum and Natural Gas Engineering Dept., METU

Date: 31.01.2018

I hereby declare that all information in this document has been obtained and presented in accordance with academic rules and ethical conduct. I also declare that, as required by these rules and conduct, I have fully cited and referenced all material and results that are not original to this work.

Name, Last Name: Gamze Yalgın

Signature:

ABSTRACT

DEVELOPMENT OF A SCREENING MODEL FOR THE CYCLIC STEAM INJECTION (CSI) PROCESS

Yalgın, Gamze
M.S., Department of Petroleum and Natural Gas Engineering
Supervisor: Prof. Dr. Mustafa Verşan Kök
Co-Supervisor: Assoc. Prof. Dr. Emre Artun

January 2018, 101 pages

Cyclic steam injection (CSI), a single-well enhanced oil recovery method for heavy oil reservoirs, is characterized with three stages: injection, soaking, and production which altogether constitute a cycle. In this study, it is aimed to develop a screening model that can be used to accept or reject a given CSI proposal from a representative performance indicator. This indicator is estimated from a large set of reservoir & CSI design characteristics, using the screening model developed. The model has been trained by using an artificial neural network (ANN) that can estimate the process performance in a given reservoir depending on the steam-injection design parameters. The data that be used for the ANN is generated using a representative numerical reservoir model, built with a commercial simulator. A large number of simulation cases are generated using the experimental design methodology to account for a large variety of scenarios, and corresponding performance indicators such as incremental oil recovery, and injection efficiency, are collected. After proper training and validation, the screening tool is ready to estimate the

performance within a fraction of a second. Sensitivity study between the tool and numerical model showed that the tool captured the problem very well. According to the 90% of testing dataset results, the tool is able to estimate efficiencies with having less than 0.2 STB/STB absolute difference error. A probabilistic assessment study for a given reservoir illustrated the practicality of the tool.

Keywords: cyclic steam injection, enhanced oil recovery, numerical simulation model, artificial neural network, data-driven screening tool

ÖZ

DÖNGÜSEL BUHAR ENJEKSİYONU (DBE) İNCELEME MODELİ GELİŞTİRME

Yalgın, Gamze
Yüksek Lisans, Petrol ve Doğal Gaz Mühendisliği Bölümü
Tez Yöneticisi: Prof. Dr. Mustafa Verşan Kök
Ortak Tez Yöneticisi: Doç. Dr. Emre Artun

Ocak 2018, 101 sayfa

Ağır petrol rezervuarları için geliştirilmiş tek kuyu da uygulanan bir petrol çıkarma yöntemi olan döngüsel buhar enjeksiyonu (DBE) bir döngü şeklinde üç aşamada gerçekleşir: enjeksiyon, yayılma, ve üretim. Bu çalışmada, temsili performans belirleyiciye göre verilen DBE işlemini onaylayan veya reddeden bir inceleme modeli oluşturmak amaçlanmıştır. Performans belirleyici, geliştirilen inceleme modelini kullanarak geniş bir rezervuar ve DBE dizayn parametrelerinden tahmin edilir. Yapay sinir ağları (YSA) ile geliştirilen model; buhar enjeksiyon dizayn parametrelerine bağlı verilen rezervuardaki DBE işlem performansını tahmin edebilir. YSA'da kullanılan veriler; simülatörde oluşturularak temsili bir nümerik rezervuar modeli kullanılarak elde edilmiştir. Simülasyonda deneysel dizayn yöntemi kullanılarak çeşitli senaryolar tanımlanıp çok sayıda durum oluşturulmuştur. Artan petrol üretimi ve enjeksiyon verimliliği gibi senaryolara karşılık gelen performans belirleyiciler toplanmıştır. Uygun geliştirme ve doğrulamadan sonra inceleme modeli saniyeler içinde performans tahmini için

hazır duruma getirilmiştir. İnceleme modeli ve nümerik rezervuar modeli arasında yapılan duyarlılık analizi sonunda inceleme modelinin problem iyi öğrendiği görülmüştür. Test veri sonuçlarının %90'ına göre inceleme modeli performansları 0.2 STB/STB'den düşük mutlak hata farkı ile tahmin etmektedir. Verilen bir rezervuar için olasılık değerlendirme çalışması inceleme modelinin kullanılabilirliğini göstermiştir.

Anahtar Kelimeler: döngüsel buhar enjeksiyonu, geliştirilmiş petrol üretimi, nümerik simülasyon modeli, yapay sinir ağları, veriye dayalı inceleme modeli

To my ‘elephant’ family

ACKNOWLEDGEMENTS

I would like to express my deepest gratitude to Assoc. Prof. Dr. Emre ARTUN for his valuable knowledge, guidance, encouragements, friendship and of course patience for my endless questions and confusions. Without his continuous confidence in my work and me, this thesis would not have been completed. I am grateful to him for being my mentor since I took the first "Reservoir Engineering" course from him.

I also present great thanks to Prof. Dr. Mustafa Verşan KÖK for the privilege to work with him and his support from the beginning.

My other biggest gratitude is to Prof. Dr. Salih SANER for his support, precious suggestions and insight on the challenges that I faced in academic life. Thanks to his fatherliness and humor, the days in Cyprus were peaceful and vivacious.

Most important thanks belong to my 'superhero' father Nadir YALGIN who always help me to face my problems and guide me to make the right decision, my 'guardian angel' mother Dilek YALGIN who always support and encourage me to the academic life with her unconditional love, my 'crazy other half' sister Özge YALGIN who always be there for me and laugh out loud together.

Special thanks goes to my 'roomie' Negar PAKZAD who shares the entire thesis, assistantship and Cyprus journey with me. I know that this journey would be more difficult without her joy, sisterhood and support. I am also thankful to many friends who do not leave me alone and give moral support despite of the distances.

Finally, I also acknowledge METU Ankara and METU NCC Petroleum and Natural Gas Engineering Departments for allowing me the opportunity to obtain a M.S. degree.

TABLE OF CONTENTS

LIST OF FIGURES

LIST OF TABLES

LIST OF SYMBOLS

A	Viscosity coefficient	*cp*
B	Viscosity coefficient	^oR
c_o	Coefficient of capillary pressure in oil/water system	*fraction*
c_g	Coefficient of capillary pressure in gas/liquid system	*fraction*
$c_{p,o}$	Heat capacity of oil	$Btu/ft^3.F$
EFF	Efficiency of CSI operation	*STB/STB*
h	Total reservoir thickness	*ft*
k	Permeability	*mD*
k_h	Horizontal permeability	*mD*
k_v	Vertical permeability	*mD*
k_{rw}	Relative permeability of water in oil/water system	*fraction*
k_{row}	Relative permeability of oil in oil/water system	*fraction*
k_{rg}	Relative permeability of gas in gas/liquid system	*fraction*
k_{rgl}	Relative permeability of liquid in gas/liquid system	*fraction*
MW	Molecular weight	*lbmole*
n	Exponent of the relative permeability	*unitless*
$N_{p,inc.}$	Incremental oil production, yearly	*bbl*
$N_{p,with\ inj.}$	Oil production with injection, yearly	*bbl*
$N_{p,without\ inj.}$	Oil production without injection, yearly	*bbl*
P_{res}	Reservoir Pressure	*psi*
p_{cow}	Capillary pressure in oil/water system	*fraction*
p_{cgl}	Capillary pressure in gas/liquid system	*fraction*
S_g	Gas saturation	*fraction*
S_{oi}	Initial oil saturation	*fraction*
S_{or}	Residual oil saturation	*fraction*
S_w	Water saturation	*fraction*
S_{wi}	Initial water saturation	*fraction*

S_{wirr}	Irreducible water saturation	*fraction*
$S_{i,inc.}$	Incremental steam injection, yearly	*bbl*
$S_{i,with\ inj.}$	Steam injection, yearly	*bbl*
t_{inj}	Steam injection time	*days*
t_{soak}	Steam soaking time	*days*
T_{res}	Reservoir temperature	^oF
T_{steam}	Steam temperature	^oF
$T_{surface}$	Surface temperature	^oF
q_{inj}	Steam injection rate	*bbl/day*
Q_{steam}	Steam quality	*fraction*
$W_{p,inc.}$	Incremental water production, yearly	*bbl*
$W_{p,with\ inj.}$	Water production with injection, yearly	*bbl*
$W_{p,without\ inj.}$	Water production without injection, yearly	*bbl*

Greek Letters

Δ	Production/Injection Differences	*Mbbl*
γ_o	Specific Gravity of oil	*fraction*
λ_o	Thermal conductivity of oil	*Btu/ft.day-F*
μ_o	Viscosity of oil	*cp*
ρ_o	Mass density of oil	lb/ft^3
Φ	Porosity	*fraction*

LIST OF ABBREVIATIONS

API	American Petroleum Institute
ANN	Artificial Neural Network
BOPD	Barrel Oil per Day
CO_2	Carbon dioxide
CSI	Cyclic Steam Injection
EOR	Enhanced Oil Recovery
GUI	Graphical User Interface
IOR	Improved Oil Recovery
NPV	Net Present Value
SAGD	Steam Assisted Gravity Drainage

CHAPTER 1

INTRODUCTION

According to Faergestad (2016), today's total world oil resources are 9 to 13 trillion bbl and British Petroleum Statistical Review of 2017 shows that only 1.7 trillion of these resources can be counted as reserves. While light oil only accounts for 30% of the total world oil resources, heavy oil and the others account for 70% of the resources which corresponds to 6.3 to 9.1 trillion bbl. The amount of light oil met the demand of world up to now; however, continuous increase in the demand for oil and the decrease in the supply of light oil resulted in the need to consider other sources like heavy oil and natural bitumen. Therefore, recovering heavy and other resources has an important role in the petroleum industry.

Light, heavy and natural bitumen are classified by their API gravities. Light oil is characterized by high API gravity and a low viscosity. On the other hand; low API and high viscosity are associated with heavy oil or natural bitumen. Heavy oil viscosity and gravity range from 100 to 10,000 cp and 20 to 10 API, respectively. Due to high viscosity and low API, heavy oil is slightly mobile in the reservoir and conventional production techniques cannot be used easily. In order to decrease viscosity and increase mobility, **enhanced oil recovery (EOR)** or **tertiary recovery** techniques are utilized.

EOR is generally applied for increasing the oil production after primary and secondary recovery. Even though these techniques can be expensive, the recovery can be increased up to 50-70%. According to reservoir characteristics and feasibilities, different EOR methods can be applied as thermal and non-thermal

methods. For increasing heavy oil recovery, thermal methods are used which are steam flooding, cyclic steam injection (CSI), steam assisted gravity drainage (SAGD), hot water flooding and in situ combustion. In this study, cyclic steam injection is considered as a recovery method for heavy oil reservoirs.

A number of studies have been conducted to improve the screening of cyclic steam injection process. These studies involve constraining reservoir models, simulating reservoirs in laboratory conditions, and using real and synthetic reservoir data. Most of the earlier screening criteria studies (Taber 1997, Ali et al. 1994, Trujillo et al. 2010) focus on limited number of reservoir properties and they are based on limited number of real cases. Even though these studies can give an idea about the applicability of CSI via quantitative comparisons, they cannot provide any production and performance results. While the studies which can predict the performance provide ranges for different parameters, they are difficult to utilize for different combinations of reservoir parameters. Therefore, they kept most of the parameters as a constant.

Modeling studies are important to simulate possible cases before applying in real life (Offeringa 1971, Pethrick et al. 1988, Scott et al. 1994, Razavi and Kharrat 2009, Mongy and Shedid 2015). Although commercial simulators analyze and forecast the production of a reservoir, they are complex and time-consuming. They require significant resources (computing, manpower, time), yet convergence problems may occur in modeling of complex EOR processes. ANN-based models have been proven to be successful for both forward and inverse modeling applications for EOR (i.e. both performance forecasting and reservoir characterization). Screening tools have been developed in this way for different EOR methods, including cyclic steam injection in naturally fractured reservoirs (Silpngarmlers et al. 2002, Parada 2008, Artun 2009, Arpacı 2014, Sun and Ertekin 2015). However, while some of the conducted studies are based on multi-layered reservoir models, they distributed the properties to each layer homogeneously and

did not consider the heterogeneity. Moreover, they neglect anisotropy of permeability, thermal properties and capillary pressures, and consider the EOR application for a short period of time.

In this study, it is aimed to develop a screening model that can predict the performance of a CSI process, once a set of reservoir characteristics and steam-injection design parameters are provided. The model is trained by using an artificial neural network (ANN) that can estimate the process performance in a given reservoir depending on the steam-injection design parameters. These parameters include steam injection rate, injected steam temperature, steam quality, durations of steam injection, soaking, and economic rate limit. The data used for the training of the ANN is generated using a representative numerical reservoir model, built with a commercial simulator (CMG, 2015).

This thesis is organized into seven chapters as follows:

- In Chapter 2, a literature survey for cyclic steam injection processes and applications of neuro-simulation in the petroleum industry are given.
- In Chapter 3, the statement of the problem and workflow are included.
- In Chapter 4, construction of the numerical model, ranges of reservoir and operational parameters are described in details. Grid sensitivity process is also explained.
- In Chapter 5, principles of artificial neural networks including its structure, and architecture, and development of the screening model are presented.
- In Chapter 6, results of numerical modeling and the screening model, analyses of the reservoir and operational parameters and a probabilistic assessment study for a given reservoir is presented. The graphical user interface (GUI) application is also presented.
- In Chapter 7, a brief summary and key conclusions are given.

CHAPTER 2

LITERATURE REVIEW

2.1 Cyclic Steam Injection

Cyclic steam injection is a single-well process for heavy oil reservoirs which means the same well is used for both injection and production. This method is also called cyclic steam stimulation and “huff and puff” steam injection. The aim of the process is to increase the temperature around the wellbore by using steam energy and decrease the viscosity of heavy oil. There are three stages: injection, soaking, and production as shown in Figure 2.1.

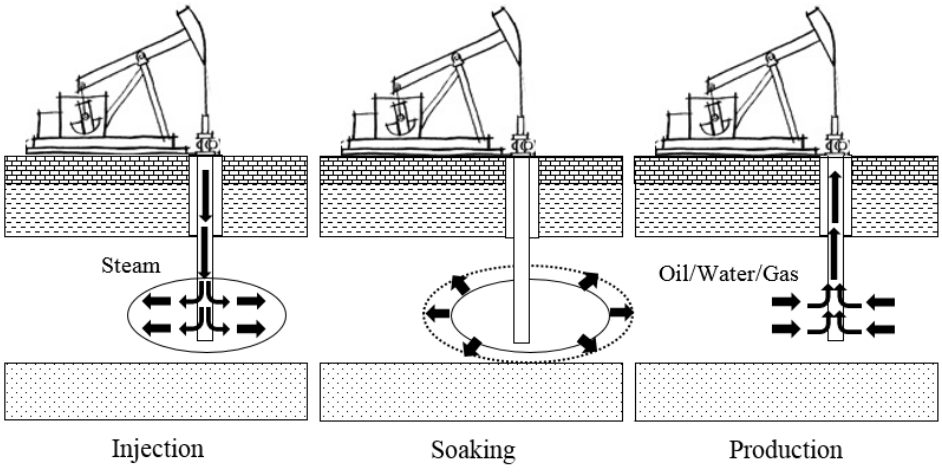

Figure 2.1 Cyclic Steam Injection Stages: injection, soaking and production.

Injection Stage: In this stage, steam is injected into the reservoir to increase the temperature. Duration of this stage is generally 3 to 4 weeks depending on the reservoir conditions (Arpacı, 2014).

Soaking Stage: After injection stage, the well is shut-in to let the steam diffuse into the formation. While the steam diffuses and increases the temperature in the reservoir, viscosity of heavy oil decreases and mobility of it increases. Duration of this stage is generally 2 to 3 weeks depending on the reservoir conditions (Arpacı, 2014). This duration should be selected properly because if it is too short, steam cannot heat the formation or if it is too long, heat can be lost and reservoir may cool again.

Production Stage: When the desired viscosity is reached, well is again put on production. Production continues until the production rate drops to an economic rate limit (Figure 2.2).

After production rate reaches to an economic limit, whole cycle of injection, soaking, and production may be repeated until it is considered to be feasible.

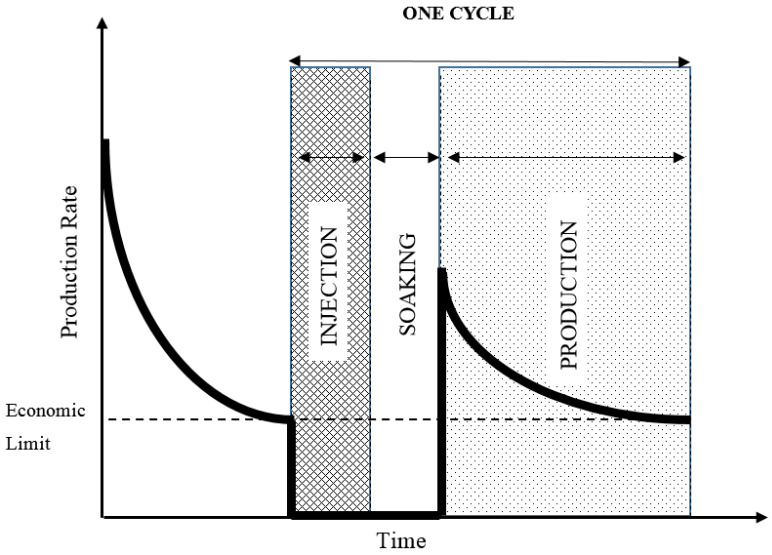

Figure 2.2 One cycle of cyclic steam injection with all stages.

In the late 1950s, a well in the Mene Grande Field located in Venezuela was backflowed due to reservoir pressure during a steam flooding process. The flow rate was increased and water cut was decreased compared to the unstimulated version of the well. This accident led to the discovery of today's cyclic steam injection process (Trebolle et al., 1993). Compared to other thermal EOR techniques, in some cases, a cyclic steam injection application may not increase the oil recovery significantly by oneself since only a limited area around the well is affected by steam. However, due to possible geological complexities like shale barriers, faults, and disconnected formations, cyclic steam injection may be the only method that can be applied successfully. For example, in some Cold Lake Field projects in Alberta where ultimate oil recovery was lower than 20%, steam flooding was not feasible because of very high oil viscosity and high conductive zones. Another example is in the Marguerite Lake Field located in Canada where in-situ combustion was tried as a posterior process and concluded with limited success (Ali, 1994).

Although CSI method is used to improve the recovery by itself, there are also some cases that it is used as a prior process to steam flooding, in-situ combustion, and CO_2 injection in order to increase the recovery factor. For instance, in some Californian fields, steam flooding applied after CSI increased total recoveries approximately to 60% (Ali, 1994). Moreover, in Duri Field located in Indonesia, the steam flood also followed the CSI operation. With this flood, the largest steam flood in the world, about 300,000 BOPD were produced from more than 3000 wells (Gael et al., 1995).

After CSI discovery, applications of this method were started in many heavy oil reservoirs and many research studies were conducted on the effects of the reservoir and operational parameters. By understanding the reservoir characteristics, steam properties, and injection conditions better, screening criteria, analytical modeling

and numerical modeling studies were conducted to implement a successful CSI operation.

By examining the real successful EOR projects and considering the main mechanism of oil-displacement for EOR methods, Taber et al. (1997) proposed a screening criteria based on oil properties and reservoir characteristics. They studied on eight different EOR or IOR (improved oil recovery) methods include gas injections (nitrogen, hydrocarbon, CO2), water flooding (polymer, alkaline), thermal methods (in-situ, steam injection) and surface mining. According to API gravity, viscosity, oil composition, oil saturation, formation type, net thickness, permeability, depth and temperature, suitable EOR methods can be selected. Moreover, Ali et al. (1974, 1997) conducted two comprehensive surveys of steam injection to specify ranges for reservoir and operational parameters. Performed tests between 1960 and 1970 were analyzed and ranges were specified as in Table 2.1.

Table 2.1 Cyclic steam injection screening criteria (Ali et al., 1997).

Depth, ft	< 3000
Reservoir Thickness, ft	> 30
Porosity, %	> 30
Permeability, mD	1000 - 2000
Initial Oil Saturation, %	> 45
API Gravity	< 15
Viscosity (@ Reservoir Condition), cp	< 4000
Steam Quality, %	80 - 85
Steam Pressure, psi	< 1400
Injection Time, days	14-21
Soaking Time, days	1-4

Trujillo et al. (2010) built a software tool to determine a feasible EOR method for a reservoir by using screening criteria. Nineteen different EOR methods including CSI can be screened with the certain reservoir rock and fluid properties; such as porosity, permeability, viscosity, API, oil saturation, thickness, depth, temperature,

pressure and lithology. After determining the suitable method, by comparing reservoir and fluid properties, analog models are selected through approximately 1000 real EOR cases to identify possible problems related to the selected EOR method. To form an opinion, this tool can be beneficial to determine the EOR method; however, results may not be accurate due to limited number of reservoir parameters and real EOR cases. Although, screening criteria studies are useful to have an idea about the applicability of CSI for a selected reservoir, production or performance data cannot be obtained.

There are also a large number of analytical model studies developed to predict the performance of a CSI process and almost all of these models used the Boberg-Lanz model and the Mark-Langenheim model to calculate heat losses and estimate the radius of the heated zone, respectively (Green and Willhite, 1998). Some of those models are Jones model (1977, oil recovery from pressure depleted gravity drainage reservoir using CSI process), Gantijo and Aziz model (1984, radial flow toward vertical wells considering fluid flow and heat conduction together), Ozkan et al. (1999, pressure drop in the wellbore), Wu et al. (2011, inflow performance for horizontal well with gravity drainage using CSI) and Saripalli et al. (2017, oil production from horizontal wells using CSI). Albeit an exact solution, existing analytical models are only homogenous systems can be solved.

When the number of parameters increases, the process gets more complex. Due to the number of unlimited combinations of reservoir and operational parameters, it is hard to find the optimum solution for a given reservoir. Offeringa (1971) developed a mathematical cyclic steam injection model by keeping most of the parameters as constants. These parameters were taken from physical laboratory models or real cyclic steam injection wells. By using different amounts of steam and lengths of a cycle, the model was calibrated and the optimum production performance of the well was predicted. However, due to keeping parameters constant, this study is limited to performance estimation only.

Another optimization study was published by Pethrick et al. (1988). A numerical model was built for cyclic steam injection process by using data of Cold Lake Field, one of the world's largest heavy oil sources located in northern Alberta. The aim of the study was to optimize the operating strategies for multiple wells and a single well. The results obtained from this study showed that reservoir modeling is useful in order to optimize CSI performance. Furthermore, by using simulation, a number of field pilot tests can be reduced and a cost-effective process can be achieved. According to Scott et al. (1994), field performances and some research studies have shown that increase in temperature by CSI may cause the occurrences of stresses and deformations. The change in heavy oil formation structure affects the permeability and water mobility of a reservoir. In their study, changes in the stress path and temperature were tried to be modeled by using testing equipment and experimental procedures. Moreover, the relations between the volume and permeability were figured out by using Cold Lake Field data. A numerical simulation modeling study conducted by Razavi and Kharrat (2009) was designed with data taken from one of the fractured heavy oil reservoirs located in Iran to find optimum recovery. Because of having less capital cost, less pressure operation and fast production period compared to steam flooding, CSI was chosen as a thermal method. Many CSI scenarios were created by changing the number of wells and directions, steam injection rates, production rates, soaking time and steam quality to determine the effect of operational parameters. They concluded that by using this thermal method, the oil recovery could be increased from 0.66% to 10% in 10 years.

Mongy and Shedid (2015) conducted a simulation study to create a suitable steam injection design for high cumulative oil recovery into a Middle Eastern heavy oil reservoir. By changing the steam properties, well completion and well spaces, different scenarios were created to analyze the effects of parameters on production performance and to optimize both cyclic and continuous steam injection.

As seen in the reviewed studies, reservoir simulators can be used to model the possible flow behaviors of a certain reservoir for forecasting the performance of a CSI. A model can be run many times with less manpower and expense in a short period of time; however a real field application can be done only once. Therefore, numerical simulation models are the most effective way to solve problems and to analyze the optimum values under different possible scenarios.

2.2 Artificial Neural Network

Artificial Neural Network (ANN) is known as a biologically inspired information-processing system. By using the relations between a problem and its solution, ANN creates connection links between them to solve similar problems like a human brain system. In 1943, a paper about the working principle of neurons was written by neurophysiologist Warren McCulloch and mathematician Walter Pitts, and in 1960, to solve a real world problem, the first neural network about a filter eliminating echoes on phone lines was developed (Kriesel, 2011). After this application, its usage started to become widespread and it was tried to be improved.

In the petroleum industry, there are a large number of artificial neural network applications as the following (McCormack, 1991);

- Exploration; identification of microfossils, analysis of gas chromatography, gravity/magnetics modeling, seismic data processing and other applications for seismic, etc.
- Drilling; drill bit quality assessment system, etc.
- Reservoir and Production; predicting water saturation (Al-Bulushi et al., 2007), analysis of pressure transient, analysis of gas well production, permeability prediction (Singh, 2005), EOR method selection (Shokir et al., 2002), etc.

For reservoir engineers especially those studying EOR methods, artificial neural network can be very useful to predict oil recovery in a given field because complex nonlinear relationships can be learned by ANN even if inputs are less precise.

Silpngarmlers et al. (2002) worked on ANN models that can predict two-phase relative permeability. Training and testing were done by using endpoint saturations, porosity, permeability, viscosity and interfacial tension as input parameters obtained from relative permeability experiments. In the same year, Shokir et al. studied on two neural networks to select a proper EOR method and check the feasibility of the selected method by considering only seven reservoir parameters which are area, porosity, permeability, reservoir depth, API gravity, viscosity and initial oil saturation. Parada (2008) created two neuro-simulation tools to screen and design different types of improved oil recovery (IOR) methods which are miscible injection, waterflooding and steam injection. The first tool predicts oil production profiles by using the reservoir and operational parameters as inputs. The second one works as an inverse ANN which predicts the operational parameters by using reservoir parameters and oil production profiles. Artun (2009) used artificial neural network based proxy models to check the feasibility of the cyclic pressure pulsing in different reservoir characteristics and to find the maximum efficiency of the project by optimization. Moreover, by developing an inverse ANN-based proxy model, optimized design parameters were provided for a given desired performance criteria. Arpacı (2014) built six different ANN models for naturally fractured reservoirs with horizontal wells to estimate the performance of CSI in a short period. Two of them predicts oil flow rate, a number of cycles, cumulative oil production, and duration of each cycle. Other two of them were built as inverse models to predict operational parameters from performance indicators. Last two out of six ANN was generated as predictors of reservoir parameters by using desired production profile and operational parameters as an inverse modeling approach. Despite built several ANN models, most of the parameters were taken as a constant include API gravity, residual oil and irreducible water saturations or neglected include anisotropy of permeability and capillary pressures. ANN-based proxy models were developed by Sun and Ertekin (2015) to be used in steam assisted gravity drainage (SAGD), and cyclic steam injection in naturally fractured reservoirs. The number of cycles for CSI, oil flow rate and cumulative oil

production can be predicted with given certain reservoir and operational parameters. These models help engineers to estimate the recovery of SAGD and CSI projects in a faster way. In addition to this, graphical user's interface was developed to provide easy access and implementation to the ANN models to the users. Although it is one of the most elaborate study in the literature, the effect of the heterogeneity, anisotropy and capillary pressures were neglected.

In all these reviewed studies, artificial neural networks were used to develop screening tools by learning the relationships between inputs and outputs. These tools compared to real field applications and simulations help to achieve desired outputs in seconds by using less manpower and energy spent.

To develop a successful CSI operation, it is important to analyze the applicability and efficiency of CSI for a given reservoir. This requires understanding the relationships between all parameters of the process and their effects on the efficiency of CSI. As mentioned in this chapter, generating a screening tool compared to field application and commercial simulators is a good option to analyze a large number of possible operational cases and design a successful CSI operation without complexity, manpower and long-computational time. Many screening tool studies about CSI operation have been conducted by neglecting the heterogeneity and some important reservoir parameters including capillary pressure and thermal properties.

CHAPTER 3

STATEMENT OF THE PROBLEM

Diversely in this study, the main objective is to develop a data-driven screening tool that can predict the performance of a CSI operation in a rapid way for all kinds of heavy oil reservoirs, once a set of reservoir characteristics and steam-injection design parameters of a reservoir are provided. It is desired to develop a tool that has the following characteristics which would also fill some of the important gaps in the existing models presented in the literature:

- The reservoir model is constructed as a five layered heterogeneous system. Different thickness, porosity, horizontal and vertical permeability values can be defined for each layer. One, two, three and four layered heterogeneous and homogeneous systems can also be created by changing these reservoir properties,
- 50 different reservoir and operational parameters are analyzed in detail and 36 of them are considered to build the screening model. By using Corey's correlations, capillary pressure and relative permeability effects are included. Moreover, thermal conductivity and heat capacity of rock and reservoir fluids are also considered.
- The screening tool can predict time dependent performance of CSI. Five artificial neural network models are developed to estimate efficiencies of any CSI operation for 10, 8, 6, 4 and 2 years.

CHAPTER 4

METHODOLOGY

In order to achieve these objectives, following steps are completed (Figure 4.1):

1. **Conceptual model construction**
   - A reservoir model is constructed using a commercial simulator (CMG, 2015) for cyclic steam injection.
2. **Data-base construction**
   - Many different scenarios with different combinations of 56 reservoir and operational parameters are run in the simulator with and without CSI.
3. **Performance data collection**
   - Incremental oil production and incremental steam injection results are collected to calculate efficiencies of 10, 8, 6, 4 and 2 years of CSI application.
   - Unreasonable cases are eliminated by checking for simulator errors and cases with only 1 cycle.
4. **Artificial Neural Network Design**
   - By using results of rest of the cases, 5 different ANN-based screening models are separately trained and tested to estimate efficiency for 10, 8, 6, 4 and 2 years of CSI application.
5. **Analysis**
   - The results of numerical simulation model and ANN are compared and the accuracy of the ANN is evaluated.

- A reservoir having similar properties with a real field is created and it is run with 10,000 different operational parameters to find optimum values for injection design.
- Monte Carlo Simulation analysis is also performed with 10,000 different cases having different reservoir parameters and same operational parameters.
- The effects of each parameter are examined by changing their maximum and minimum values in the base case and tornado charts are constructed with results of the numerical model and screening model.

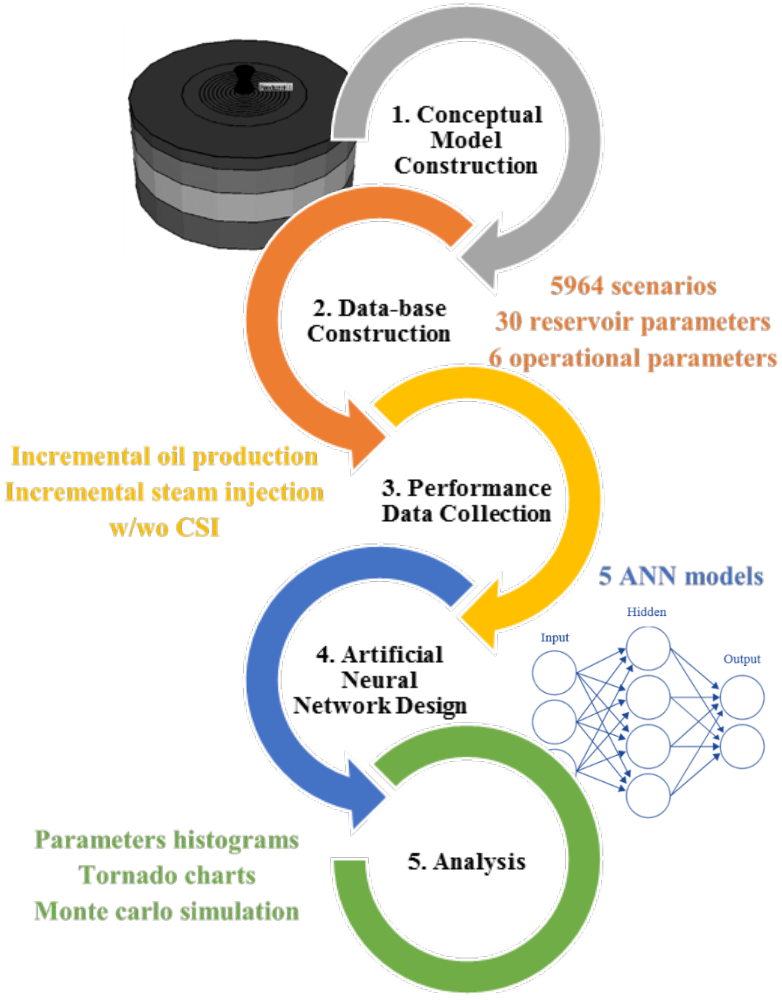

Figure 4.1 Summarized workflow of the study.

CHAPTER 5

RESERVOIR MODEL CONSTRUCTION

In order to train and test ANN models, a database was created by using a reservoir simulation model in CMG - Thermal & Advanced Processes Reservoir Simulator (STARS). This simulator can design thermal and compositional applications such as steam flooding, in-situ combustion, foam flooding and cyclic steam injection (CMG, 2015).

The reservoir model was predicated on a CMG STARS template constructed by Aziz et al. (1987) with some changes (CMG, 2015). The model was defined as a radial heterogeneous reservoir with 12 logarithmically distributed grid points in the radial direction and five layers as seen in Figure 5.1. A well was drilled in the center of the grids to be used as a producer and an injector for CSI operation. 50 different reservoir rock-fluid and 6 operational parameters were used to build the model.

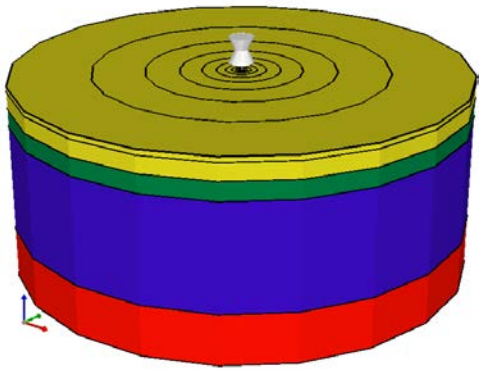

Figure 5.1 A three-dimensional view of constructed reservoir model for CSI operation (CMG, 2015).

5.1 Reservoir Rock - Fluid Parameters

Some fluid parameters indicated in Table 5.1 were taken from the Aziz et al.'s template or assumed as a constant. In addition to them, thermal conductivity of water and thermal expansion of oil were determined as 8.3 Btu/ft.day.F (Schön, 2011) and 3.96E-4 1/F (Souraki et al., 2002), respectively.

Table 5.1 Constant fluid parameters

WATER	Molecular weight, lb/lbmole	18.02		(CMG, 2015)
	Critical pressure, psi	3206.2		
	Critical temperature, ^oF	705.4		
	Coefficients in power-law correlation for temperature dependence of gas-phase viscosity	A, cp/R	1.13E-5	
		B	1.075	
	Mass density, lb/ft^3	0		
	Compressibility, 1/^oF	0		
	Thermal expansion, 1/^oF	0		
	Heat capacity, Btu/lbmole.F	0		
	Coefficients of the correlation for temperature dependence of component viscosity in the liquid phases.	A, cp	0	
		B, ^oR	0	
OIL	Critical pressure, psi	0		
	Critical temperature, ^oF	0		
	Coefficients in power-law correlation for temperature dependence of gas-phase viscosity	A, cp/R	0	
		B	0	
	Compressibility, 1/F	5.0E-6		

Porosity reference pressure, psi	14.7	ASSUMPTIONS
Surface pressure, psi	14.7	
Surface temperature, ^oF	60	
Reference pressure for fluid properties, psi	14.7	
Reference temperature for T-dependent and thermal properties, ^oF	60	

Apart from abovementioned parameters, 27 varying reservoir parameters were also used to construct the model:

1. Thermal conductivity of oil (Btu/ft.day.F)
2. Thermal conductivity of gas (Btu/ft.day.F)
3. Thermal conductivity of formation rock (Btu/ft.day.F)
4. Thermal conductivity of upper/lower formation rock (Btu/ft.day.F)
5. Heat capacity of formation rock (Btu/ft^3.F)
6. Heat capacity of upper/lower formation rock (Btu/ft^3.F)
7. Porosity (fraction)
8. Molecular weight of oil (lb/lbmole)
9. Reservoir pressure (psi)
10. Initial water saturation (fraction)
11. Initial oil saturation (fraction)
12. Well drainage area (acres)
13. Reservoir depth (ft)
14. Reservoir thickness (ft)
15. Permeability (mD)
16. Anisotropy of permeability (k_v/k_h) (fraction)
17. Rock compressibility (1/psi)
18. Density (lb/ft^3)
19. Reservoir temperature (^oF)
20. Heat capacity of oil (Btu/lbmole.F)
21. Viscosity coefficient of A (cp)
22. Viscosity coefficient of B (^oR)
23. Residual oil saturation (fraction)
24. Irreducible water saturation (fraction)
25. Exponential coefficient for relative permeability (unitless)
26. Capillary pressure coefficient of oil (unitless)
27. Capillary pressure coefficient of gas (unitless)

According to studies of Eppelbaum et al. (2014) and Schön (2011), wide range of thermal properties were specified as seen in Table 5.2. Thermal conductivity of oil (λ_o) is depend on reservoir temperature (T_{res}) and specific gravity (γ_o) of oil; therefore, it was calculated from following equation in order to get an accurate value:

$$\lambda_o = \frac{1.62}{\gamma_o}[1 - 3(T_{res}) * 10^{-4}] \quad (5.1)$$

Table 5.2 Ranges for thermal properties.

		Eppelbaum et al. (2014)	Schön (2011)	In this study	
				min	max
Thermal conductivity of gas		-	0.37	0.3	1.0
Thermal conductivity of formation rock	Limestone	31	9-87	10	90
	Sandstone	33-48	13-90		
Thermal conductivity of upper/lower formation rock	Shale	-	8-59	10	60
Heat capacity of formation rock	Limestone	34	31-64	25	125
	Sandstone	24 - 32	26-114		
Heat capacity of upper/lower formation rock	Shale	-	33-54	33	54

Moreover, two screening criteria (Table 5.3) were investigated to determine range of some properties which are porosity, molecular weight, reservoir pressure, initial water saturation. It was assumed that reservoirs are saturated with only water (S_{wi}) and oil (S_{oi}) at initial state:

$$S_{oi} + S_{wi} = 1 \tag{5.2}$$

Wide and reasonable ranges for well drainage area, reservoir depth and thickness, permeability ratio of k_v/k_h, rock compressibility, and API gravity of oil were specified. In this study, range of API gravity was used from 10 to 20 due to heavy oil characterization and with API value, density (ρ_o) was calculated by following equations to use in simulator as an input.

$$\text{API} = \frac{141.5}{\gamma_o} - 131.5 \tag{5.3}$$

$$\gamma_o = \frac{\rho_o}{62.4} \tag{5.4}$$

Each layer may have different thickness, porosity and permeability values. Lorenz coefficient is used to state the degree of heterogeneity within the simulated reservoir. The minimum "zero" value indicates that reservoir is completely homogeneous; on the other hand, the maximum value "one" is a signal for completely heterogeneous system (Dykstra and Parsons, 1950). This coefficient was calculated by a code prepared by Liber Eleutherios in 2008 (MATLAB, 2013) to be used as an input in ANN models.

Reservoir temperature (T_{res}) is a depth and surface temperature ($T_{surface}$) dependent parameter; therefore, it was calculated with following equation:

$$T_{res} = T_{surface} + \frac{Depth}{70} \tag{5.5}$$

According to Wright (2014), changes in heat capacity of oil ($c_{p,o}$) can be estimated from graphs or Equation 5.7. The equation is related with API, reservoir temperature and molecular weight (MW). In this study, equation was used:

$$\begin{gathered} c_{p,o}{}' = [(-1.39 * 10^{-6})\, T_{res} + (1.847 * 10^{-3})]API \\ + \\ (6.312 * 10^{-6})T_{res} + 0.352 \end{gathered} \tag{5.6}$$

$$c_{p,o} = c_{p,o}{}' * MW \tag{5.7}$$

Increase in viscosity causes an increase in residual oil saturation by decreasing the mobility of oil. Due to that, viscosity is an important guideline for numerical simulation to apply successful CSI operation. Although viscosity can be identified by using a viscosity-temperature table, in this model, it was calculated with reservoir temperature, viscosity coefficients A and B. Range of these coefficients were specified by considering interval between 100 cp and 10,000 cp. These parameters were used in Andrade's oil viscosity correlations (Sun and Ertekin 2016):

$$\mu_o = A + e^{\frac{B}{T_{res}+460}} \tag{5.8}$$

In order to include the relative permeability tables as variables; ranges for residual oil saturation (S_{or}), irreducible water saturation (S_{wirr}) and exponential coefficient for relative permeability (n) were determined (Table 5.3) and Corey's three-phase relative permeability correlation were used to construct relative permeability tables (Arpacı, 2014, and Sun and Ertekin, 2016):

Oil/Water System

$$k_{rw} = \left(\frac{S_w - S_{wirr}}{1 - S_{or} - S_{wirr}}\right)^n \tag{5.9}$$

$$k_{row} = \left(\frac{1 - S_{or} - S_w}{1 - S_{or} - S_{wirr}}\right)^n \tag{5.10}$$

Gas/Liquid System

$$k_{rg} = \left(\frac{S_g}{1 - S_{wirr}}\right)^n \tag{5.11}$$

$$k_{rgl} = \left(\frac{1 - S_g - S_{wirr}}{1 - S_{wirr}}\right)^n \tag{5.12}$$

where k_{rw}, k_{row}, k_{rg} and k_{rgl} denote relative permeability to water, oil to water, gas and gas to liquid, respectively. S_w is water saturation and S_g is gas saturation.

In this study, capillary effects were also considered by using Corey's capillary pressure correlation with specified ranges for capillary pressure coefficient of oil (c_o) and gas (c_g). Capillary pressure tables were constructed with following equations:

Oil/Water System

$$p_{cow} = \frac{c_o}{\sqrt{\frac{S_w - S_{wirr}}{1 - S_{or} - S_{wirr}}}} \tag{5.13}$$

Gas/Liquid System

$$p_{cgl} = \frac{c_g}{\sqrt{\frac{1 - S_g - S_{wirr}}{1 - S_{wirr}}}} \tag{5.14}$$

where p_{cow} is capillary pressure in water-oil system and p_{cgl} is capillary pressure in gas-liquid.

All determined wide and reasonable ranges were as in Table 5.3. Furthermore, several CSI applied field properties (Table 5.4) were investigated to be sure that ranges are suitable for real cases.

Table 5.3 Screening criteria and determined ranges of reservoir parameters.

	Arpacı (2014)		**Sun and Ertekin (2016)**		**In this study**	
	min	**max**	**min**	**max**	**min**	**max**
Porosity	0.15	0.40	0.18	0.35	0.10	0.40
Molecular W.	600		420	700	200	600
Res. Pressure	500	3,500	600	1,200	500	2,000
Ini. Water Sat.	0.15	0.60	0.10	0.40	0.10	0.50
Area	-	-	35	104	5	30
Depth	1,000	10,000	-	-	500	5000
Thickness	40	200	30	120	10	500
Permeability	20	200	500	2,000	1	2,000
k_v/k_h	1.0		1.0		0.01	1.0
Rock Comp.	5E-4		-	-	3.00E-6	1.00E-5
API Gravity	6		10	25	10	20
Visc. Coef. A	visc-temp table		1.00E-4	5.00E-3	0.01	0.05
Visc. Coef. B			6,000	7,600	5,000	6,500
Res. Oil Sat.	0.15		0	0.05	0.1	0.3
Ir. Water Sat.	0.25		0.05	0.15	0.1	0.3
Rel. Perm. Exp.	2-2.5		2	4	2	4
Cap. Pres. Coef. oil	0		0	0	1	4
Cap. Pres. Coef. gas	0		0	0	0.1	0.3

Table 5.4 Reservoir parameters of steam injected fields.

	Midway-Sunset (Monarch)	**Midway-Sunset (Potter)**	**Guadalupe**	**Kern River**	**Cymric**	**Huntingon Beach**	**Cox Penn**	**Tia Juana**	**Los Perales**	**Duri**
	Hazlett et al. (1997)	Counihan (1977) Mohammadi et al. (1989)	Mohammadi and McCollum (1989)	Chu and Tremble (1975)	Fong et al. (2001)	Adams and Khan (1969)	Chiou and Murer (1989)	Salazar et al. (1987)	Pascual (2001)	Gael et. al (1995)
Depth	-	1,600	2,800	900	1,230	2,000-2,400	1,400-1,600	1,250	3,116	500
h	400	437	40	89	225	50-100	75	98-157	13	120
φ	0.3	0.32-0.34	0.35	0.30	0.49	0.38	0.26	0.38	0.28	0.34
k	200-1,500	2,150-2,500	1,550	3,000	2	2,300	750-1,500	3,000	500	1,500
S_{oi}	80	64-70	-	50	43	-	80	85	-	53
API Gravity	14	11-12	9	12	13	12-13	14-16	12	10-17	20
T_{res}	95	120	130	95	100	110-115	80	102-104	-	100
P_{res}	-	20	300	50	-	600-1,200	275	560-630	1,207	100
μ_o, @ T_{res}	2,300	1,630	560	4,000	354	940-3,700	2,000	3,000-10,000	-	330

5.2 Operational Parameters

The data-driven screening model can estimate the process performance in a given reservoir depending on the steam-injection design parameters. These design parameters include steam injection rate (q_{inj}), injected steam temperature (T_{steam}), steam quality (Q_{steam}), durations of steam injection (t_{inj}), soaking (t_{soak}), and economic rate limit. After investigating real CSI field applications and screening criteria, wide and reasonable ranges were determined for operational parameters (Table 5.5).

Table 5.5 Operational parameters of steam injected fields and screening criteria.

		q_{inj}	T_{steam}	Q_{steam}	t_{inj}	t_{soak}	Eco.rate limit
Midway-Sunset (Monarch) Hazlett et al. (1997)		650	450	0.70	10	10	-
Kern River Chu and Tremble (1975)		1,000	470	0.80	20	8	-
Cymric Fong et al. (2001)		500	-	-	6	4	-
Huntingon Beach Adams and Khan (1969)		1,300-1,350	-	0.80	-	-	-
Cox Penn Chiou and Murer (1989)		240-888	530-625	0.25-0.80	18-44	8-47	-
Los Perales Pascual (2001)		820	625	0.65-0.70	18	-	-
Duri Gael et. al (1995)		2,000	432	0.80	21	5	-
Arpacı (2014)	**min**	350	450	0.70	5	5	-
	max	5,000	750	1.00	50	50	-
Sun and Ertekin (2016)	**min**	600	450	0.70	10	10	20
	max	1,500	750	1.00	50	20	40
In this study	**min**	500	450	0.70	10	10	5
	max	2,000	700	1.00	60	30	25

"TRIGGER" keyword (CMG, 2015) was implemented to add a condition to apply cyclic steam injection. After simulation started with injection, well was put on production until economic rate limit was reached and then, new injection-production cycle starts again. All these parameters were constant for each cycle of one case; however, they were changed in every case by randomly selecting from ranges. Despite the constant parameters, production period was varied in each cycle of one case according to economic rate limit. Therefore, the number of cycles was also different for each case.

5.3 Grid Sensitivity Analysis

Smaller grid sizes provide more accurate results in numerical modeling studies; however, execution time takes longer. Therefore, it is important to find best grid sizes having shorter runtime with reasonable results (Shin et al., 2012). In this study, a reservoir was created with the base values of parameters (can be seen in Section 5.4 as a table) and grid sensitivity was performed. Firstly, the reservoir model was divided in R-θ-Z grids to create 3-D model (Figure 5.2) and run with different dimensions in the θ direction (360^o, 90^o and 60^o).

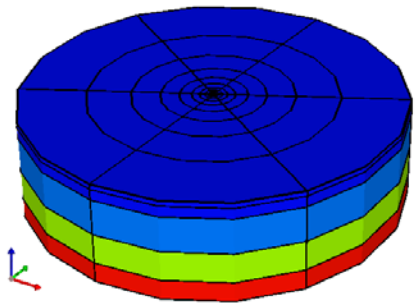

Figure 5.2 Division of grids in R-θ-Z dimensions for constructed reservoir model (CMG, 2015).

The production differences (Figure 5.3) and the elapsed time of the simulator (Figure 5.4) indicated that increase in grids affect the production and computation time. The more grids means longer computation time; therefore, according to the

low percentages of the production differences, the model was constructed as 2-D by not taking into account the θ direction.

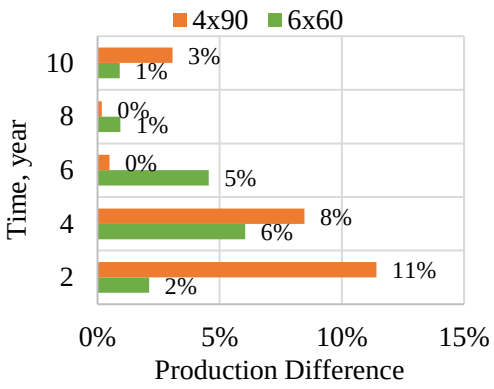

Figure 5.4 Absolute production difference compared with 1 grid model (360º).

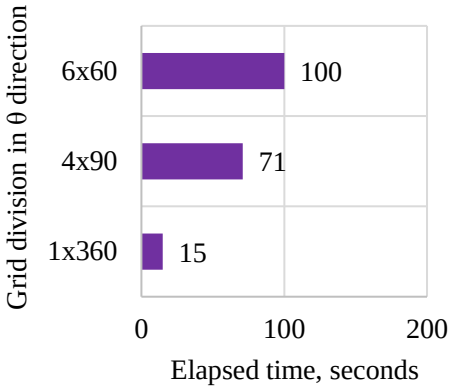

Figure 5.4 The elapsed times for 60º with 6 grids, 90º with 4 grids and 360º with 1 grid.

Secondly, after creating 2-D model, grid sizes were changed in R direction and cumulative oil productions, cumulative water productions, cumulative steam injections and elapsed time of simulation were collected (Figure 5.5 and Figure 5.6).

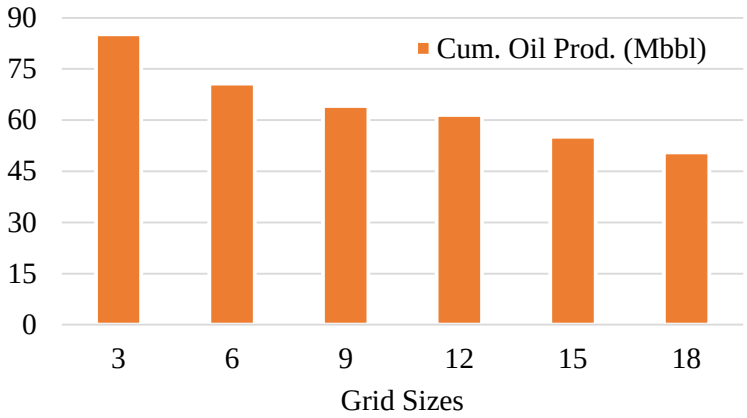

Figure 5.5 Cumulative oil productions of different grid sizes.

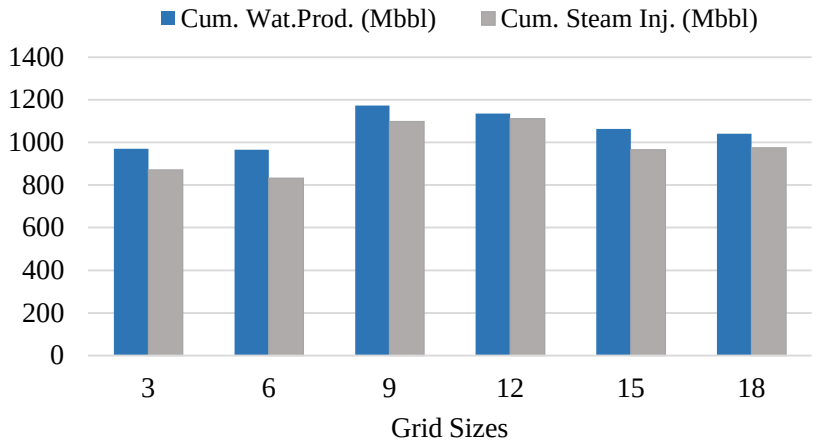

Figure 5.6 Cumulative water productions and cumulative steam injections of different grid sizes.

Table 5.6 shows all cumulative values and their change ratios according to previous less grid sizes. By comparing these values, with 61.5 Mbbl cumulative oil production, 1136 Mbbl cumulative water production, 1112 Mbbl cumulative steam injection and 11 seconds runtime, 12 grid points was found to be the most reasonable one respect to others.

Table 5.6 Cumulative values and change ratios.

Grid Sizes	Cum. Oil Prod. (Mbbl)	Δ	Cum.Water Prod. (Mbbl)	Δ	Cum. Steam Inj. (Mbbl)	Δ	Elapsed Time (sec)
3	85.1		970.4		871.9		1
6	70.7	-17%	966.0	0%	832.6	5%	4
9	64.1	-9%	1172.9	-21%	1098.6	-32%	9
12	**61.5**	**-4%**	**1136.3**	**3%**	**1111.6**	**-1%**	**11**
15	55.1	-10%	1063.3	6%	966.4	13%	14
18	50.6	-8%	1040.7	2%	975.5	-1%	15

An exponentially increasing grid distribution was suitable for this model because it was constructed as a radial reservoir. A linear equation was created by using best fit for distributions of 5, 10, 15, 20, 25 and 30 acres (Figure 5.7).

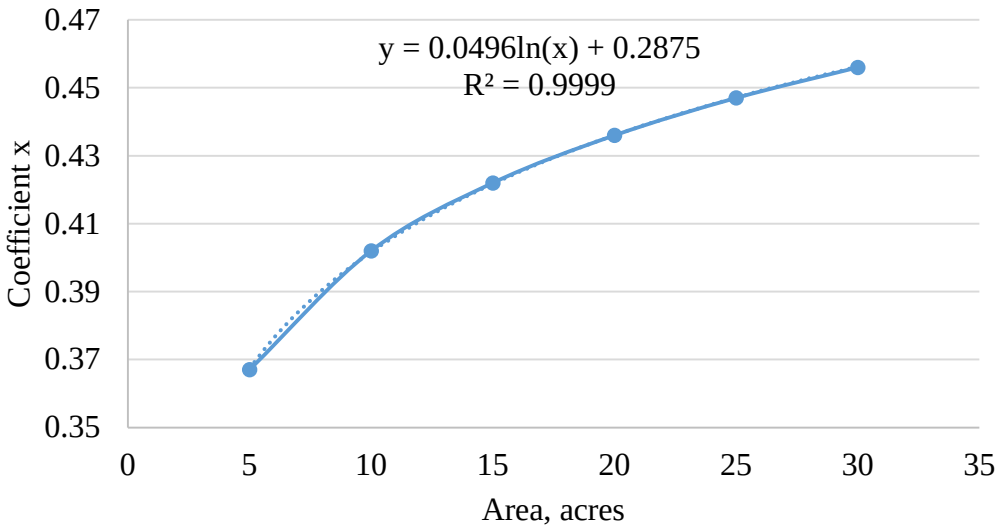

Figure 5.7 Best fit equation.

The distribution of grid points for well drainage area between 5 and 30 acres were calculated from following equations:

$$x = 0.0496 * \ln(\text{area}) + 0.2875 \quad (4.15)$$

$$\text{grid size} = \exp(x * \#\text{ofgrid}) \quad (4.16)$$

# of grid	1	2	…	11	12
Grid sizes	exp(x)	exp(x*2)	…	exp(x*11)	exp(x*12)

5.4 Generation of the Dataset

The list of parameters used as input in the screening model and their ranges were determined as in Table 5.7.

Table 5.7 Screening model inputs and their ranges.

#	Parameters	Unit	In this study		
			min	**base**	**max**
1	Well drainage area	acres	5	18	30
2	Total reservoir thickness	ft	10	255	500
3	Reservoir depth	ft	500	2,750	5000
4	k_v/k_h	fraction	0.01	0.5	1.0
5	Average porosity	fraction	0.10	0.30	0.40
6	Average permeability	mD	1	200	2,000
7	Rock compressibility	1/psi	3.00E-6	6.50E-6	1.00E-5
8	Heat cap. of fm	$Btu/ft^3.F$	25	75	125
9	Therm. conductivity of fm	Btu/ft.day.F	10	50	90
10	Therm. conductivity of oil	Btu/ft.day.F	calculated		
11	Therm. conductivity of gas	Btu/ft.day.F	0.3	0.7	1.0
12	Heat capacity of u/l fm	$Btu/ft^3.F$	33	44	54
13	Therm. cond. of u/l fm	Btu/ft.day.F	10	35	60
14	Molecular weight of oil	lb/lbmole	200	400	600
15	Density of oil	lb/ft^3	calculated		
16	Specific gravity of oil	fraction	calculated		
17	API gravity	API	10	15	20
18	Heat capacity of oil	Btu/lbmole.F	calculated		
19	Viscosity coefficient A	cp	0.01	0.03	0.05
20	Viscosity coefficient B	^oR	5,000	5,750	6,500
21	Residual oil saturation	fraction	0.10	0.20	0.30
22	Irreducible water saturation	fraction	0.10	0.20	0.30
23	Relative perm. exponent	unitless	2	3	4
24	Capillary pres. coef. of oil	unitless	1	2.3	4
25	Capillary pres. coef. of gas	unitless	0.1	0.2	0.3
26	Reservoir pressure	psi	500	1,250	2,000
27	Reservoir temperature	^oF	calculated		
28	Initial water saturation	fraction	0.10	0.30	0.50
29	Initial oil saturation	fraction	calculated		
30	Steam temperature	^oF	450	575	700
31	Steam quality	fraction	0.70	0.85	1.00
32	Steam injection rate	bbl/day	500	1,250	2,000
33	Injection time	day	10	35	60
34	Soaking time	day	10	20	60
35	Economic rate limit	bbl/day	5	15	25
36	Lorenz coefficient	fraction	calculated		

All selected parameters except permeability were uniformly distributed in their own ranges. In reality, most of the permeability values are between 50 and 100 mD; therefore, lognormal distribution was selected to be realistic. Porosity, permeability and thickness values were selected for one layer and then, for other four layer, values were selected from first layer's values. Therefore, distribution of average porosity, average permeability and total thickness were not seen uniform and lognormal. Unfortunately, some scenarios were eliminated after the run. One part of these could not be simulated by the simulator because of "convergence error". Some numerical controls were set to check the model (e.g. material balance error is set to not exceed 1E-4). The other part did only one cycle CSI process in 10 years since flow rates did not reach economic rate limit. After elimination, 5964 scenarios were obtained for training and testing the screening model. Histogram plots of new data set showed that elimination of scenarios did not affect the distributions (Figure 5.8 - 5.11).

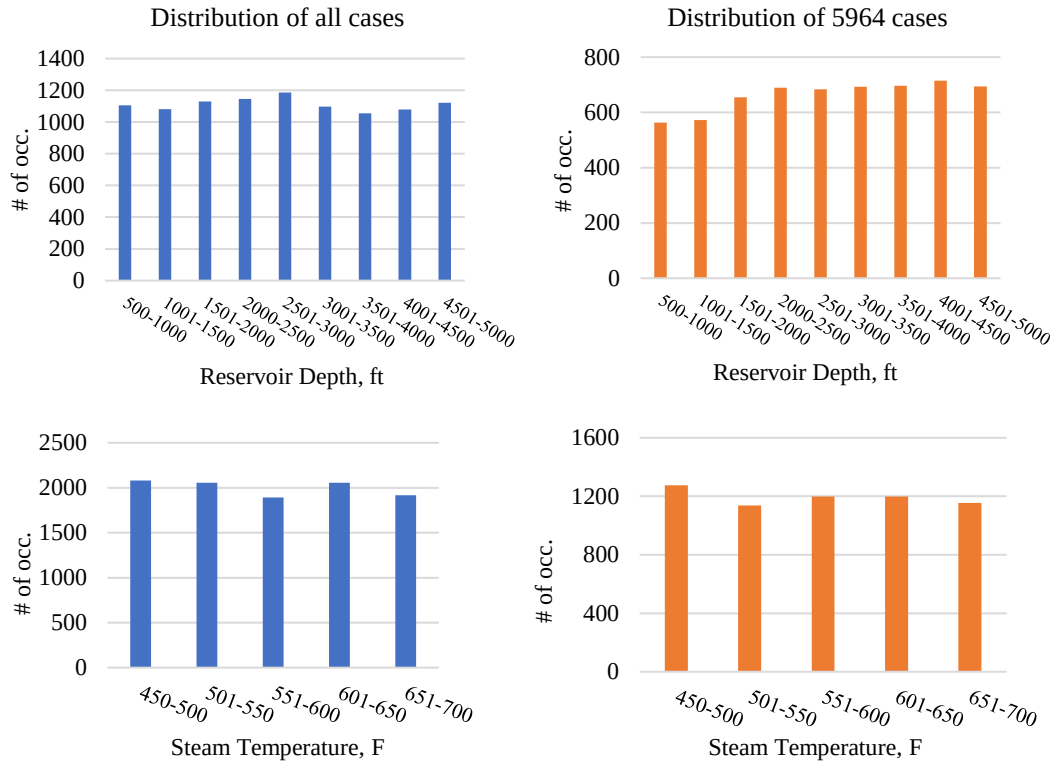

Figure 5.8 Example uniform distributions of reservoir and operational parameters.

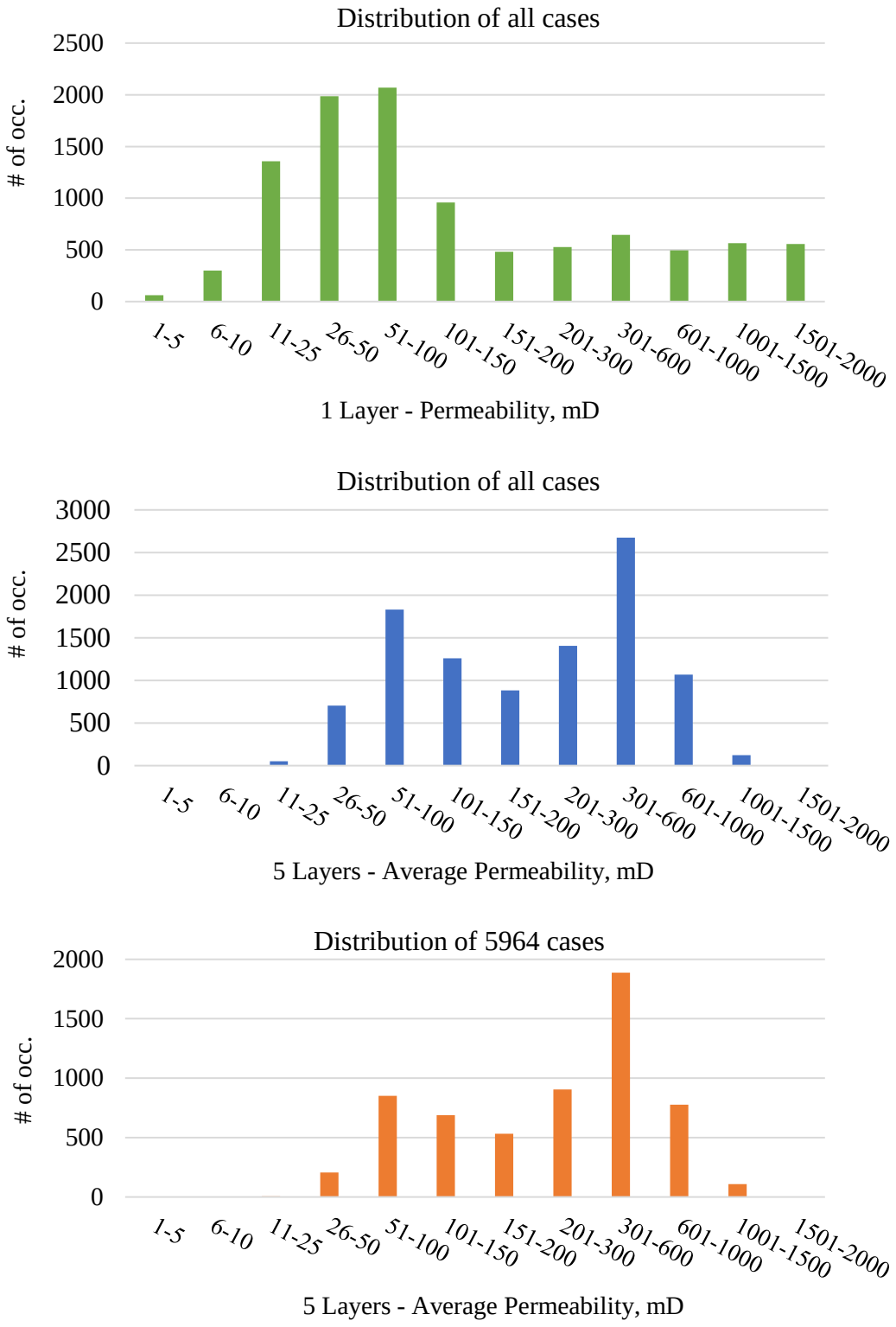

Figure 5.9 Distribution of permeability for one layer and five layers.

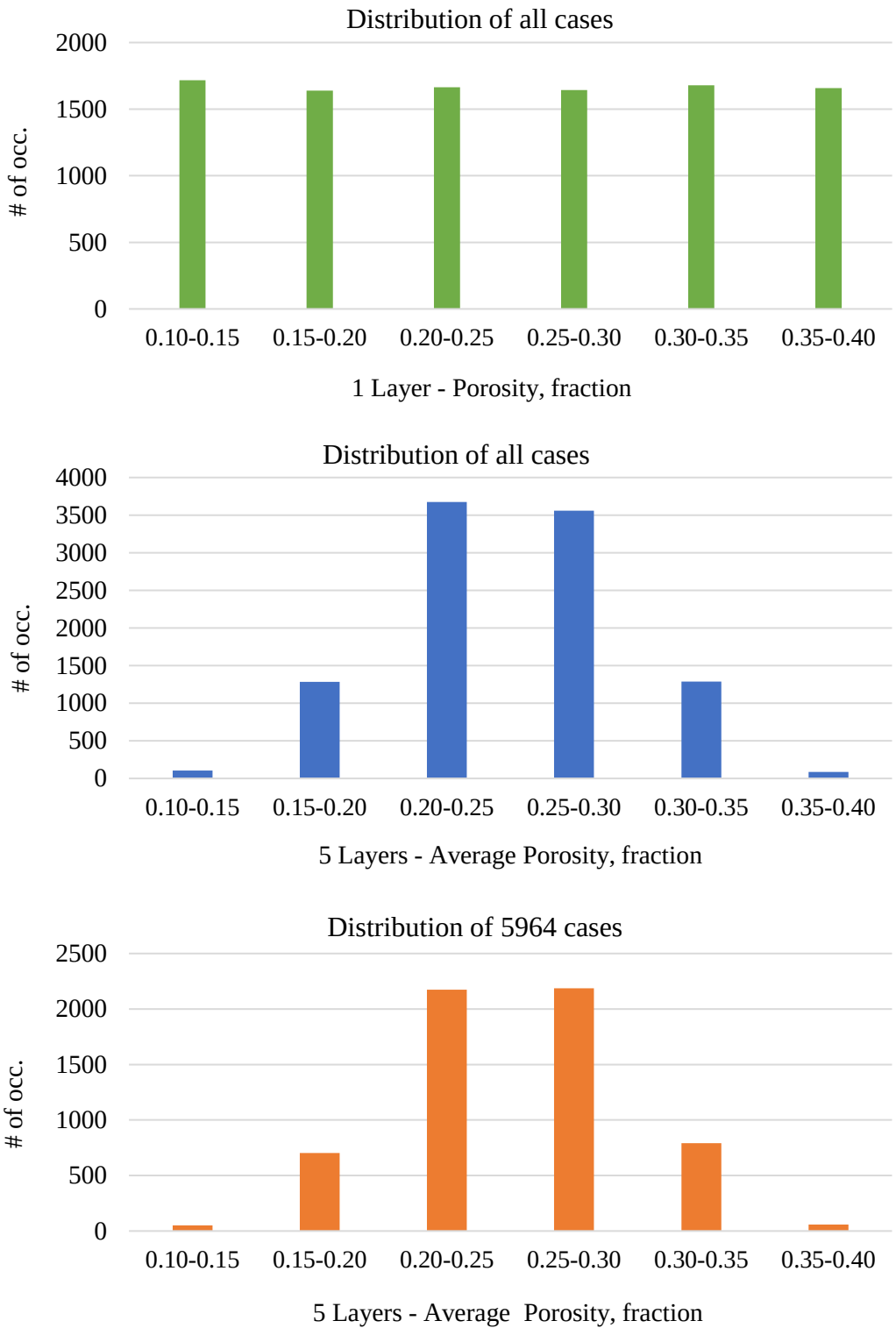

Figure 5.10 Distributions of porosity for one layer and five layers.

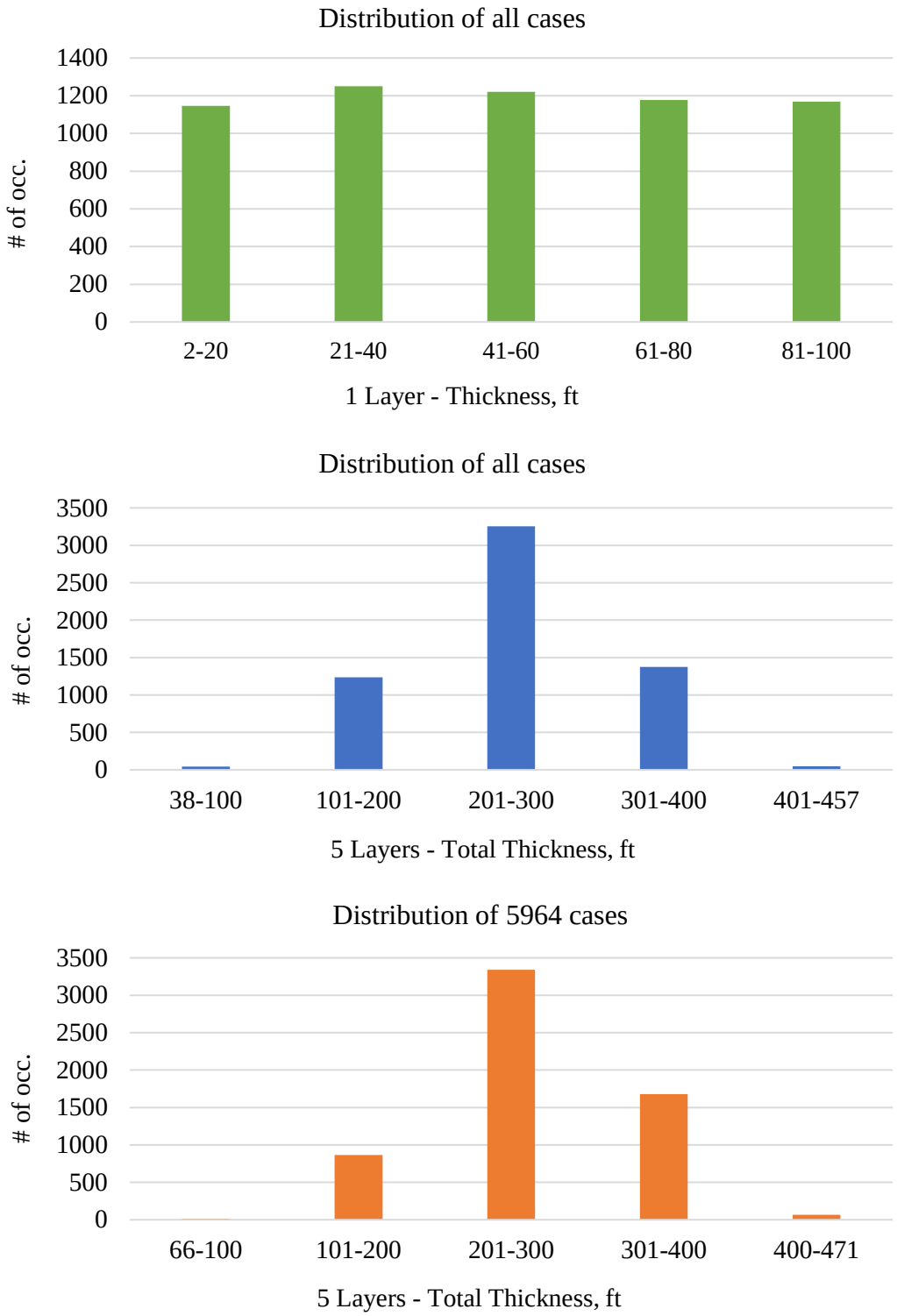

Figure 5.11 Distributions of porosity and thickness for one layer and five layers.

Two simulator templates, seen in Appendices A and B, were created for “with” and “without” CSI operation. Each case was simulated in both situations and cumulative oil production, cumulative water production and cumulative steam injection for 10 years were collected as outputs. Then, efficiencies were calculated as follows:

1. Yearly production and injection were calculated for 10 years and then, incremental values were found by subtracting ‘without injection’ values from ‘with injection’ values:

Yearly oil prod. : $$(N_{p,inc.})_n = (N_{p,with\ inj.})_n - (N_{p,without\ inj.})_n \quad (5.17)$$

Yearly water prod. : $$(W_{p,inc.})_n = (W_{p,with\ inj.})_n - (W_{p,without\ inj.})_n \quad (5.18)$$

Yearly steam inj. : $$(S_{i,inc.})_n = (S_{i,with\ inj.})_n \quad (5.19)$$

n:1, 2, 3, 4…10 years

2. By using these incremental values for 10 years, present values (PV) were calculated for 10, 8, 6, 4 and 2 years with 10% interest rate (i), separately (Figure 5.12).

PV oil prod. : $$(PV_{Np})_n = \sum_{j=1}^{n} \frac{(N_{p,inc.})_j}{(1+i)^j} \quad (5.20)$$

PV water prod. : $$(PV_{Wp})_n = \sum_{j=1}^{n} \frac{(W_{p,inc.})_j}{(1+i)^j} \quad (5.21)$$

PV steam inj. : $$(PV_{Si})_n = \sum_{j=1}^{n} \frac{(S_{i,inc.})_j}{(1+i)^j} \quad (5.22)$$

n:2,4,6,8 and 10 years

Time, year		1	2	3	4	5	6	7	8	9	10
Incremental (Yearly)	**Oil Prod.**	$(N_{p,inc.})_1$	$(N_{p,inc.})_2$	...	...	...	...	...	...	...	$(N_{p,inc.})_{10}$
	Steam Inj.	$(S_{i,inc.})_1$	$(S_{i,inc.})_2$	...	...	...	...	...	...	...	$(S_{i,inc.})_{10}$

PVs for 2 years
PVs for 4 years
PVs for 6 years
PVs for 8 years
PVs for 10 years

Figure 5.12 Calculation of present values for different period of time.

3. Efficiencies of CSI operations for 10, 8, 6, 4 and 2 years were calculated following equation:

$$(\mathrm{EFF})_n = \frac{(\mathrm{PV_{Np}})_n}{(\mathrm{PV_{Si}})_n} \tag{5.23}$$

n:2,4,6,8 and 10 years

Each efficiency was used as an output of different ANN models (Figure 5.13). Same training, validation and testing data sets were used to build data-driven screening models.

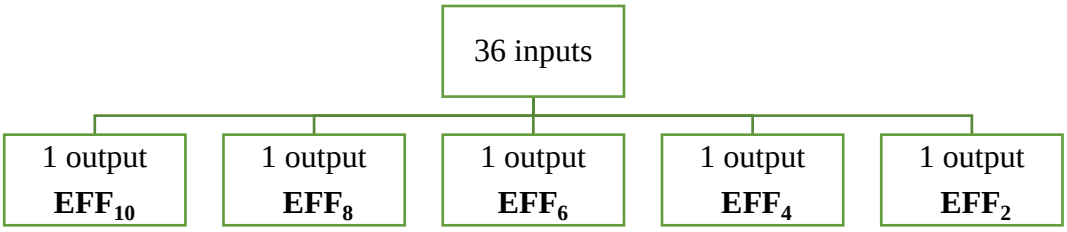

Figure 5.13 Five different ANN models with same inputs.

CHAPTER 6

SCREENING TOOL DEVELOPMENT

Reservoir modeling can be a costly and time consuming process in complex reservoirs because of the necessity of a comprehensive reservoir description. With a reasonable range of error in accuracy and computational efficiency, a screening tool can be used to reduce extensive time and energy spent in simulation and modeling studies.

Data driven modeling approach was followed to develop the screening tool. The principle about data driven modeling is based on learning the relationship between inputs and outputs of a system by using a data set without explicit knowledge of physical behavior of the system. There are a number of computational intelligence techniques used for data-driven modeling. Artificial neural networks, fuzzy rule-based systems and genetic algorithm are among the most popular ones (Abrahart et al., 2008).

Artificial neural network (ANN) approach was selected to model the data driven screening tool. ANN is very powerful to understand non-linear and complex relationships between inputs and outputs. By creating regression models, input & output mapping can be performed.

An artificial neural network is characterized by the following:

a. The connection pattern between neurons which represents the architecture of the ANN.

b. The method of determination of weights on the connections and its training algorithm.

6.1 Structure and Architecture of Artificial Neural Network

The idea of ANN is similar with human brain system. A human brain contains approximately 100 billion neurons that receive, process and transmit information among themselves (Kriesel, 2011). The structure and working principle of ANN mimic the human brain like a mathematical model representation of biological nervous system (Figure 6.1). Similarly, in an ANN model, an information is received from dendrites to process in cell body and transmitted by synapses to other neuron.

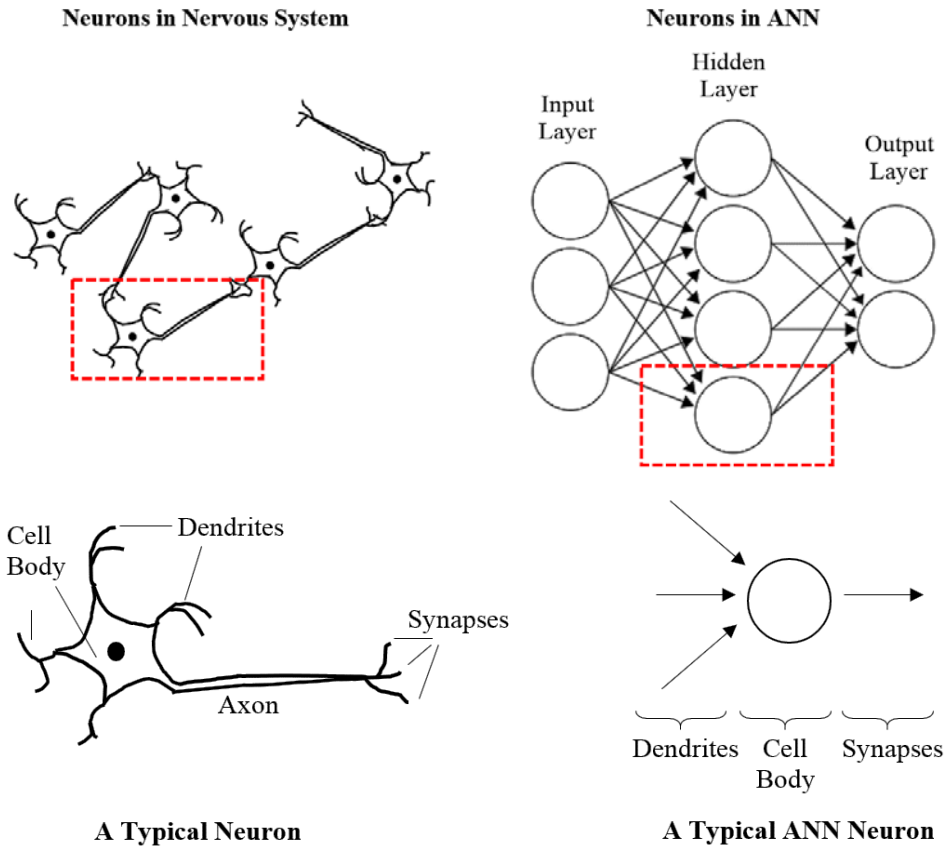

Figure 6.1 Structure of neurons in human brain and ANN.

The architecture of an ANN model can be defined as the arrangement of neurons and the connections between them. According to its classification, ANN is divided into two: single layer and multilayer as seen in Figure 6.2. While single layer is formed only input and output layers, multilayer has extra one or more layers to connect input and output layers. These extra layers, named as "**hidden layers**", can be helpful in complex problems to be solved. The number of hidden layers and neurons in each hidden layer are determined based on complexity of the problem which can be defined as the number of input and output neurons.

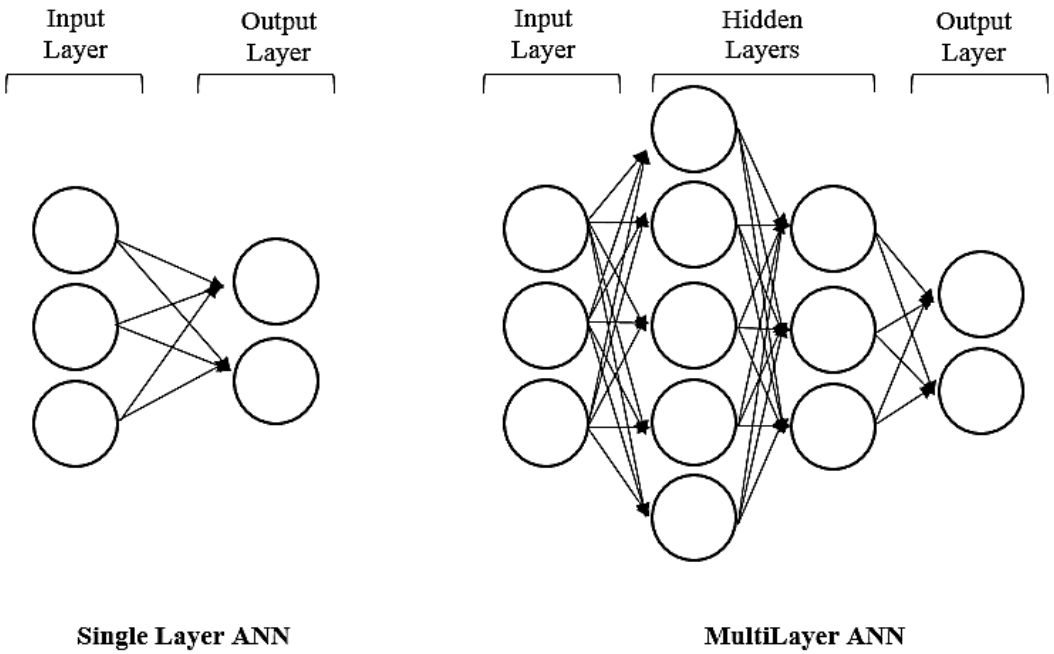

Figure 6.2 ANN classification for architecture.

6.2 Weights and Training of Artificial Neural Network

Determination of weights between layers is another important characterization aspect for ANN modeling. A weight refers to the strength of connection between two neurons. By showing that how neurons have an influence on solution, weights

have a direct relationship with the learning process. They are calibrated based on inputs and outputs to become ideal connections in network.

Learning system behavior is a critical issue about ANN. While there are a number of different learning algorithms, the most common way of calibration of weights can be completed in two steps; forward propagation and back propagation.

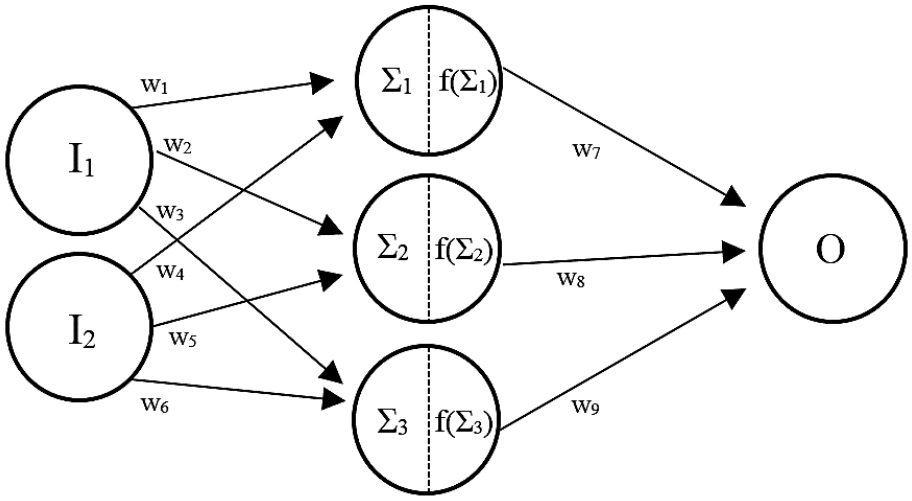

Figure 6.3 Example ANN model with one hidden layer.

1. Forward propagation: Inputs (I_1 and I_2) and output (O') are normalized between -1 and +1, separately. A set of weights are randomly selected between 0 and 1. The product of inputs and their selected weights (w) are summed for each hidden layer's neuron. A transfer function (f) is applied to the hidden layer sums (Σ) to obtain hidden layer outputs (Figure 6.3).

$$\Sigma_1 = I_1 * w_1 + I_2 * w_4 \quad (6.1)$$

$$\Sigma_2 = I_1 * w_2 + I_2 * w_5 \quad (6.2)$$

$$\Sigma_3 = I_1 * w_3 + I_2 * w_6 \quad (6.3)$$

More than ten different transfer functions can be used in forward propagation. Linear function, log sigmoid function, step function and hyperbolic tangent sigmoid function are the most common ones (Kulga, 2010):

- In linear function, hidden layer output (f) can be found with the multiplication of input (Σ) by a constant (K). (Figure 6.4a)

$$f(\Sigma) = K * \Sigma \tag{6.4}$$

- In log sigmoid function, hidden layer outputs get values between 0 and 1 by using following equation and produce "S" shape curve. (Figure 6.4b)

$$f(\Sigma) = \frac{1}{1 + e^{-\Sigma}} \tag{6.5}$$

- In step function, hidden layer outputs can get two values, 1 and -1, based on inputs. (Figure 6.4c)

$$f(\Sigma) \begin{cases} 1 & \text{if } \Sigma > 0 \\ -1 & \text{if } \Sigma < 0 \end{cases} \tag{6.6}$$

- In hyperbolic tangent sigmoid function, hidden layer outputs get values between -1 and 1 by using following equation and produce again "S" shape curve like log sigmoid function. (Figure 6.4d)

$$f(\Sigma) = \frac{e^{\Sigma} - e^{-\Sigma}}{e^{\Sigma} + e^{-\Sigma}} \tag{6.7}$$

Calculated hidden layer outputs are multiplied with randomly determined weights and summed to obtain the final output (O') as in Equation 6.8. Calculated output (O') is compared with the target output (O).

$$O' = f(\Sigma)_1 * w_7 + f(\Sigma)_2 * w_8 + f(\Sigma)_3 * w_9 \tag{6.8}$$

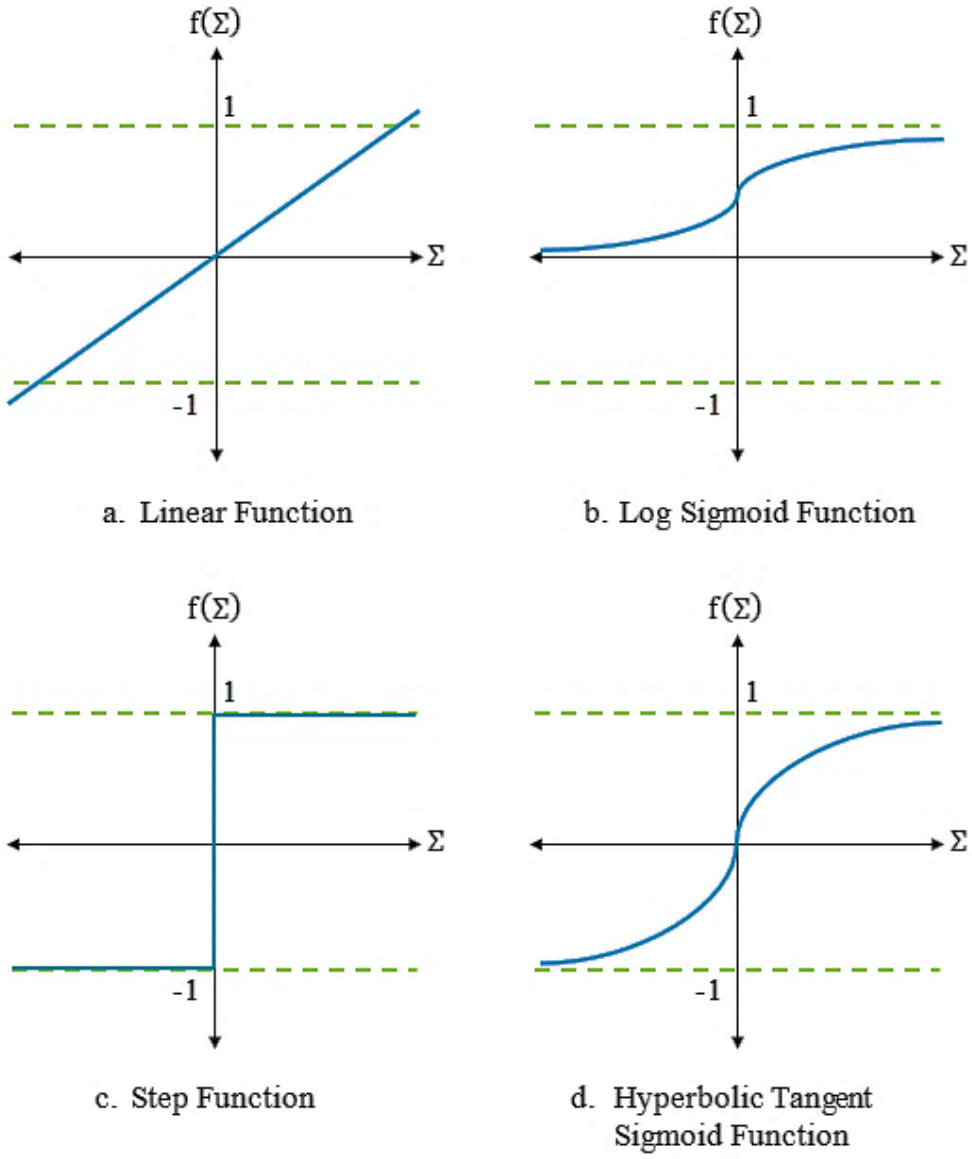

Figure 6.4 Common transfer functions.

2. Back propagation: The margin of error of the output is measured and weights are calibrated correspondingly to decrease the error based on "Generalized Delta Rule". Both steps are repeated until weights are adjusted to ideal ones. Data set is divided into three as training, validation and testing. Training data set is used to calibrate the weights. Validation data set is used to show how training process goes: generalization or memorization. To avoid memorizing, during the training period,

the error of validation is monitored. If the error of validation increases while the training error decreases, this shows that ANN memorized the pattern instead of generalizing. Testing data set is used to assess generalization capabilities of the neural network (Arpacı, 2014).

6.3 Application of Artificial Neural Network to Screening-Model Development

As mentioned in the previous chapter, 5964 cases were created randomly with 36 parameters and efficiencies of these cases were calculated for 2, 4, 6, 8 and 10 years. More inputs and outputs mean more complexity in ANN applications. Therefore, in this thesis, instead of creating an ANN with five different time periods, five different ANNs were built to predict performance of CSI for each period.

Before training ANN models, all inputs and outputs were prepared. Each input parameter and output was normalized linearly between -1 and +1 in itself because all of them have different scale. For instance, while porosity ranges between 10 % and 40 %, reservoir depth ranges between 500 ft and 5000 ft. For both parameters, minimum values and maximum values were considered as -1 and +1, respectively and the remaining values were distributed proportionally.

5964 cases were distributed into training, validation and testing data sets with 80 %, 10 % and 10 % proportions, respectively (training data set - 4772 cases, both validation and testing data sets - 596 cases). It is important to train models with different parameters and efficiency values; therefore, in order to avoid using similar cases, efficiency values were distributed manually into the data sets. It was aimed that training, validation and testing data sets have all possible efficiency values from

minimum to maximum. Same data sets were used to train all ANN models as seen in Figure 6.5.

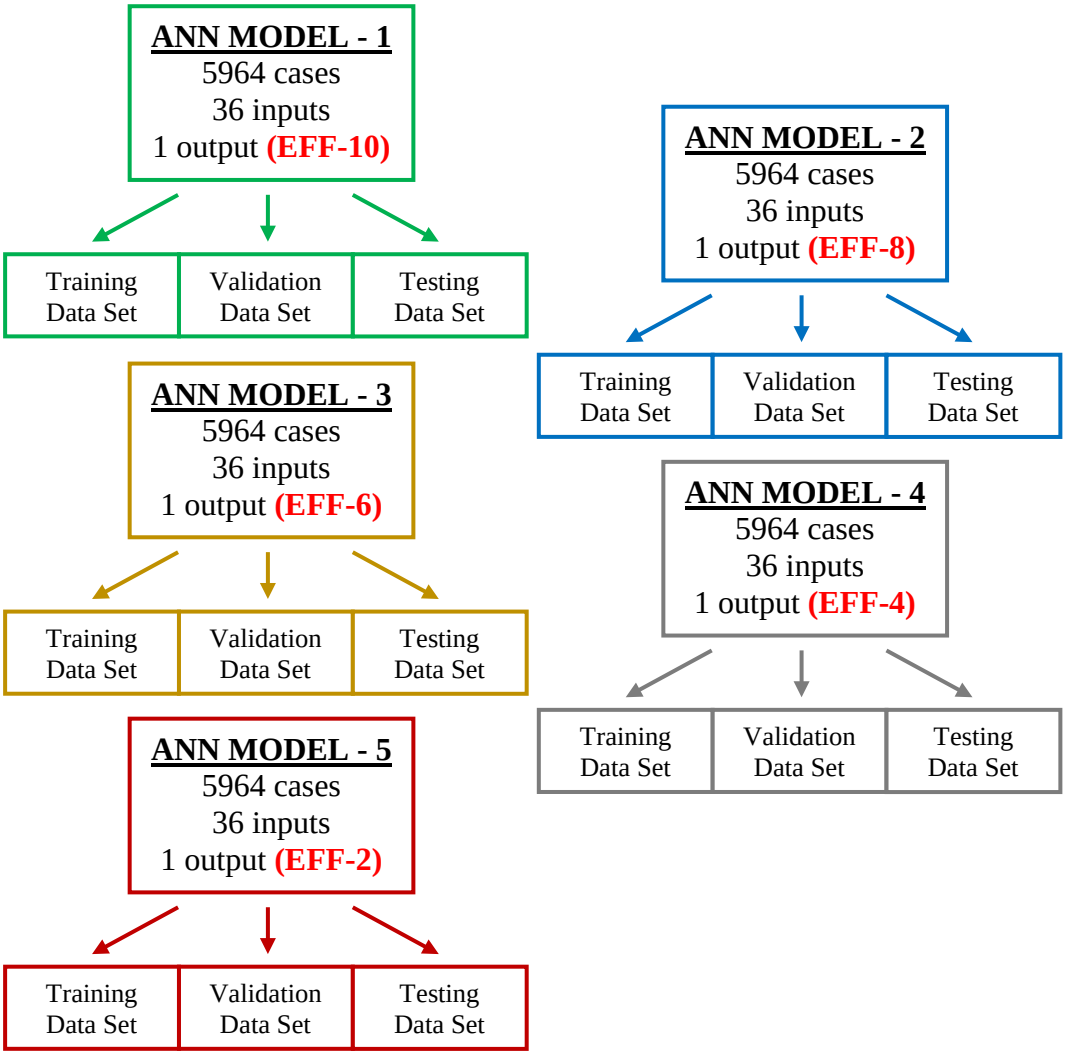

Figure 6.5 Data sets distributions for ANN models.

The most appropriate ANN structures were generated for each ANN model by using the trial and error method. Different number of hidden neurons and hidden layers were used and their effects on training were observed. By comparing regressions of the training, validation and testing data sets, the best training structures for each

ANN models were selected. In Figure 6.6, there are example regression graphs taken from training of ANN Model – 5.

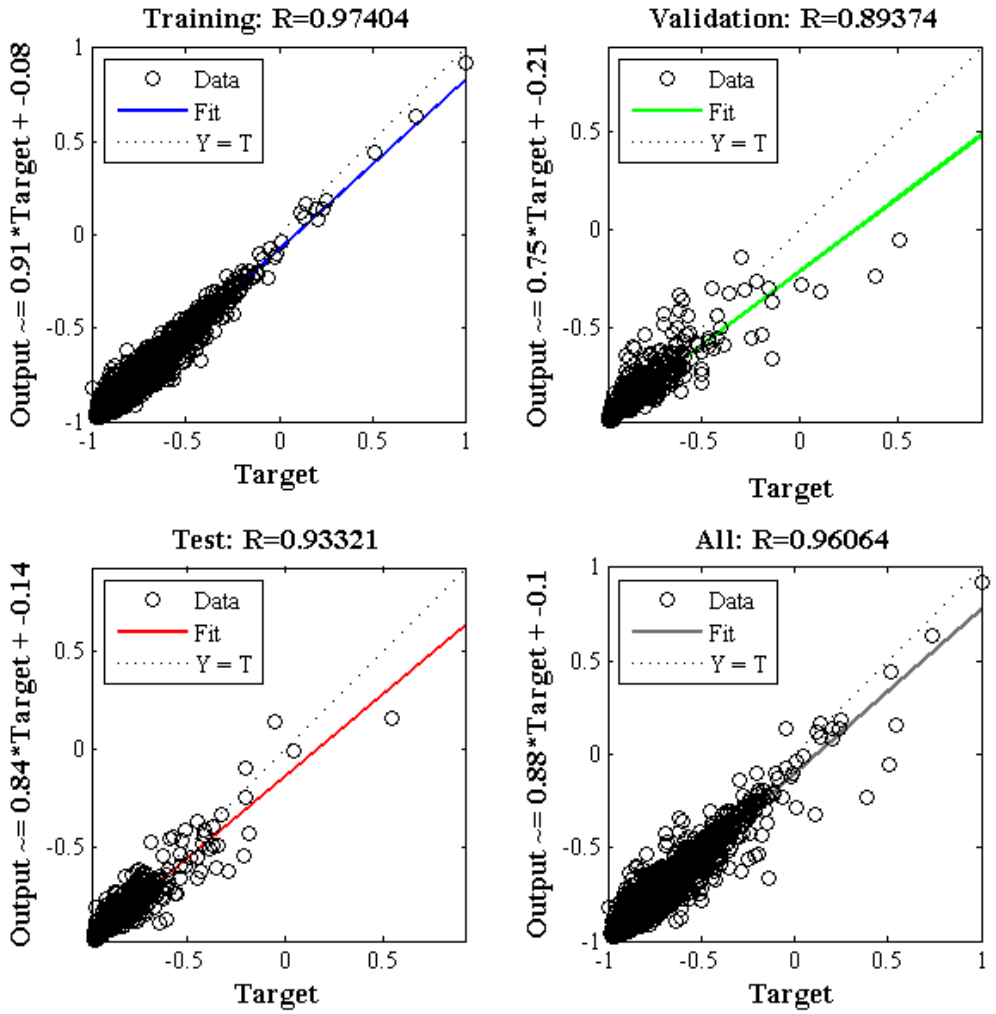

Figure 6.6 Regression graphs for 12th training trial (ANN Model – 5).

All structure trials and regressions for ANN Model – 5 can be seen in Table 6.1 and Figure 6.7. As much as possible, the highest regressions were tried to be achieved. After 14 trials, 11th and 12th trials having close regressions were compared and 12th one with the highest testing regression was selected.

- 11th Trial: Training R= 0.971 Validation R=0.910 Testing R=0.892
- 12th Trial: Training R= 0.974 Validation R=0.894 Testing R=0.933

Table 6.1 Number of neurons and layers tested for building ANN Model – 5.

Training trials	Number of Neurons in 1. Hidden Layer	Number of Neurons in 2. Hidden Layer	Total Neurons in Hidden Layers
1	100	-	100
2	90	-	90
3	80	-	80
4	70	-	70
5	60	-	60
6	50	-	50
7	40	-	40
8	40	20	60
9	50	10	60
10	40	10	50
11	30	20	50
12	30	10	40
13	25	15	40
14	35	5	40

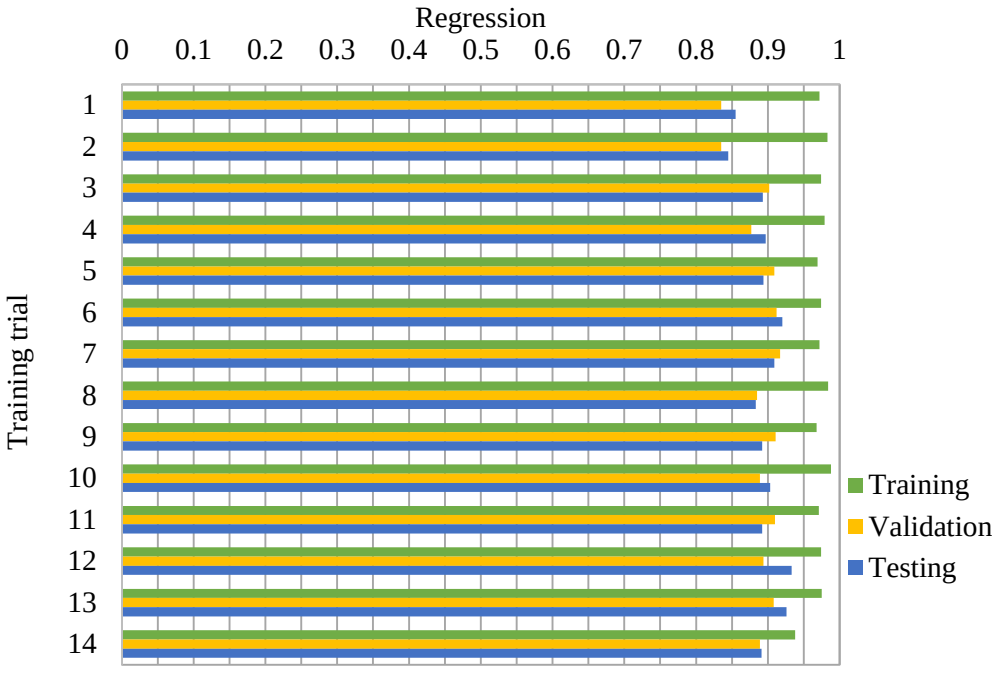

Figure 6.7 Regression values for all training trials.

CHAPTER 7

RESULTS AND DISCUSSIONS

In this chapter, results obtained from the numerical simulator and the screening model are analyzed in detail. A number of cases are investigated to ascertain the effects of the reservoir and operational parameters and by carrying out a sensitivity study, the accuracy of the ANN is evaluated. Moreover, a reservoir model having similar properties with The Liaohe Oilfield is created and optimization studies are performed for operational parameters.

7.1 Analyses of Reservoir and Operational Parameters

After creating the dataset using the numerical simulator, best 500 cases, having the highest efficiencies, are selected to analyze the effects of the reservoir and operational parameters on efficiency. This selection is made separately for 10, 8, 6, 4 and 2 years to analyze in detail. For each parameter, histograms are plotted, and their distributions in their ranges are analyzed to infer the effects. Exact conclusions cannot be achieved from these histograms since a large number of varying different parameters affect the performance indicators at the same time.

In yearly parametric analysis, it is seen that there is no significant difference between them. However, distributions of some parameters according to their ranges change.

The histogram of viscosity shows that the efficiency decreases as long as viscosity increases (Figure 7.1). **T**he cases having between 100 and 200 cp viscosity have lower efficiencies since the performance indicators were calculated by incremental production and injection values. For these cases, they have high base productions and there is no need to inject steam to the reservoir.

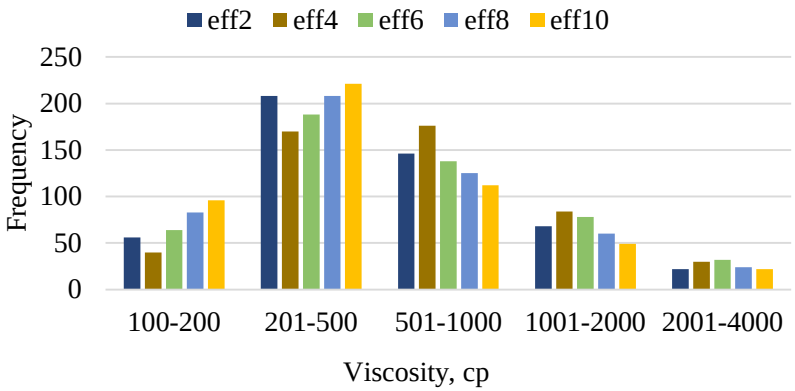

Figure 7.1 Distribution of viscosity for best 500 cases.

The following three histograms show that some parameters affect the efficiency positively. The increase in area, reservoir pressure, formation compressibility and anisotropy of permeability increase the efficiency (Figure 7.2 – 7.5).

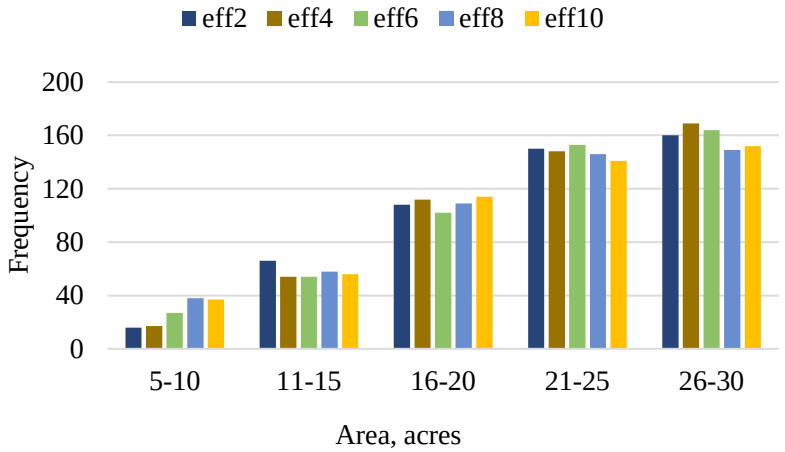

Figure 7.2 Distribution of area for best 500 cases.

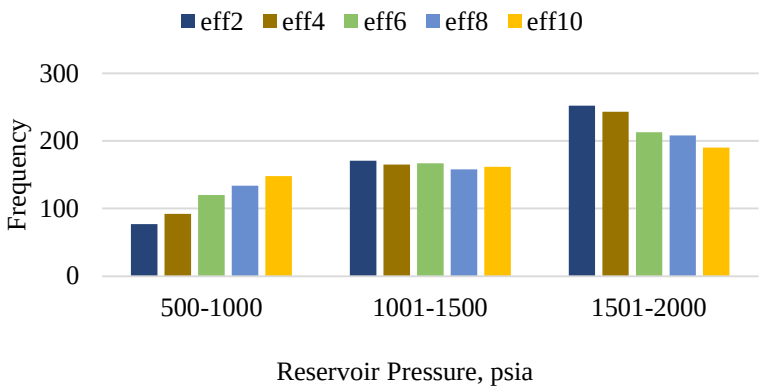

Figure 7.3 Distribution of reservoir pressure for best 500 cases.

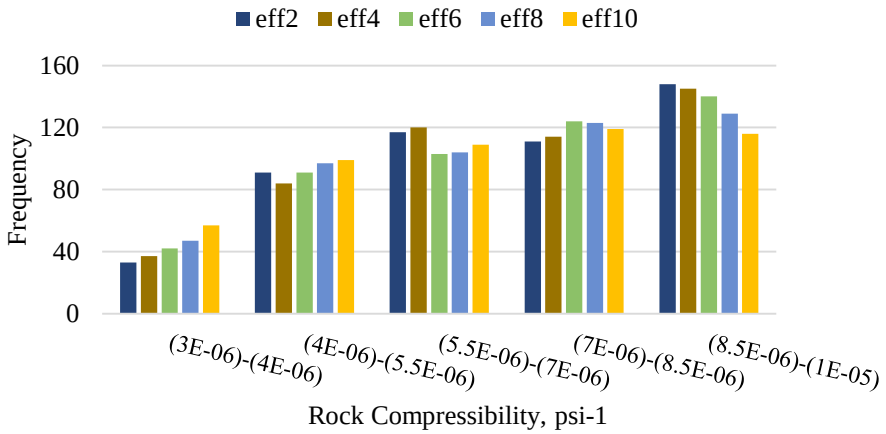

Figure 7.4 Distribution of reservoir pressure for best 500 cases.

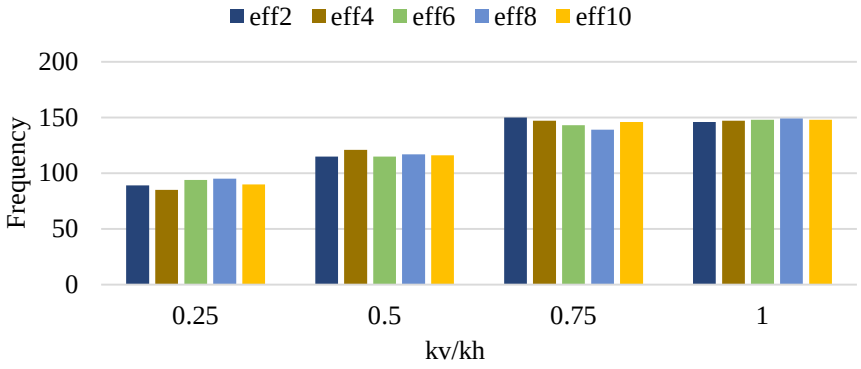

Figure 7.5 Distribution of anisotropy of permeability for best 500 cases.

Relative permeability data is one of the critical physical properties for the production. Corey's exponential coefficient for relative permeability (n) states the pore size distribution. In the model for each case, this number is taken as constant for oil/water and gas/liquid systems. Therefore, only pore size distribution can be analyzed. The solid line is for a wide range of pore sizes (n=2) while the dashed line shows a medium range pore sizes (n=4) (Figure 7.6). As seen in the Figure 7.7, more uniform pore size distribution helps to increase efficiency.

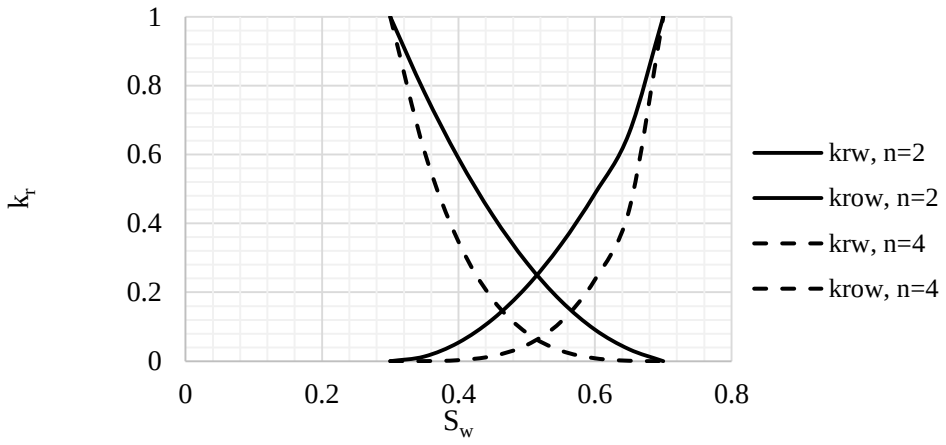

Figure 7.6 Two different pore size distribution.

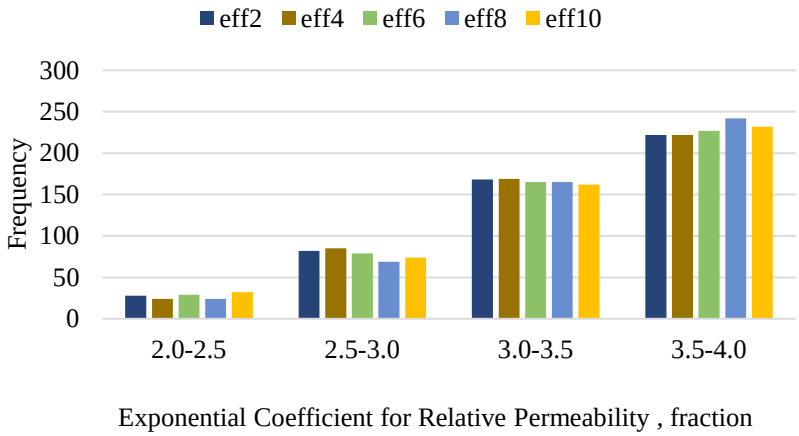

Figure 7.7 Distribution of exponential coefficient for relative permeability for best 500 cases.

According to Corey's equations, capillary pressure and coefficients are directly proportional. As seen in Figure 7.8, to extract water from the pores, more pressure is needed and this means, oppositely, oil can flow more easily in the pores. However, the histogram show that the effect of them is very small for the efficiencies (Figure 7.9).

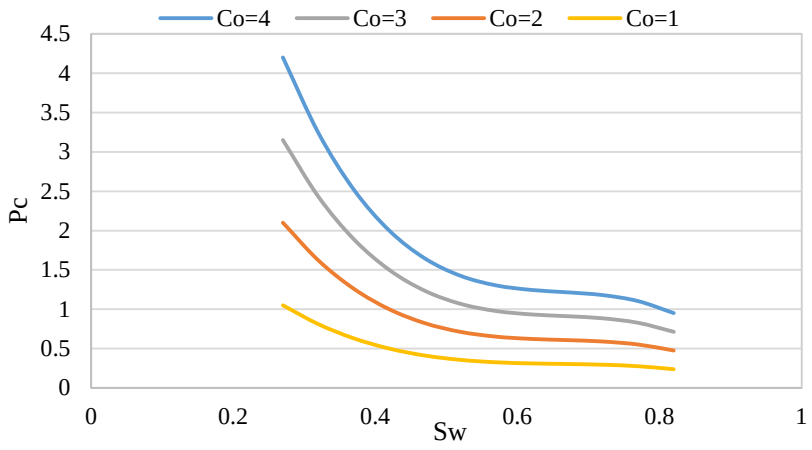

Figure 7.8 Capillary pressure vs. water saturation graph for different capillary pressure coefficients of oil

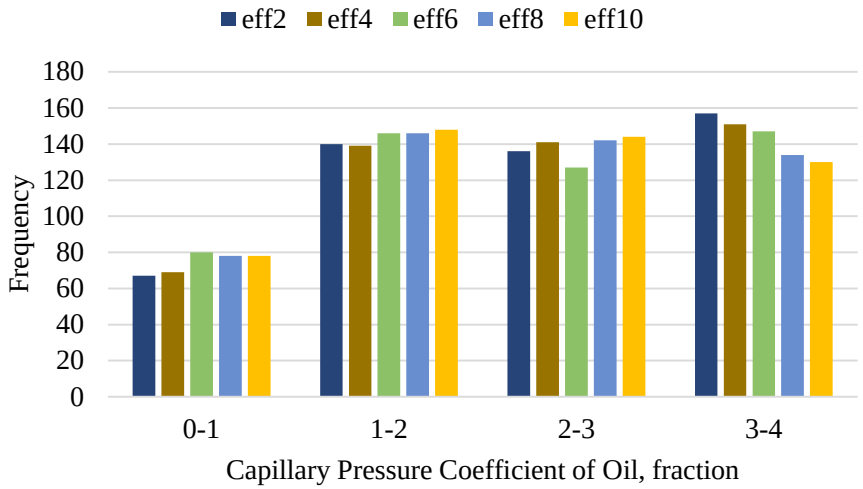

Figure 7.9 Distribution of capillary pressure coefficient of oil for best 500 cases.

The ranges for operation parameters were determined after detailed literature review. Therefore, all values were optimum and distributed uniformly. The distribution of steam temperature, steam quality and soaking time can be seen in Figure 7.10 – 12.

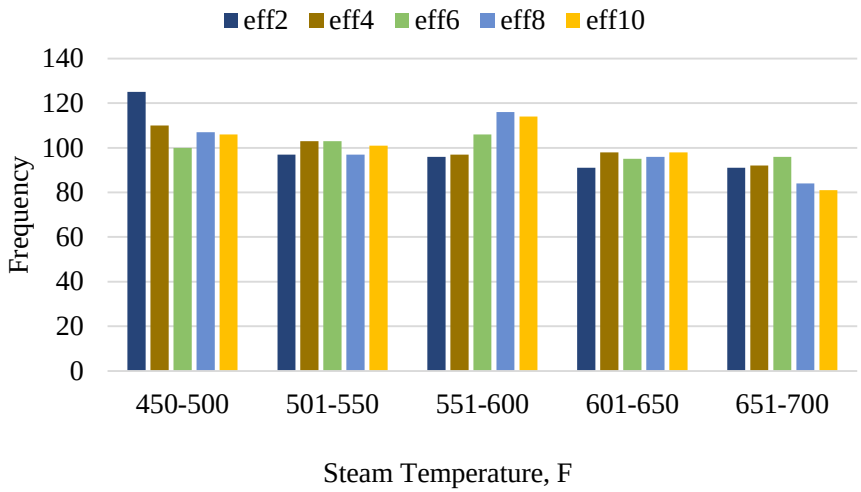

Figure 7.10 Distribution of steam temperature for best 500 cases.

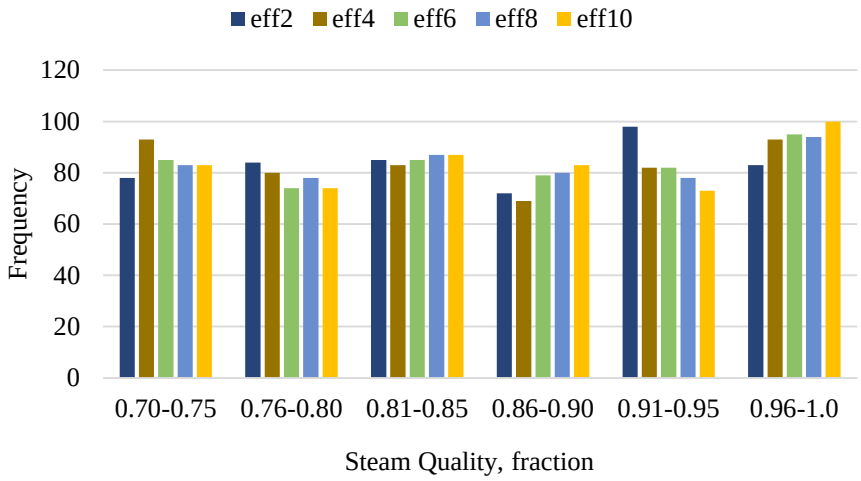

Figure 7.11 Distribution of steam quality for best 500 cases.

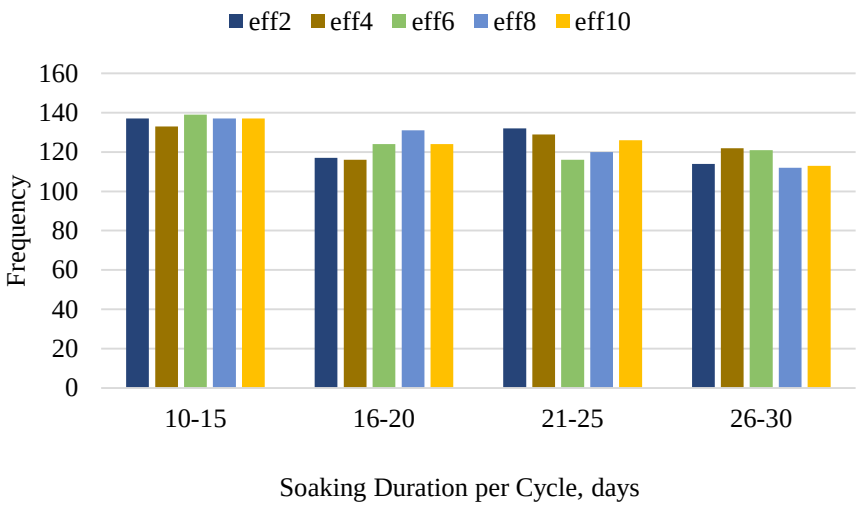

Figure 7.12 Distribution of soaking duration per cycle for best 500 cases.

For injection duration per cycle, histogram (Figure 7.13) shows that cases with less injection time have high performance with cyclic steam injection process in 2 years period of time. When the operation time increases to 6 and more years, the effect of the parameter decreases.

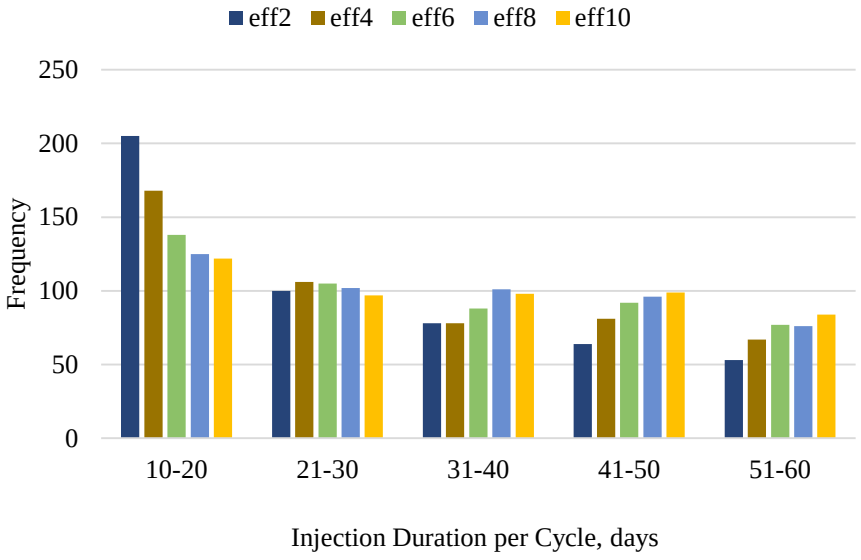

Figure 7.13 Distribution of injection duration per cycle for best 500 cases.

7.2 Accuracy of the Screening Tool

Development of the screening tool is the most important part of this thesis and the stages are given in the previous chapter in detail. By using different number of hidden neurons and hidden layers, trial and error method is applied and the most appropriate structures for ANN models are determined as in Table 7.1.

Table 7.1 Determined number of neurons and hidden layer for all models.

ANN Model	# of hidden neurons		Regressions		
	Layer 1	Layer 2	Training	Validation	Testing
1 – EFF10	50	10	0.977	0.932	0.931
2 – EFF8	40	-	0.959	0.901	0.917
3 – EFF6	30	10	0.941	0.865	0.894
4 – EFF4	30	10	0.967	0.870	0.905
5 – EFF2	30	10	0.974	0.894	0.933

Prediction capabilities of ANN models were assessed by comparing numerical model outputs with ANN model outputs. The comparison graphs for testing data set of ANN models can be seen in Figures 7.14 to 7.18. The darker line shows the numerical model outputs and the lighter one is data-driven model outputs. The overlapping of these two lines shows that the models can predict the efficiency values as much as precise.

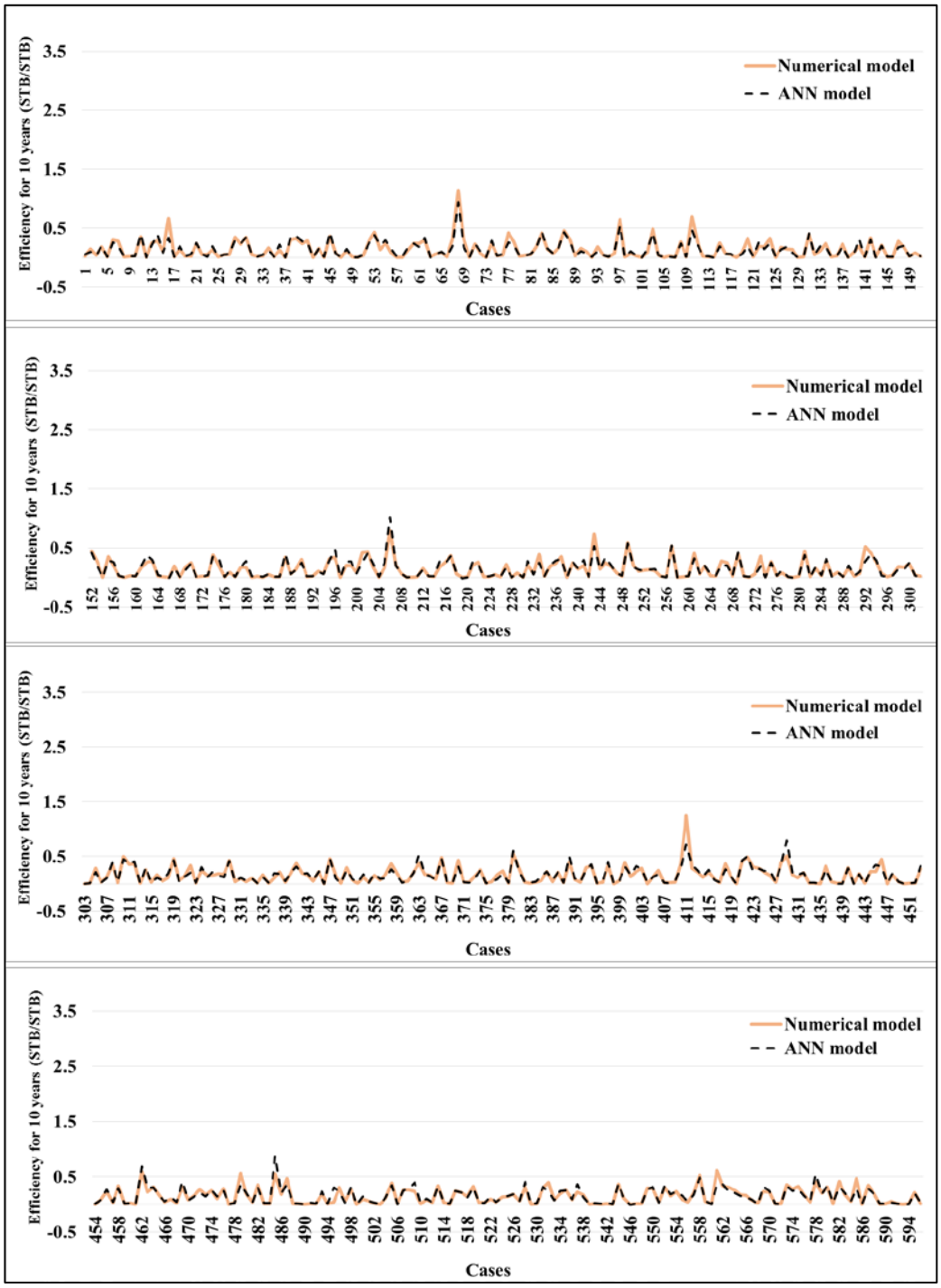

Figure 7.14 The comparison of original output and ANN output for testing data set of Model – 1.

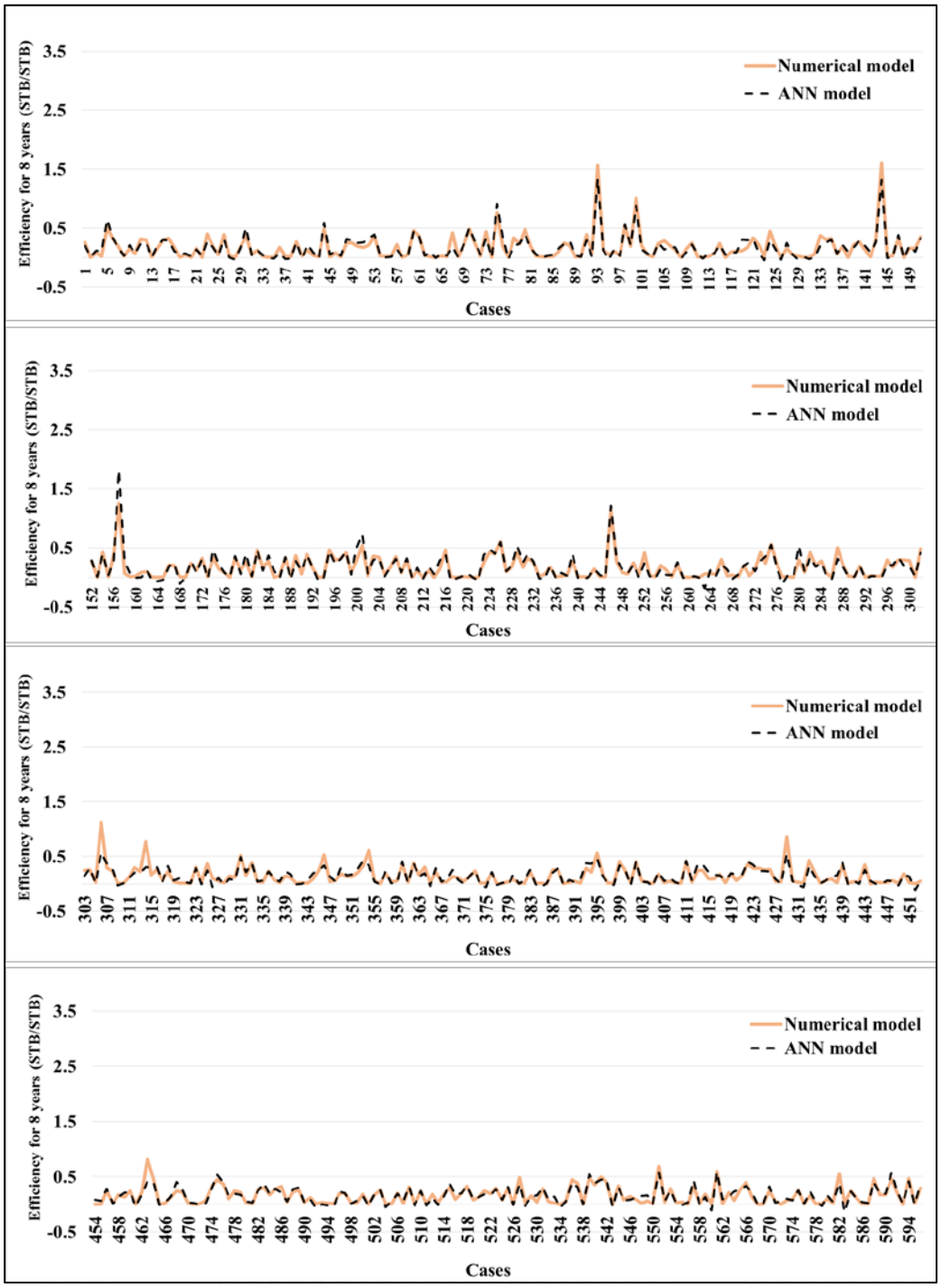

Figure 7.15 The comparison of original output and ANN output for testing data set of Model – 2.

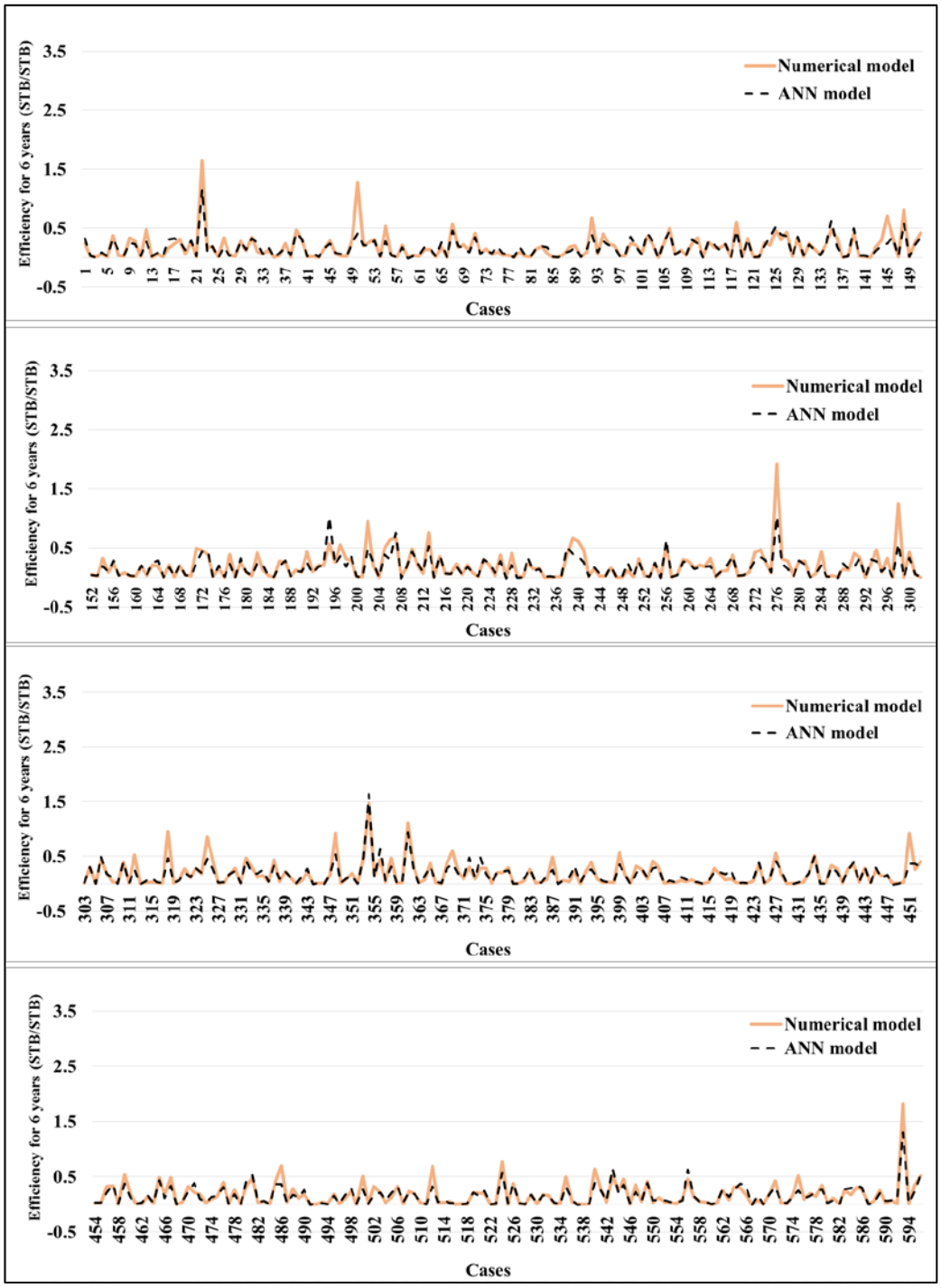

Figure 7.16 The comparison of original output and ANN output for testing data set of Model – 3.

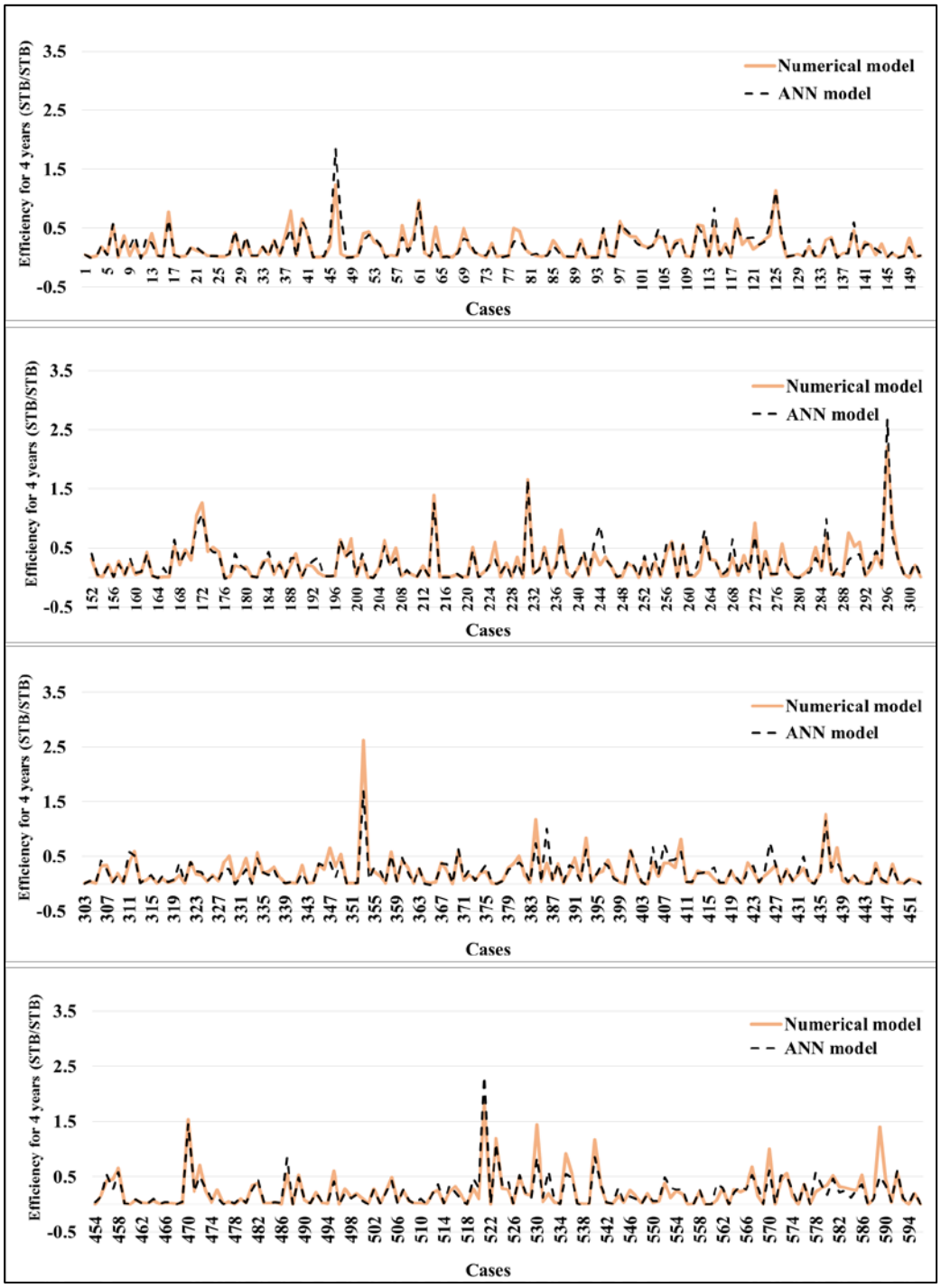

Figure 7.17 The comparison of original output and ANN output for testing data set of Model – 4.

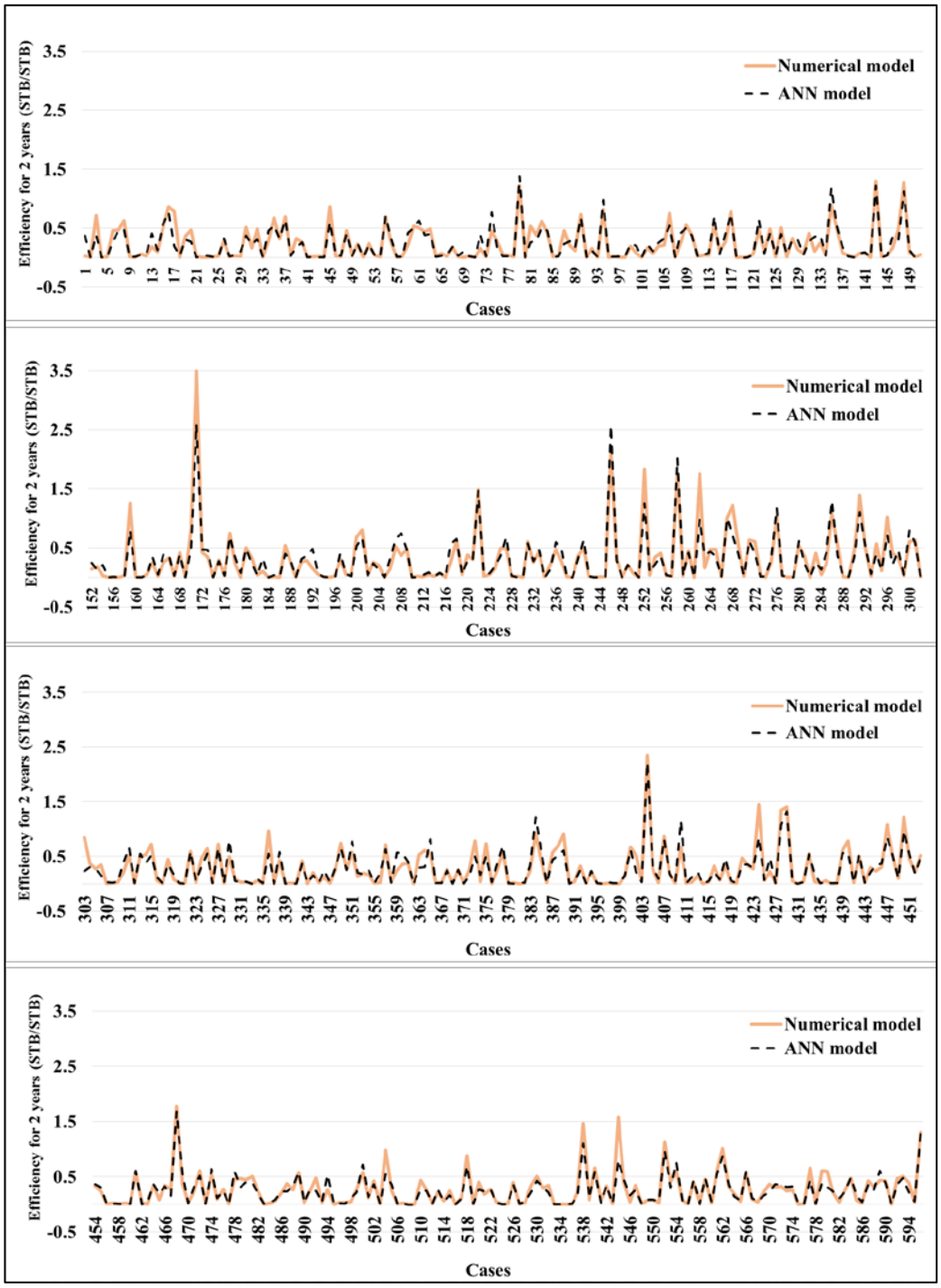

Figure 7.18 The comparison of original output and ANN output for testing data set of Model – 5.

The error of prediction for each case was calculated by taking absolute difference between numerical simulator output and ANN output (Equation 7.1). In order to analyze the error distribution in testing data set, the frequency percentages of error were plotted (Equation 7.2). Figure 7.19 shows that for each model, only 10% of cases have higher than 0.2 STB/STB absolute difference error. If all testing data set is examined, this number can be considered as high error. However, checking errors for each case, especially peak values, would be more realistic. For instance, the efficiency of case 171 in Model – 5 (Figure 7.18) is calculated as 3.50 STB/STB from the numerical model and estimated as 2.60 STB/STB from the ANN model. For this case, 0.9 STB/STB absolute difference error can be ignored and the prediction can be considered as sufficient.

$$\text{Error} = |\text{Eff}_{\text{simulator}} - \text{Eff}_{\text{ANN}}| \tag{7.1}$$

$$\%\text{Error} = \frac{\text{Frequency of Error}}{\text{Total Case Number}} \text{ x } 100 \tag{7.2}$$

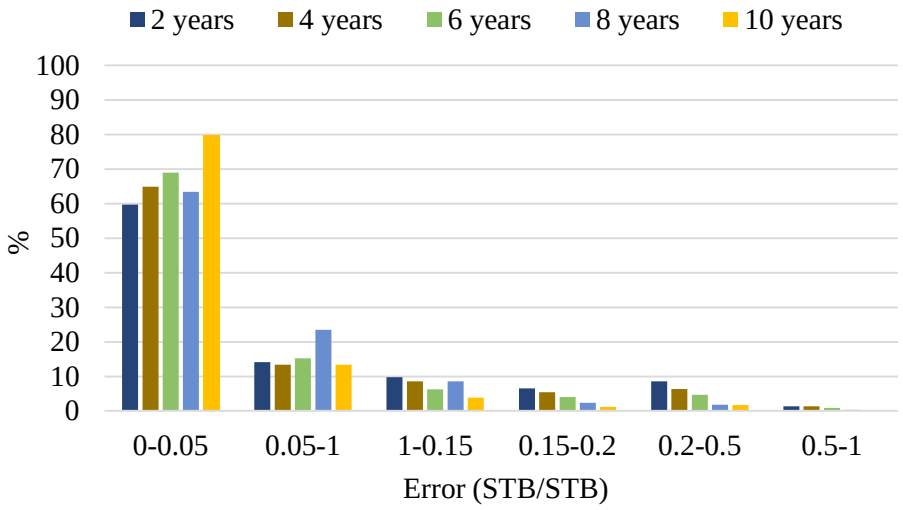

Figure 7.19 Histogram of ANN Model - 5 testing data set.

7.3 Sensitivity to Reservoir and Operational Parameters

The sensitivity study shows the accuracy of the data-driven model by comparing the parametric order with numerical model. The average values of all parameters were used to create a reservoir model, and its efficiency value was taken as a base. 58 cases were constructed by changing one parameter at a time to its maximum and minimum values to analyze each parameter's influence on the efficiency. These cases were run using both the commercial numerical simulator and the screening tool. Parameters were sorted largest to smallest according to their effects on efficiency and tornado charts were plotted for first 15 parameters. (Figure 7.20 – 7.24).

The cases created with lowest values are stated with the lighter bars, and the highest values are the darker ones. By using the results of the data driven model and numerical model, the analyses are performed for all years separately. It is seen that all efficiencies are affected positively by increasing initial oil saturation, irreducible water saturation, the exponential coefficient of relative permeability and decreasing initial water saturation, viscosity coefficients, residual oil saturation. More detailed analyses should be performed for each parameter to examine the exact conclusion about the effects of the parameters. The similarities in the order of the data-driven model and numerical model results show that the screening tool captured the problem very well.

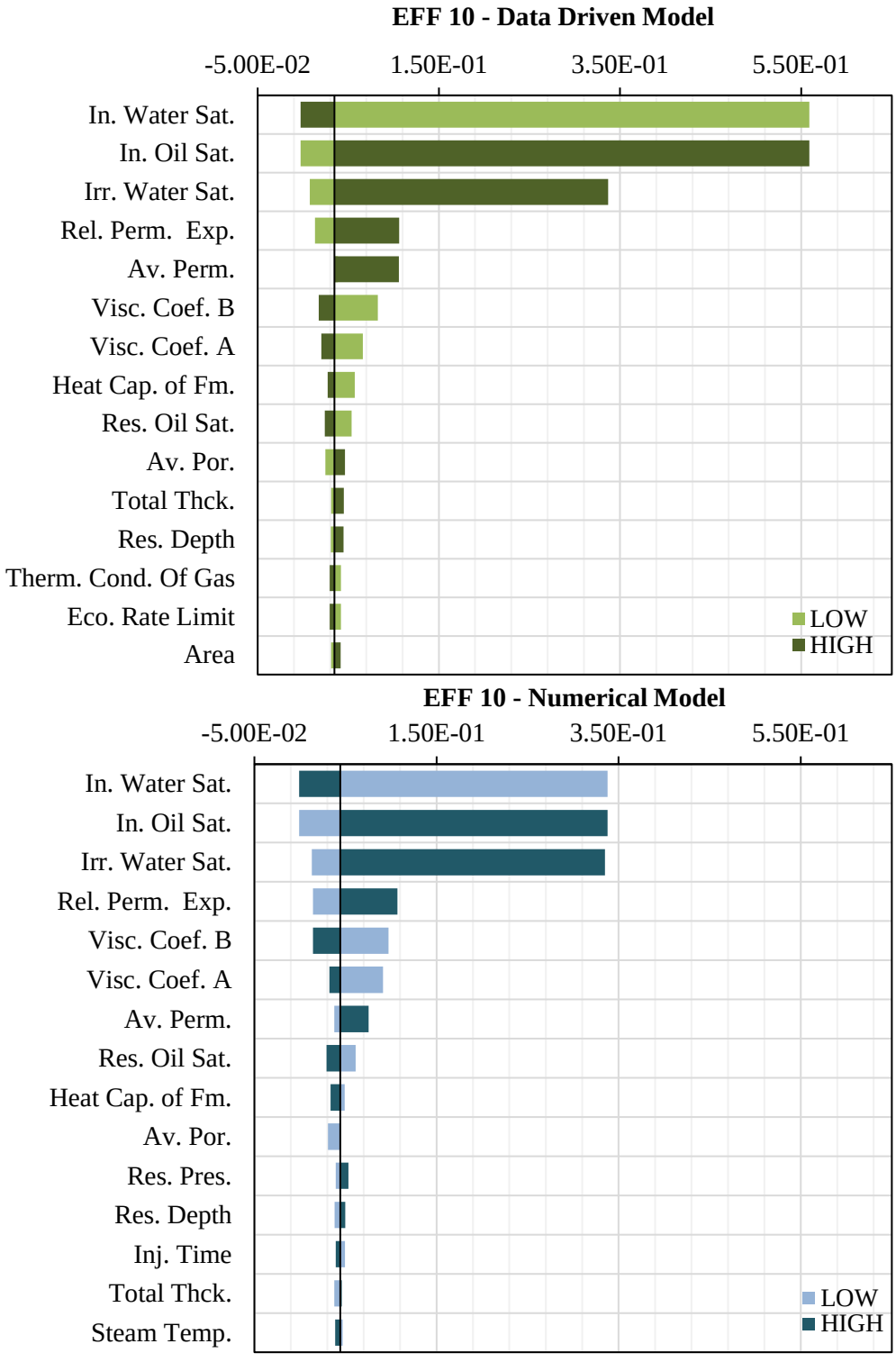

Figure 7.20 Parametric accuracy comparison between Data-driven model and Numerical model for 10 years

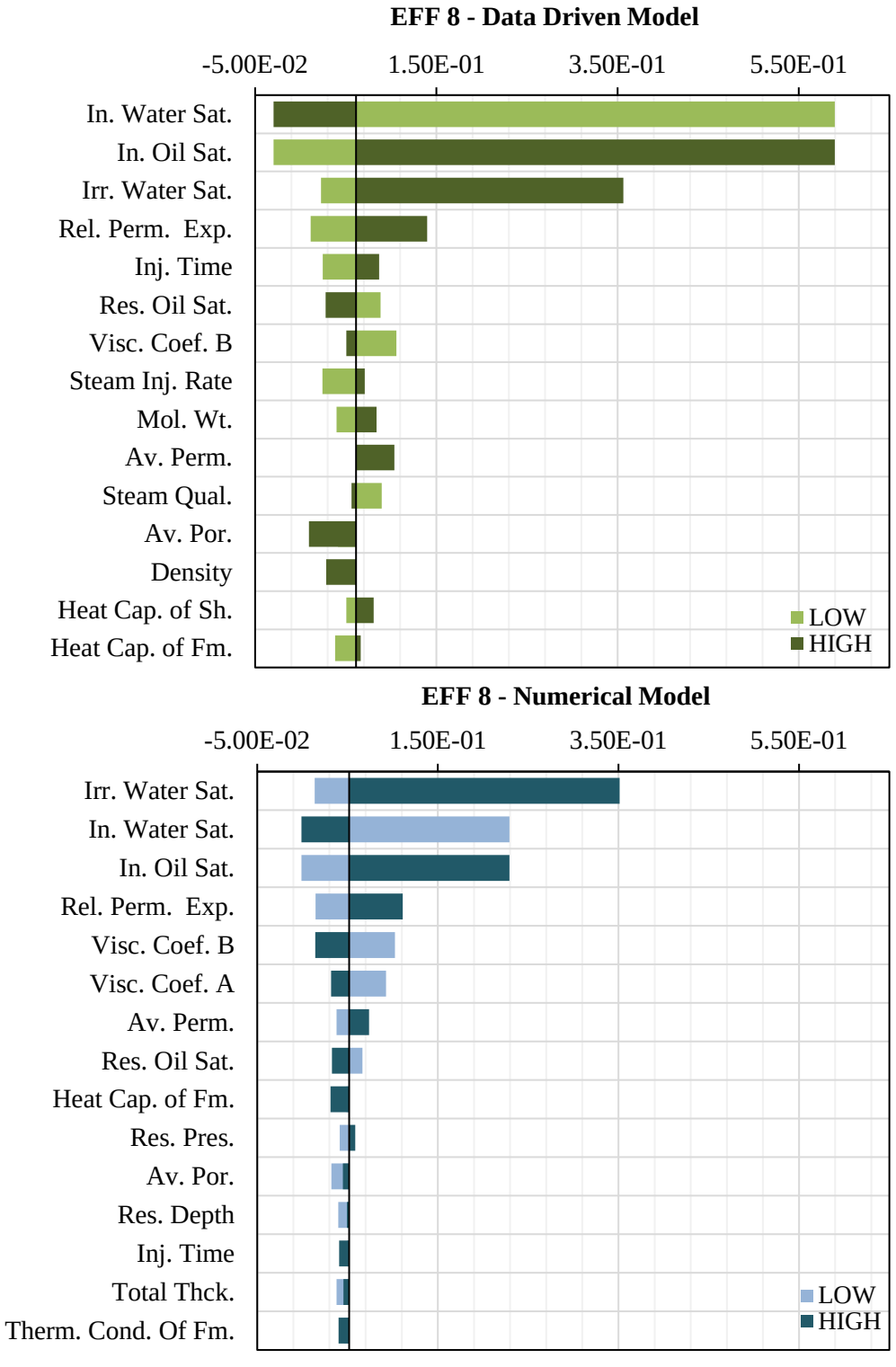

Figure 7.21 Parametric accuracy comparison between Data-driven model and Numerical model for 8 years

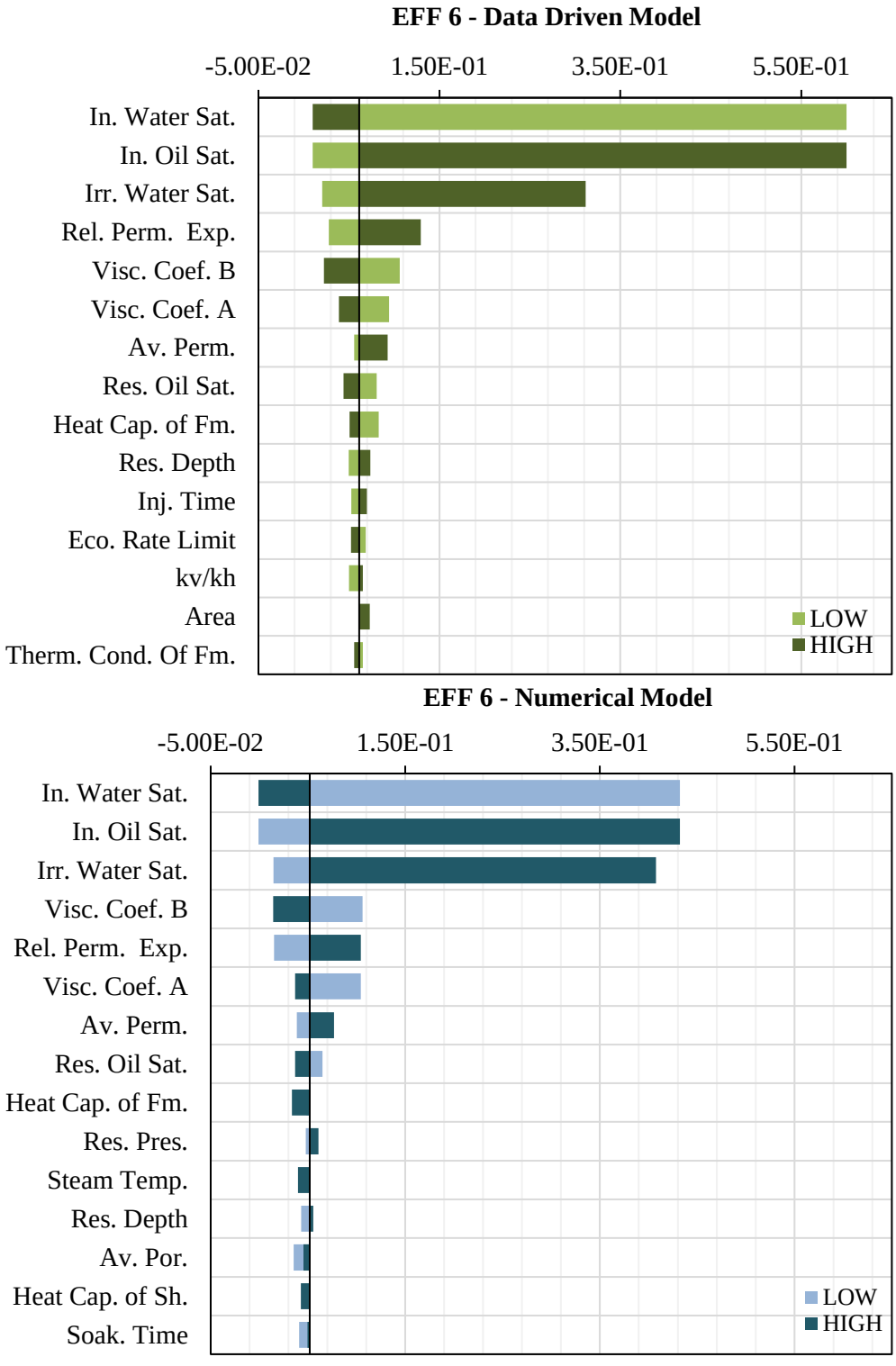

Figure 7.22 Parametric accuracy comparison between Data-driven model and Numerical model for 6 years

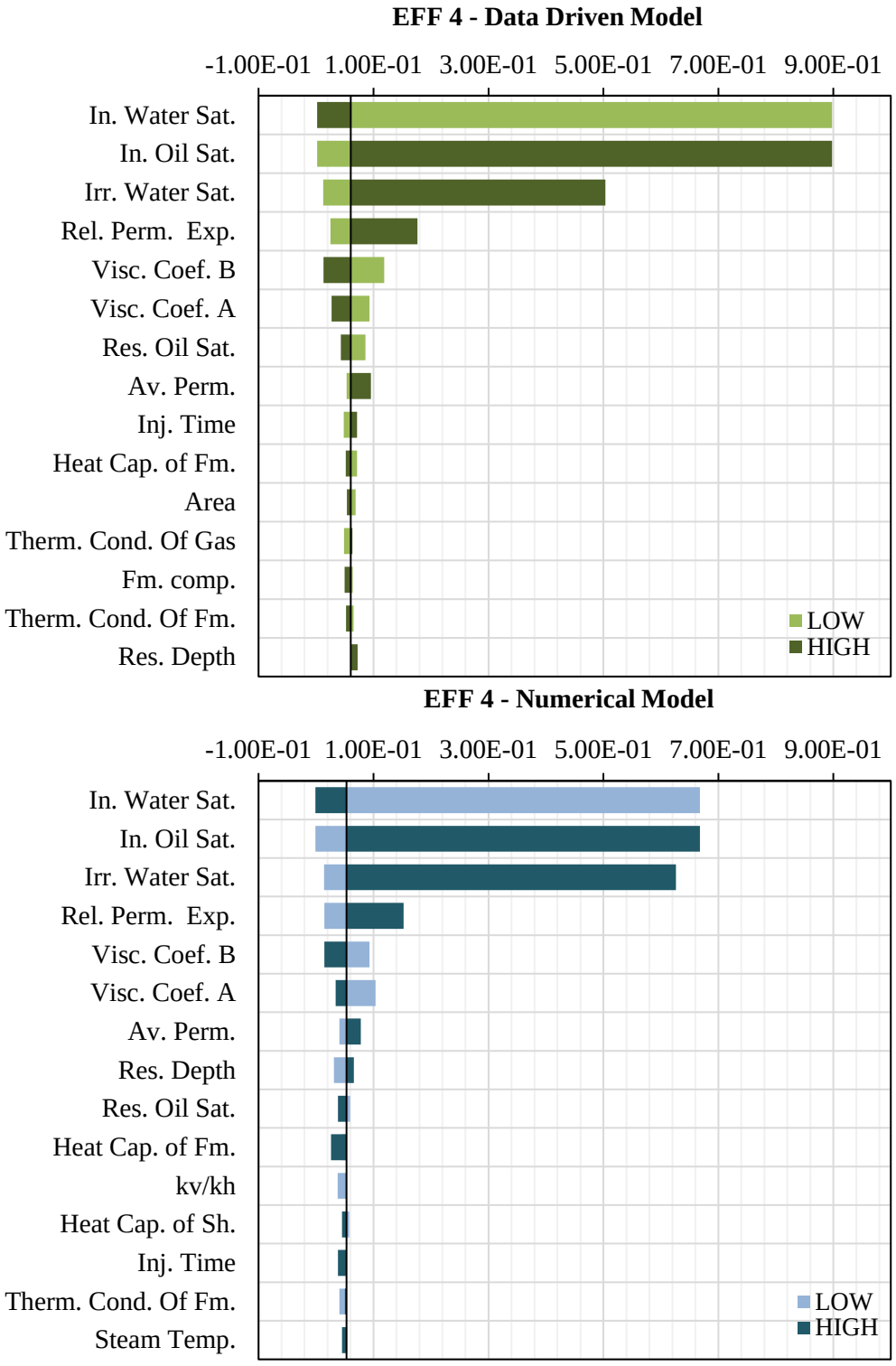

Figure 7.23 Parametric accuracy comparison between Data-driven model and Numerical model for 4 years

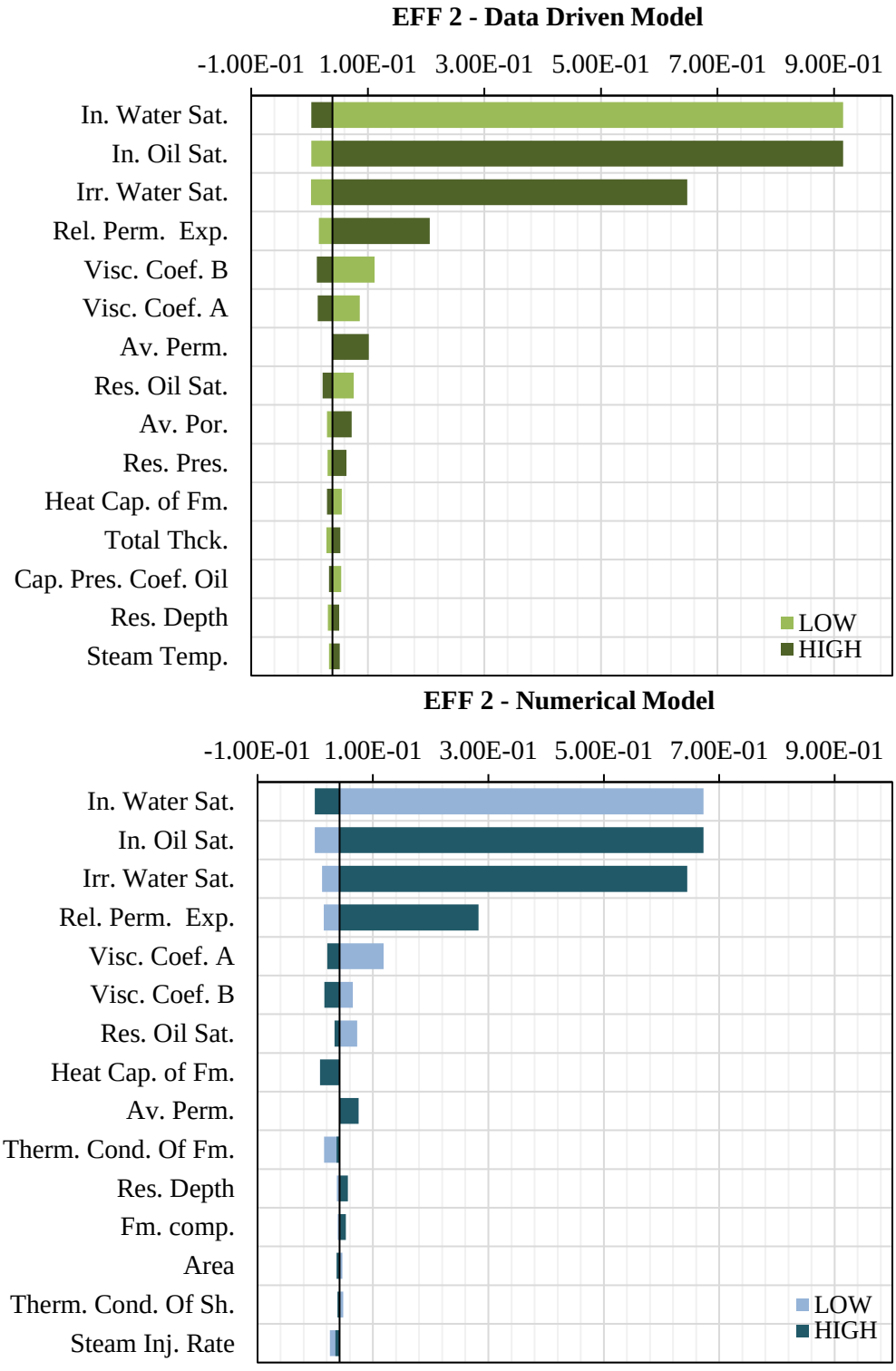

Figure 7.24 Parametric accuracy comparison between Data-driven model and Numerical model for 2 years

7.4 Probabilistic Assessment of CSI in a Given Reservoir

Two studies were conducted separately as an implementation of the screening tool. In each study, 10,000 cases were created and run into the screening tool to produce distributions of possible efficiency values. These probabilistic approaches help to quantify the uncertainty in variables and the risk involved in potential decisions.

a. Specific reservoir parameters:

Different CSI applications in a specific reservoir are analyzed. Reservoir parameters are taken from The Liaohe Oilfield; having a favorable CSI operation in Northeast China (Wang et al., 2017) and operational parameters are selected randomly. Only a few reservoir parameters were out of this study's range; therefore, adjusting them to given ranges did not result in a significant deviation from the reality. Table 7.2 and 7.3 show the reservoir and operational parameters.

Table 7.2 The ranges of the operational parameters of The Liaohe Oilfield (Wang et al., 2017).

Operational Parameters	**Unit**	
Steam temperature	^{o}F	500 – 700
Steam quality	fraction	0.75 – 0.90
Steam injection rate	bbl/day	500 – 700
Injection time	day	10 – 30
Soaking time	day	10 – 20
Economic rate limit	bbl/day	10 – 20

Table 7.3 The values of the reservoir parameters of The Liaohe Oilfield (Wang et al., 2017).

Reservoir Parameters	**Unit**	
Well drainage area	acres	18
Total reservoir thickness	ft	91
Reservoir depth	ft	2863
Anisotropy of permeability	fraction	0.5
Average porosity	fraction	0.29
Average permeability	mD	1644
Rock compressibility	1/psi	1.00E-5
Heat capacity of formation	$Btu/ft^3.F$	36.5
Therm. conductivity of formation	Btu/ft.day.F	24.2
Therm. conductivity of gas	Btu/ft.day.F	0.52
Heat capacity of upper/lower formation	$Btu/ft^3.F$	35
Therm. cond. of upper/lower formation	Btu/ft.day.F	16.9
Molecular weight of oil	lb/lbmole	600
API gravity	API	11.7
Viscosity coefficient A	cp	0.045
Viscosity coefficient B	^oR	6,400
Residual oil saturation	fraction	0.27
Irreducible water saturation	fraction	0.30
Relative permeability exponent	unitless	4
Capillary pressure coefficient of oil	unitless	2.3
Capillary pressure coefficient of gas	unitless	0.2
Reservoir pressure	psi	1175
Initial water saturation	fraction	0.32
Lorenz coefficient	fraction	0.054

Due to having limited real production data, one-to-one comparison cannot be made. However, expectation curve shows that the uncertainty in the efficiency of CSI application can be quantified by reading corresponding values for cumulative probabilities of 90%, 50%, and 10%. An example curve can be seen in Figure 7.25. There is a 90% chance that the efficiency for 2 years will be at least 0.570 STB/STB

and a 10% chance that it will be at least 0.880 STB/STB. Probabilities for other models can be seen in Table 7.4.

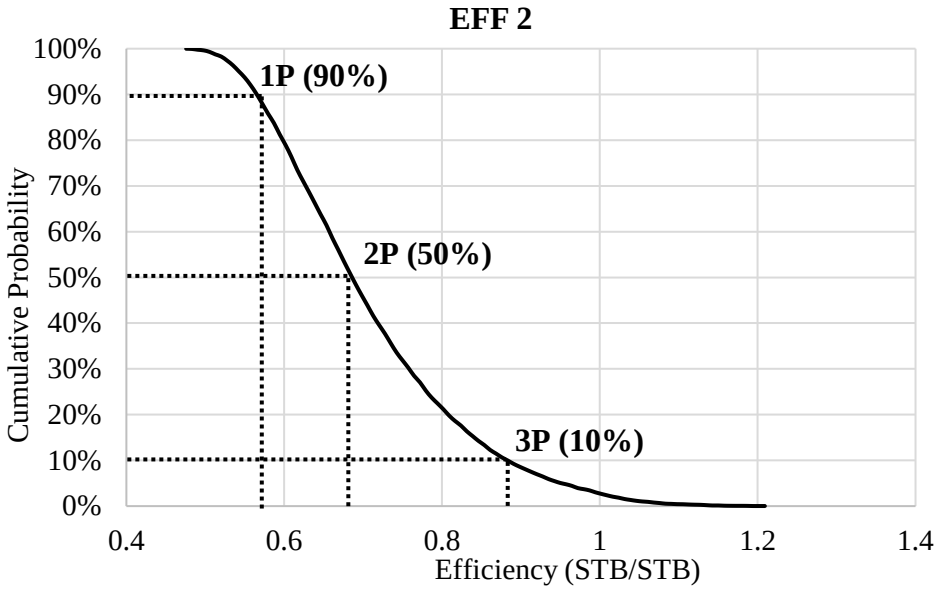

Figure 7.25 Probabilistic estimation of efficiency-2 years for given range operational parameters.

Table 7.4 Yearly probabilistic approach for given range operational parameters.

	1P (90%)	**2P (50%)**	**3P (10%)**
Model 1 (EFF 10)	0.106	0.141	0.170
Model 2 (EFF 8)	0.204	0.242	0.280
Model 3 (EFF 6)	0.178	0.198	0.219
Model 4 (EFF 4)	0.196	0.250	0.355
Model 5 (EFF 2)	0.570	0.690	0.880

By considering economic aspects as well, the efficiency of the CSI process can be interpreted more realistically. Therefore, oil prices and steam prices are included in the efficiency calculations (Equation 7.3). To include both optimistic and pessimistic scenarios, oil and steam prices are selected randomly from 20 to 100 $/bbl and 5 to 15 $/bbl, respectively. Expectation curve indicates that the efficiency of CSI for this reservoir will be 1.90 STB/STB with 90% expectation and 8.70 STB/STB with 10% expectation (Figure 7.26). For all models, Table 7.5 summarizes all results obtained.

$$(\text{EFF\_cost})_n = (\text{EFF})_n \frac{(\text{Oil Price})_n}{(\text{Steam Cost})_n} \tag{7.3}$$

n:2,4,6,8 and 10 years

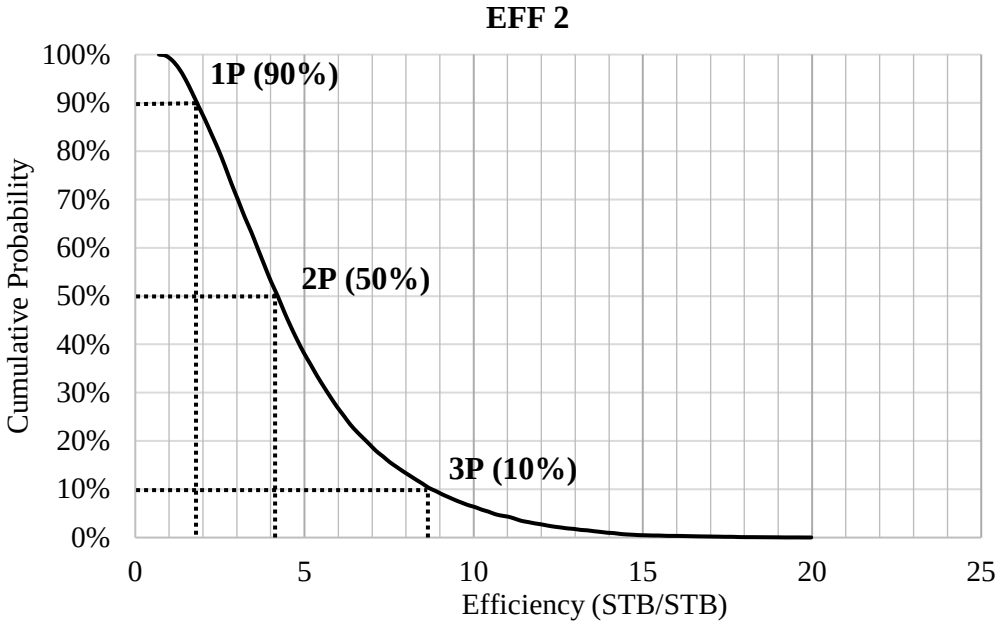

Figure 7.26 Expectation curve for cost-efficiency- 2 years.

Table 7.5 Yearly probabilistic approach with Economic Study-1.

	1P (90%)	**2P (50%)**	**3P (10%)**
Model 1 (EFF 10)	0.35	0.84	1.78
Model 2 (EFF 8)	0.62	1.48	3.00
Model 3 (EFF 6)	0.50	1.20	2.50
Model 4 (EFF 4)	0.68	1.51	3.30
Model 5 (EFF 2)	1.90	4.20	8.70

b. Reservoir parameters in a range:

In this part of the study, it is considered as if there is uncertainty in reservoir parameters of a specific field and they were selected from a narrow range. For instance, a general range for the area is between 5 and 30 acres in the screening tool. The drainage area is known as around 18 acres, but it is not certain. A narrow range is selected as from 15 to 20 acres. For all reservoir parameters, the same idea is applied, and 10,000 cases are created according to narrow ranges. Same CSI operation was applied to all cases by using constant operational parameters. Expectation curve and probabilities for all models can be seen in Figure 7.27 and Table 7.6, respectively.

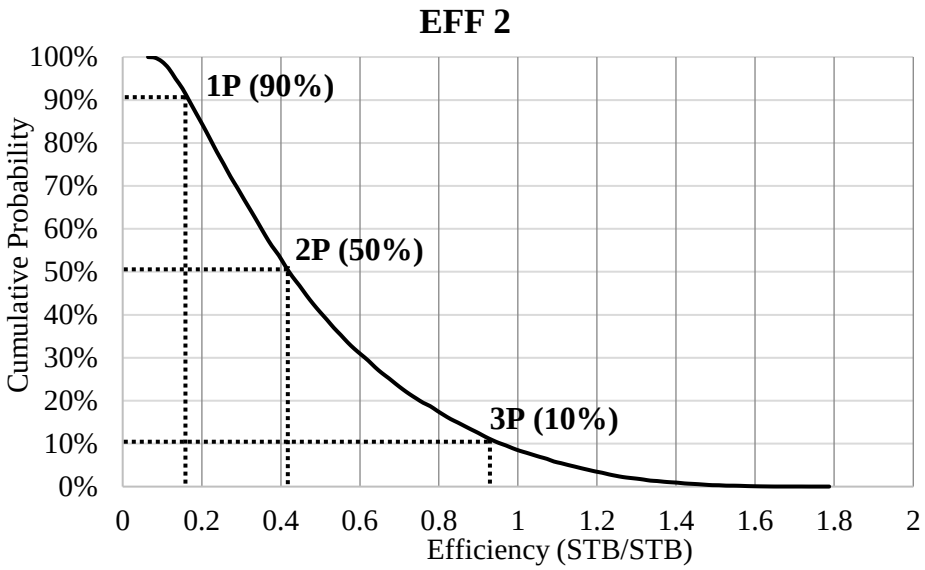

Figure 7.27 Probabilistic estimation of efficiency-2 years for given range reservoir parameters.

Table 7.6 Yearly probabilistic approach for given range reservoir parameters.

	1P (90%)	**2P (50%)**	**3P (10%)**
Model 1 (EFF 10)	0.030	0.060	0.100
Model 2 (EFF 8)	0.045	0.095	0.175
Model 3 (EFF 6)	0.085	0.122	0.170
Model 4 (EFF 4)	0.080	0.140	0.270
Model 5 (EFF 2)	0.170	0.420	0.940

Table 7.7 shows probabilistic estimates of efficiencies when prices are also considered.

Table 7.7 Yearly probabilistic approach with Economic Study-2.

	1P (90%)	**2P (50%)**	**3P (10%)**
Model 1 (EFF 10)	0.11	0.34	0.84
Model 2 (EFF 8)	0.20	0.55	1.40
Model 3 (EFF 6)	0.31	0.75	1.60
Model 4 (EFF 4)	0.35	0.88	2.21
Model 5 (EFF 2)	0.80	2.50	7.50

These examples illustrate the practicality of the screening tool that was developed. A large range of uncertainties can be incorporated easily which would help to understand the risks involved in the CSI application in a given reservoir.

7.5 Graphical User Interface Application

The calculation of efficiency for five different time periods in one ANN model is a complex problem; therefore, in order to avoid complexity, five different ANN models for each time periods are created. Thus, the models with one output can be trained without problems and they can be used to predict the efficiencies more accurately. However, by using these models, finding the efficiencies is not a user friendly system. Creating a graphical user interface (GUI) is a convenient way of increasing the practicality of the models. Five models are combined in a screening tool GUI by using in-built functions of MATLAB (R2013a).

In this chapter, features of this GUI application are presented which includes both deterministic and probabilistic approaches:

Deterministic Approach is based on certain values (best estimates) for each parameter of a given reservoir and a given set of operational parameters.

Probabilistic Approach is based on a range of values for each parameter of a given reservoir and a given set of operational parameters. Since uncertainty in parameters is taken into account, this approach gives more realistic results compared to deterministic approach, by quantifying the uncertainty.

In the screening tool, 23 reservoir, 6 operational and 2 economical parameters can be entered as inputs, besides, there are two options for thickness, porosity and permeability parameters. While these parameters can be specified for each layer with “Layer by Layer Values” option, they can also be defined as total thickness, average porosity and permeability, and Lorenz coefficient with “Total/Average Values” option (Figure 7.28).

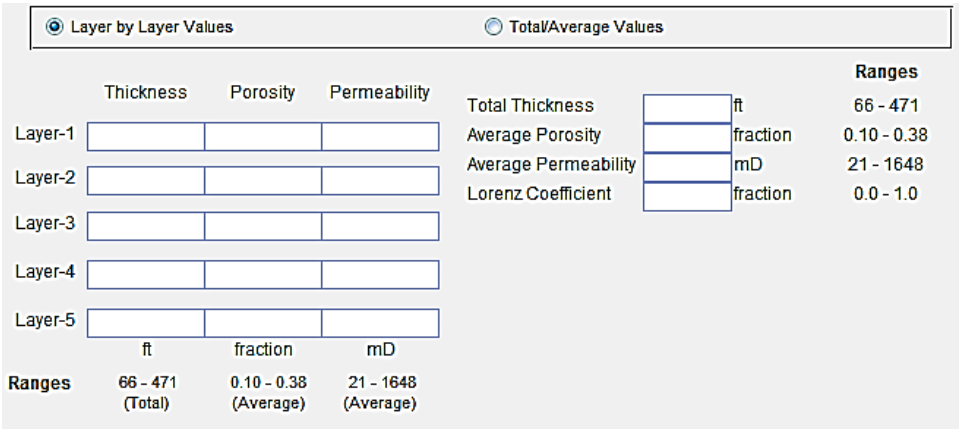

Figure 7.28 Specification of thickness, porosity and permeability for deterministic approach.

In “Layer by Layer Values” option, by taking two or more layers as a one layer, system can be adjusted to different numbers of layers as required. For instance, a

two layered system, having 36 and 20 ft thicknesses, can be entered as seen in Figure 7.29. For probabilistic approach, for one to four layered systems, narrow ranges should be specified (Figure 7.30).

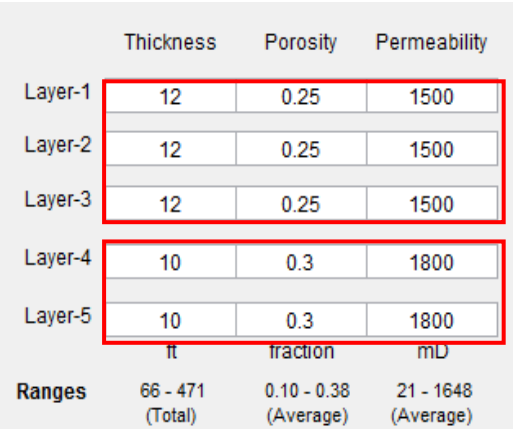

	Thickness	Porosity	Permeability
Layer-1	12	0.25	1500
Layer-2	12	0.25	1500
Layer-3	12	0.25	1500
Layer-4	10	0.3	1800
Layer-5	10	0.3	1800
	ft	fraction	mD
Ranges	66 - 471 (Total)	0.10 - 0.38 (Average)	21 - 1648 (Average)

Figure 7.29 Two layered system for deterministic approach.

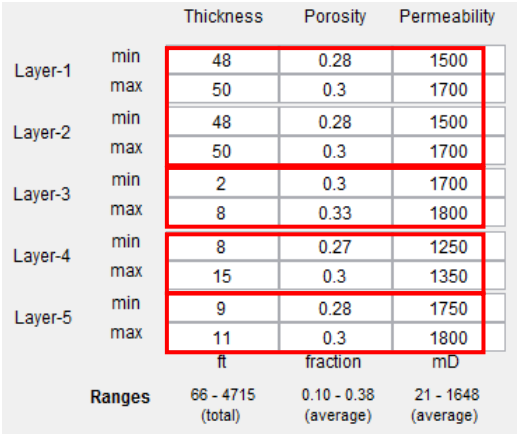

		Thickness	Porosity	Permeability
Layer-1	min	48	0.28	1500
	max	50	0.3	1700
Layer-2	min	48	0.28	1500
	max	50	0.3	1700
Layer-3	min	2	0.3	1700
	max	8	0.33	1800
Layer-4	min	8	0.27	1250
	max	15	0.3	1350
Layer-5	min	9	0.28	1750
	max	11	0.3	1800
		ft	fraction	mD
Ranges		66 - 4715 (total)	0.10 - 0.38 (average)	21 - 1648 (average)

Figure 7.30 Four layered system for probabilistic approach.

Buttons and Their Functions

In deterministic and probabilistic approaches, there are the "Excel" buttons connected to pre-processed Microsoft Excel (2013) file in order to import input data. User can use either this button or GUI screen to enter the input parameters to the tool.

In deterministic approach, one of the "Calculate" buttons is related with viscosity (Figure 7.31). In the tool, to calculate viscosity of oil, viscosity coefficient A and B should be entered. For the one who do not know these values, a viscosity calculation part is created. Proper values can be found with trial and error method by setting the desired viscosity.

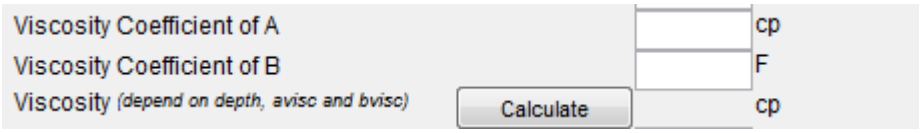

Figure 7.31 Viscosity determination part in deterministic approach.

The other "Calculate" button in deterministic approach is used to calculate efficiencies for five different time periods and to accept or reject a given CSI proposal from a representative performance indicator. By considering oil price and steam cost, certain efficiency values can be obtained. If an economic efficiency is above 1, it is indicating that the income is greater than steam cost. If it is below 1, than the cost is more than the income. The same button is also created in the probabilistic approach. Compared with the deterministic approach, for probabilistic approach, the efficiencies are calculated with 90, 50 and 10% expectations. User can identify all possible scenarios within determined ranges and analyze the performance of CSI process in the selected reservoir.

The last button group is related to the "Expectation curve". There are five different buttons to plot expectation curves for different time periods: 10, 8, 6, 4 and 2 years. When the efficiencies are calculated, the expectation graph for 2 years is plotted as a default. User can plot other curves by selecting the desired time period.

Figure 7.32 and 7.33 indicate example simulations of the tool for The Liaohe Oilfield as deterministic and probabilistic approach, respectively.

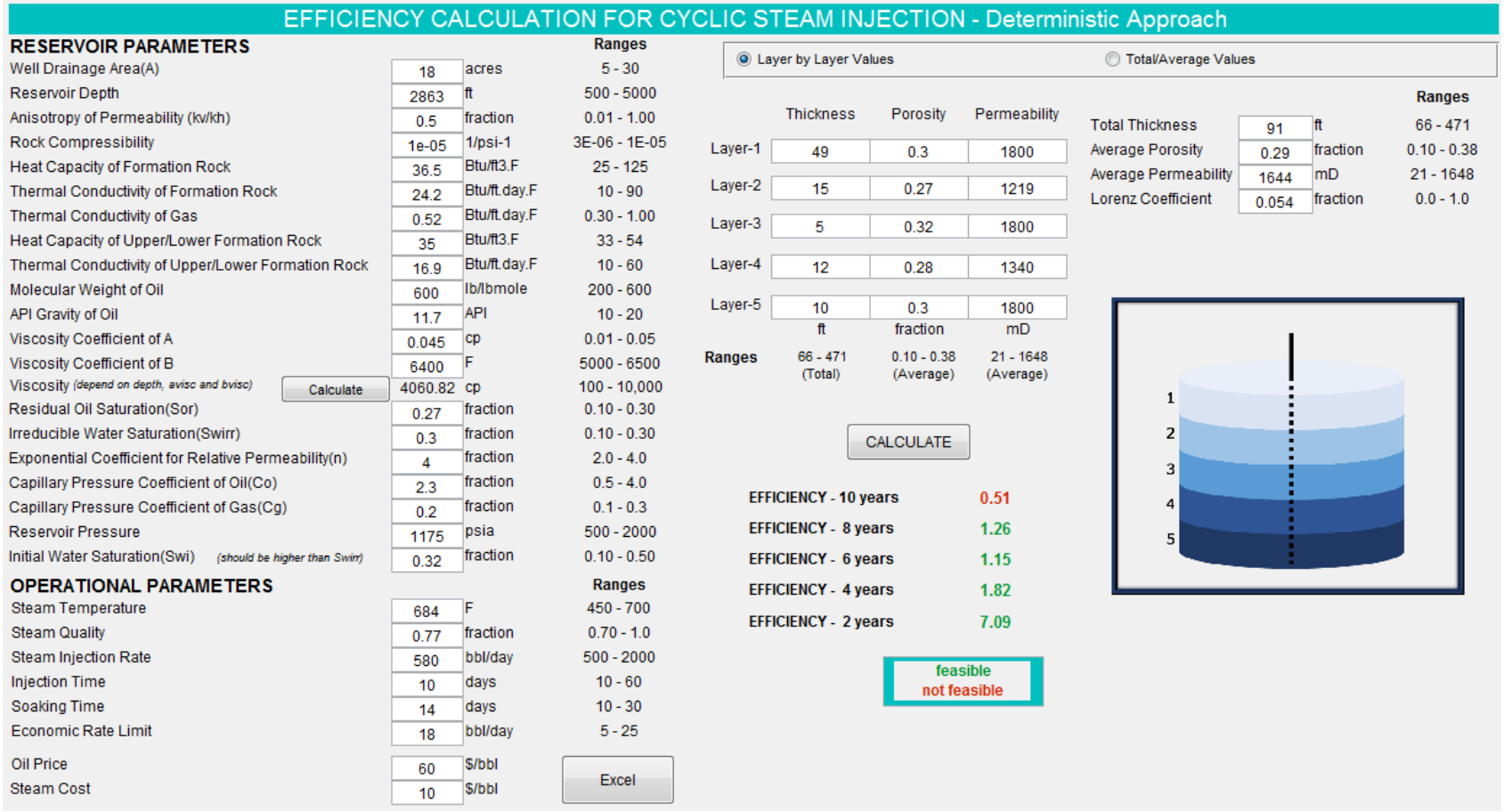

Figure 7.32 Deterministic approach for The Liaohe Oilfield by using the screening tool.

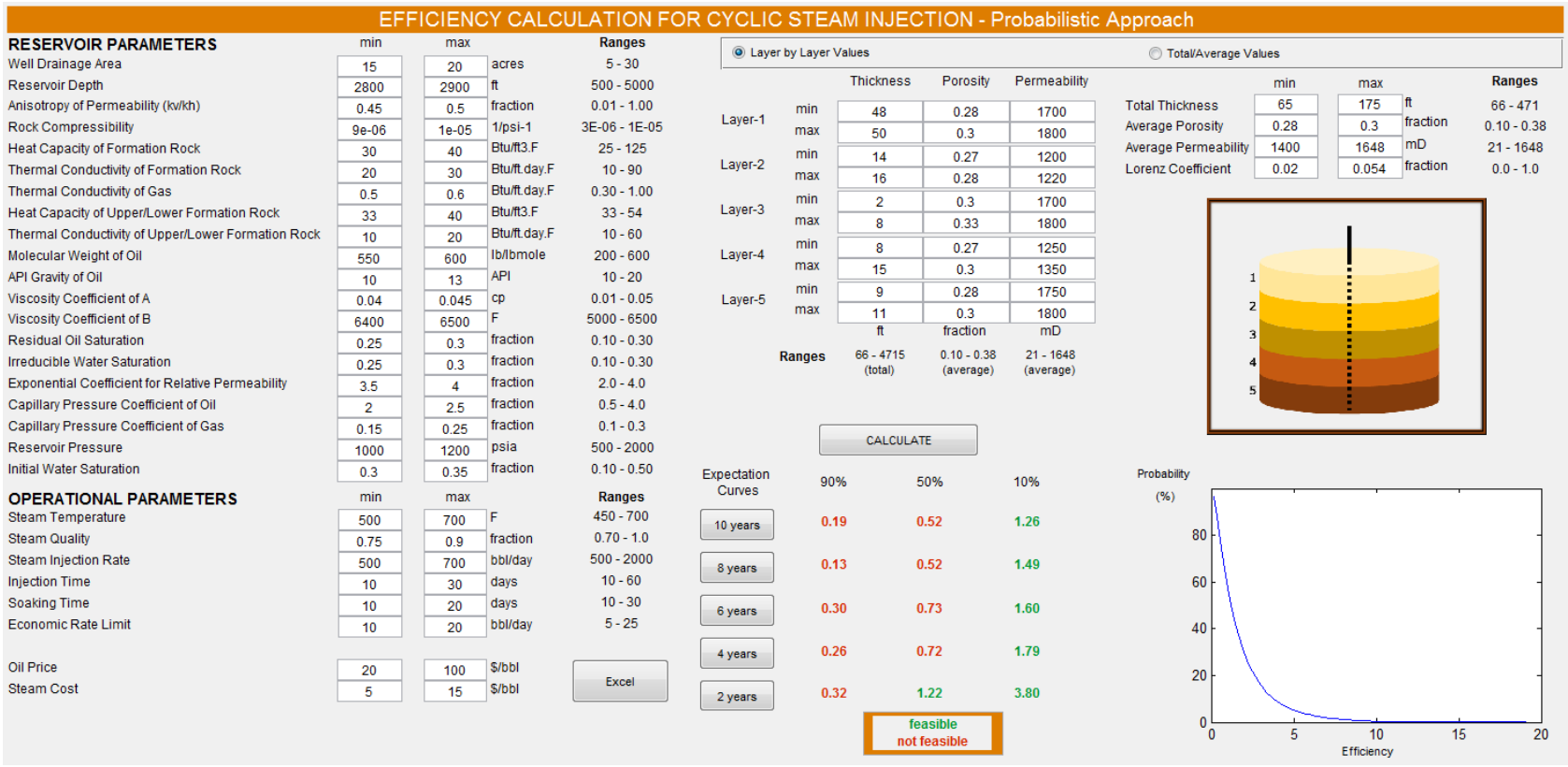

Figure 7.33 Probabilistic approach for The Liaohe Oilfield by using the screening tool.

CHAPTER 8

CONCLUSIONS

In this study, a five layered heterogeneous reservoir model is constructed using a commercial simulator to study cycle steam injection process. 50 different parameters including capillary pressure, relative permeability and thermal properties are considered. A dataset is created with many different scenarios with different combinations of these parameters with predefined statistical distributions and ranges taken from the literature. After running these scenarios, incremental oil production and incremental steam injection results for 10 years are collected to calculate efficiencies at 2-year intervals. By training and testing with the input parameters and efficiencies, a neural-network based screening tool is developed for estimating the performance of a CSI operation for all kinds of heavy oil reservoirs in a rapid way.

In order to evaluate the effects of the parameters, detailed parametric analyses are performed. After development of the screening tool, a sensitivity study is conducted and the accuracy of the screening tool is evaluated. As a practical example for the screening tool, the Liaohe Oilfield is used and the efficiencies are calculated with both deterministic and probabilistic approaches.

The key conclusions drawn from this study are listed as follows:

1. Five different ANN models are created separately to predict each time period due to the complexity of the building one ANN model with five different time periods. This helped to improve the training performance.
2. To train these models precisely, it is important to distribute the cases uniformly in train, validation and testing sets.

3. With a validation study, performed by comparing screening tool results with simulator results, it is seen that the screening tool captures the flow dynamics of CSI process and can predict the efficiency of any reservoir within the ranges.
4. Selecting the parameters out of the ranges decreases the accuracy of the prediction of efficiencies.
5. The screening tool can output the performance of a selected CSI operation by estimating the efficiency within a reasonable accuracy, eliminating convergence issues with simulators.
6. Significant resources such as manpower, computing and time are not required to use the screening tool.
7. The increase in initial oil saturation, irreducible water saturation and the exponential coefficient of relative permeability increases the efficiencies.
8. The decrease in initial water saturation, residual oil saturation and the viscosity coefficients increases the efficiencies.
9. While soaking time does not affect the efficiency, the increase in injection time affects the efficiencies negatively.
10. Considering oil price and steam cost is important to analyze the efficiency values with a more realistic perspective.

CHAPTER 9

RECOMMENDATIONS FOR FUTURE WORK

This study can be further improved with the following items:

1. Instead of using 10 years production period in simulator model, number of cycles can be considered to run the model.
2. The number of parameters can be decreased and influential parameters can be focused on more effectively.
3. Steam generation options and their costs can be integrated into the screening tool. For example, solar-energy assisted steam generation, a potential application of steam generators for the seasonal availability of the sunlight throughout the year in most parts of the world, can be integrated to the tool by studying the feasibility aspect.
4. For further economic analysis, facility and operational costs can be also incorporated.
5. Optimum operational parameters can be calculated by including an optimization routine in the GUI application.

REFERENCES

Abrahart, R. J., See, L. M., Solomatine, D. P. (2008). Practical hydroinformatics. Chapter 2: Data-driven modelling: Concepts, approaches and experiences. Water Science 17 and Technology Library 68, c Springer-Verlag Berlin Heidelberg 2008.

Adams, R. H., Khan, A. M. (1969). Cyclic steam injection project performance analysis and some results of a continuous steam displacement pilot. Society of Petroleum Engineers. doi:10.2118/1916-PA.

Al-Bulushi, N., Araujo, M., Kraaijveld, M., Jing, X. D. (2007). Predicting water saturation using artificial neural networks (ANNs). Society of Petrophysicists and Well-Log Analysts. 1st Annual Middle East Regional SPWLA Symposium-Abu Dhabi.

Ali, S. M. F. (1974). Current status of steam injection as a heavy oil recovery method. The Journal of Canadian Petroleum Technology. JCPT74-01-06.

Ali, S. M. F. (1994). CSS – Canada's super strategy for oil sands. The Journal of Canadian Petroleum Technology. JCPT94-09-01.

Ali, S. M. F., Jones, J., Meldau, R. F. (1997). Practical Heavy Oil Recovery. Chapter 6, pp 6-5.

Arpaci, B. (2014). Development of an artificial neural network for cyclic steam stimulation method in naturally fractured reservoirs. Master's Thesis, The Pennsylvania University.

Artun, E. (2008). Optimized design of cyclic pressure pulsing in naturally fractured reservoirs using neural-network based proxy models. Ph.D. Thesis, the Pennsylvania State University, University Park, Pennsylvania.

Aziz, K., Ramesh, A. B., Woo, P. T. (1987). Fourth SPE comparative solution project: Comparison of steam injection simulators. Society of Petroleum Engineers. doi:10.2118/13510-PA.

British Petroleum. (2017). BP Statistical Review of World Energy June 2017. London.

Chiou, R. C. S., Murer, T. S. (1989). Cyclic steam pilot in gravity drainage reservoir. Society of Petroleum Engineers. doi:10.2118/SPE-19659-MS.

Chu, C., Tremble, A. E. (1975). Numerical simulation of steam displacement field performance applications. Society of Petroleum Engineers. doi:10.2118/5016-PA.

Counihan, T. M. (1977). A successful in-situ combustion pilot in the Midway-Sunset Field, California. Society of Petroleum Engineers. doi:10.2118/6525-MS.

CMG 2015. CMG STARS Reservoir Simulation Software, Computer Modeling Group Ltd. Calgary, Alberta, Canada.

Dietrich, J. K. (1981). Relative permeability during cyclic steam stimulation of heavy-oil reservoirs. Society of Petroleum Engineers. doi:10.2118/7968-PA.

Dykstra, H., Parsons, R. (1950). The prediction of oil recovery by water flood, secondary recovery of oil in the United States, 2nd ed. American Petroleum Institute.

Eleutherios, L. (2008). Lorenz curve MATLAB code.

Eppelbaum, L., Kutasov I., Pilchin A. (2014). Thermal properties of rocks and density of fluids. Applied Geothermics, Lecture Notes in Earth System Sciences. Chapter 2, pp 99-149.

Faergestad, I. M. (2016). Heavy Oil. The Defining Series. Schlumberger-Oilfield Review.

Fong, W. S., Lederhos, L., Skow, L. A., Evola, G. M., Choi, J. (2001). Analysis of a successful cyclic steam process at Cymric Field, California. Society of Petroleum Engineers. doi:10.2118/69702-MS.

Gael, B. T., Gross, S. J., McNaboe, G. J. (1995). Development planning and reservoir management in the Duri steam flood. Society of Petroleum Engineers. doi:10.2118/29668-MS.

Gontijo, J. E., Aziz, K. (1984). A simple analytical model for simulating heavy oil recovery by cyclic steam in pressure-depleted reservoirs. Society of Petroleum Engineers. doi:10.2118/13037-MS.

Green, D. W., Willhite G.P. (1998). Enhanced Oil Recovery. SPE Textbook Series Volume 6. Chapter 8, pp 310-330.

Hazlett, W. G., Love, C. L., Chona, R. A., Rajtar, J. M. (1997). Simulation of development strategies for a mature Midway-Sunset cyclic-steam project. Society of Petroleum Engineers. doi:10.2118/37552-MS.

Jones, J. (1977). Cyclic steam reservoir model for viscous oil, pressure depleted gravity drainage reservoirs. Society of Petroleum Engineers. doi:10.2118/6544-MS.

Kriesel, D. (2011). A brief introduction to neural networks. In University of Bonn Seminar Proceeding. Chapter 2, pp 13-31.

Kulga, I. B. (2010). Development of an artificial neural network for hydraulically fractured horizontal wells in tight gas sands. Master's Thesis, The Pennsylvania University.

MATLAB R2013a. Matrix Laboratory. The Mathworks Inc. Natick, Massachusetts, United States.

Microsoft Excel (2013). Spreadsheet Software. Microsoft Corporation. Albuquerque, New Mexico, United States.

McCormack, M. P. (1991). Neural networks in the petroleum industry. Research 2: Breakthroughs for the '9Os. Society of Exploration Geophysicists. RE2.1.

Mohammadi, S. S., McCollum, T. J. (1989). Steam-foam pilot project in Guadalupe Field, California. Society of Petroleum Engineers. doi:10.2118/15054-PA.

Mohammadi, S. S., Van Slyke, D. C., Ganong, B. L. (1989). Steam-foam pilot project in Dome-Tumbador, Midway-Sunset Field. Society of Petroleum Engineers. doi:10.2118/16736-PA.

Mongy, M. A., Shedid, S. A. (2015). Feasibility of cyclic and continuous steam injections into a Middle-Eastern heavy oil reservoir: A simulation approach. Society of Petroleum Engineers. doi:10.2118/175741-MS.

Offeringa, J. (1971). A mathematical model of cyclic steam injection. World Petroleum Congress. 8th World Petroleum Congress, June, Moscow, USSR.

Ozkan, E., Sarica, C., Haci, M. (1999). Influence of pressure drop along the wellbore on horizontal-well productivity. Society of Petroleum Engineers. 25502-MS.

Parada, C. H. (2008). An artificial neural network based tool-box for screening and designing improved oil recovery methods. Ph.D. Thesis, The Pennsylvania State University, University Park, Pennsylvania.

Pascual, M. R. (2001). Cyclic steam injection pilot, Yacimiento Los Perales. Society of Petroleum Engineers. doi:10.2118/69632-MS.

Pethrick, W. D., Sennhauser, E. S., Harding, T. G. (1988). Numerical modelling of cyclic steam stimulation in Cold Lake oil sands. The Journal of Canadian Petroleum Technology. JCPT88-06-07.

Prats, M. (1982). Thermal Recovery. SPE Monograph Series Vol. 7, pp 227.

Razavi, S. D., Kharrat, R. (2009). Application of cyclic steam stimulation by horizontal well in Iranian heavy oil reservoirs. Sharif University of Technology. Scientia Iranica. Vol. 16, No.2, pp 125-139.

Salazar, A., Sanchez, N., Martinez, C., Colonomos, P. (1987). Simulation of field results of cyclic steam/gas injection in the Bolivar Coast, Western Venezuela. Society of Petroleum Engineers. doi:10.2118/16732-MS.

Saripalli, H. K., Salari, H., Saeedi, M., Hassanzadeh, H. (2017). Analytical modelling of cyclic steam stimulation (CSS) process with a horizontal well configuration. The Canadian Journal of Chemical Engineering. Volume 96, Issue 2, pp 573-589.

Schön, J. H. (2011). Handbook of Petroleum Exploration and Production: Physical properties of rocks a workbook. Volume 8, pp 343-350.

Scott, J. D., Proskin, S. A., Adhikary, D. P. (1994). Volume and permeability changes associated with steam stimulation in an oil sands reservoir. Petroleum Society of Canada. The Journal of Canadian Petroleum Technology. JCPT94-07-06.

Shin, H., Hwang, T., Chon, B. (2012). Optimal grid system design for SAGD simulation. Society of Petroleum Engineers. doi:10.2118/157900-MS.

Shokir, E. M. E.-M., Goda, H. M., Sayyouh, M. H., Fattah, K. A. (2002). Selection and evaluation EOR method using artificial intelligence. Society of Petroleum Engineers.

Silpngarmlers, N., Guler, B., Ertekin, T., Grader, A. S. (2002). Development and testing of two-phase relative permeability predictors using artificial neural networks. Society of Petroleum Engineers. doi:10.2118/79547-PA.

Singh, S. (2005). Permeability prediction using artificial neural network (ANN): A case study of Uinta Basin. Society of Petroleum Engineers. doi:10.2118/99286-STU.

Souraki, Y., Ashrafi, M., Karimaie, H., Torsaeter, O. (2012). Experimental analyses of Athabasca bitumen properties and field scale numerical simulation study of effective parameters on SAGD performance. Energy and Environment Research, Vol. 2, No. 1, pp. 140–156.

Sun, Q., Ertekin, T. (2015). The development of artificial-neural-network-based universal proxies to study steam assisted gravity drainage (SAGD) and cyclic steam stimulation (CSS) processes. Society of Petroleum Engineers. doi:10.2118/174074-MS.

Sun, Q., Ertekin, T. (2016). Structuring an artificial intelligence based decision making tool for cyclic steam stimulation processes. Journal of Petroleum Science and Engineering, Volume 154, June 2017, pp 564-575

Taber, J. J., Martin, F. D., Seright, R. S. (1997). EOR Screening Criteria Revisited - Part 1: Introduction to Screening Criteria and Enhanced Recovery Field Projects. Society of Petroleum Engineers. doi:10.2118/35385-PA.

Trebolle, R. L., Chalot, J. P., Colmenares, R. (1993). The Orinoco heavy-oil belt pilot projects and development strategy. Society of Petroleum Engineers. doi:10.2118/25798-MS.

Trujillo Portillo, M. L., Mercado Sierra, D. P., Maya, G. A., Castro Garcia, R. H., Soto, C. P., Perez, H. H., Gomez, V. (2010). Selection methodology for screening evaluation of enhanced-oil-recovery methods. Society of Petroleum Engineers. doi:10.2118/139222-MS.

Wang, Y., Ren S., Zhang L., Peng X., Pei S., Cui G., Liu Y. (2017). Numerical study of air assisted cyclic steam stimulation process for heavy oil reservoirs: Recovery performance and energy efficiency analysis. Fuel 211 (2018) pp 471–483.

Wang, Y., Zhang L., Deng J., Wang Y., Ren S., Hu C. (2017). An innovative air assisted cyclic steam stimulation technique for enhanced heavy oil recovery. Journal of Petroleum Science and Engineering 151 (2017) 254–263.

Wright, W. (2014). Simple equations to approximate changes to the properties of crude oil with changing temperature. Retrieved from: http://www.petroskills.com/blog/entry/crude-oil-and-changing-temperature?page=3#.WJw9_W996M8

Wu, Z., Vasantharajan, S., El-Mandouh, M., Suryanarayana, P. V. (2011). Inflow performance of a cyclic-steam-stimulated horizontal well under the influence of gravity drainage. Society of Petroleum Engineers. doi:10.2118/127518-PA.

APPENDIX A

AN EXAMPLE SIMULATOR TEMPLATE WITH CSI

```
**================  INPUT/OUTPUT CONTROL  ================
RESULTS SIMULATOR STARS
*INTERRUPT *STOP
*TITLE1 'DEVELOPMENT OF A SCREENING MODEL FOR THE CYCLIC STEAM
INJECTION (CSS) PROCESS'
*INUNIT *FIELD   ** output same as input
*OUTPRN *GRID *PRES *SW *SO *SG *TEMP *Y *X *W *SOLCONC *OBHLOSS
*VISO *VISG
*OUTPRN *WELL *ALL
*WRST 200
*WPRN *GRID 200
*WPRN *ITER 200
*WSRF SECTOR TIME
*OUTSRF *GRID *PRES *SO *SG *TEMP

**=============  GRID AND RESERVOIR DEFINITION  =============
*GRID *RADIAL 12 1 5 *RW 0    ** Zero inner radius matches previous treatment
**  Radial blocks:  small near well;  outer block is large
**  well drainage area: 20
*DI *IVAR 1.55 2.39 3.70 5.72 8.85 13.69 21.17 32.74 50.64 78.33 121.14 187.37
*KDIR DOWN
*DJ *CON 360  **  Full circle
*DK *KVAR 4 13 14 82 39
*DEPTH 1 1 1 2495
*POR *KVAR 0.17 0.18 0.24 0.28 0.20
*PERMI *KVAR 239 480 698 38 571
*PERMJ *EQUALSI
*PERMK *EQUALSI  / 2.22
*END-GRID
*ROCKTYPE 1
*CPOR 7.542063e-06
*PRPOR 14.7
*ROCKCP 104
*THCONR 37
*THCONW 8.3
*THCONO 1.60
*THCONG 0.51
*HLOSSPROP  *OVERBUR 38 59  *UNDERBUR 38 59
```

```
** ================== FLUID DEFINITIONS ==================
*MODEL 2 2 2   ** Components are water and dead oil.  Most water
               ** properties are defaulted (=0).  Dead oil K values
               ** are zero, and no gas properties are needed.
*COMPNAME      "Water"    "OIL"
**                -----          -----
   *CMM           18.02          584
   *PCRIT         3206.2         0       ** These four properties
   *TCRIT         705.4          0       ** are for the gas phase.
   *AVG           1.13e-5        0       ** The dead oil component does
   *BVG           1.075          0       ** not appear in the gas phase.
   *MASSDEN       0              62.0
   *CP            0              5.e-6
   *CT1           0              3.94e-4
   *CPL1          0              1
   *AVISC         0              0.02211
   *BVISC         0              6067
*PRSR 14.7
*TEMR 60
*PSURF 14.7
*TSURF 60

** ============== ROCK-FLUID PROPERTIES ==============
*ROCKFLUID
*SWT   **  Water-oil relative permeabilities
**   Sw        Krw         Krow       Pcow
**  ----    --------     -------    -------
    0.25    0.000000    1.000000   9.438175
    0.30    0.000137    0.670959   7.161045
    0.35    0.001964    0.429810   5.489804
    0.40    0.009323    0.259687   4.326815
    0.45    0.028147    0.145385   3.574438
    0.50    0.066320    0.073393   3.135036
    0.55    0.133587    0.031935   2.910968
    0.60    0.241489    0.011022   2.804598
    0.65    0.403306    0.002518   2.718286
    0.70    0.634020    0.000222   2.554394
    0.75    1.000000    0.000000   2.215283
*SLT   **  Liquid-gas relative permeabilities
**   Sl        Krg         Krog       Pcog
**  ----    --------     -------    -------
    0.25    1.000000    0.000000   1.160117
    0.30    0.754187    0.000038   0.945986
    0.35    0.567366    0.000486   0.772615
    0.40    0.417203    0.002212   0.635640
    0.45    0.298681    0.006539   0.530694
    0.50    0.207121    0.015214   0.453413
    0.55    0.138190    0.030386   0.399431
    0.60    0.087904    0.054597   0.364382
```

```
   0.65     0.052635    0.090767    0.343902
   0.70     0.029117    0.142185    0.333624
   0.75     0.014455    0.212505    0.329183
   0.80     0.006135    0.305732    0.326214
   0.85     0.002032    0.426225    0.320351
   0.90     0.000428    0.578684    0.307230
   0.95     0.000030    0.768150    0.282484
   1.00     0.000000    1.000000    0.241748

** ================  INITIAL CONDITIONS  ================
*INITIAL
** Automatic static vertical equilibrium
*VERTICAL *DEPTH_AVE
*REFPRES 1009
*REFBLOCK 1 1 1
*TEMP *CON 96
*SW *CON 0.38
*SO *CON 0.62

** ================  NUMERICAL CONTROL  ================
*NUMERICAL   ** All these can be defaulted.  The definitions
          ** here match the previous data.
*SDEGREE GAUSS
*DTMAX 90
*NORM     *PRESS 200  *SATUR 0.2   *TEMP 180  *Y 0.2   *X 0.2
*RUN

** ==============  RECURRENT DATA  ======================
*DATE 2017 06 01
  *DTWELL 0.01
    ** INJECTOR:  Constant pressure steam injection type
  *WELL 1 'Injector 1' *VERT 1 1
  *INJECTOR *MOBWEIGHT EXPLICIT 'Injector 1'
  *INCOMP WATER  1.0  0.0
  *TINJW 520
  QUAL 0.76
  *OPERATE *MAX *STW   946  CONT      ** Maximum water rate
  *PERFV 'Injector 1'
            1  1000000.00
            2  1000000.00
            3  1000000.00
            4  1000000.00
            5  1000000.00
  ** PRODUCER:  Constant liquid rate type
  *WELL 2 'Producer 1' *VERT 1 1
  *PRODUCER 'Producer 1'
  *OPERATE *MAX *STL    10000  CONT  ** Starting liquid rate
  **          rad  geofac  wfrac  skin
  GEOMETRY  K  0.25  1.0  1.0  0.0
```

```
      PERF      GEO  'Producer 1'
  **   UBA       ff    Status   Connection
     1 1 1      1     OPEN    FLOW-FROM  'SURFACE'  REFLAYER
     1 1 2      1     OPEN    FLOW-FROM  1
     1 1 3      1     OPEN    FLOW-FROM  2
     1 1 4      1     OPEN    FLOW-FROM  3
     1 1 5      1     OPEN    FLOW-FROM  4
ALTER 'Injector 1'
946
SHUTIN 'Producer 1'
OPEN 'Injector 1'
TRIGGER 'produce'
ON_WELL 'Injector 1' STW-CI > 42570
APPLY_TIMES 100 INCREMENT 42570
SHUTIN 'Injector 1'
TRIGGER 'soak'
ON_ELAPSED 'time' treltd > 16
OPEN 'Producer 1'
TRIGGER 'check'
ON_WELL 'Producer 1' STO-RP > 14
TRIGGER 'check2'
ON_ELAPSED 'time' treltd > 1.0
TRIGGER 'inject'
ON_WELL 'Producer 1' STO-RP < 14
SHUTIN 'Producer 1'
OPEN 'Injector 1'
END_TRIGGER
END_TRIGGER
END_TRIGGER
END_TRIGGER
END_TRIGGER
TIME 365
TIME 760
TIME 1095
TIME 1460
TIME 1825
TIME 2190
TIME 2555
TIME 2920
TIME 3285
TIME 3650
STOP
```

APPENDIX B

AN EXAMPLE SIMULATOR TEMPLATE WITHOUT CSI

```
**================  INPUT/OUTPUT CONTROL  ================
RESULTS SIMULATOR STARS
*INTERRUPT *STOP
*TITLE1 'DEVELOPMENT OF A SCREENING MODEL FOR THE CYCLIC STEAM
INJECTION (CSS) PROCESS'
*INUNIT *FIELD   ** output same as input
*OUTPRN *GRID *PRES *SW *SO *SG *TEMP *Y *X *W *SOLCONC *OBHLOSS
*VISO *VISG
*OUTPRN *WELL *ALL
*WRST 200
*WPRN *GRID 200
*WPRN *ITER 200
*WSRF SECTOR TIME
*OUTSRF *GRID *PRES *SO *SG *TEMP

**=============  GRID AND RESERVOIR DEFINITION  =============
*GRID *RADIAL 12 1 5 *RW 0    ** Zero inner radius matches previous treatment
**  Radial blocks:  small near well;  outer block is large
**  well drainage area: 20
*DI *IVAR 1.55 2.39 3.70 5.72 8.85 13.69 21.17 32.74 50.64 78.33 121.14 187.37
*KDIR DOWN
*DJ *CON 360  **  Full circle
*DK *KVAR 4 13 14 82 39
*DEPTH 1 1 1 2495
*POR *KVAR 0.17 0.18 0.24 0.28 0.20
*PERMI *KVAR 239 480 698 38 571
*PERMJ *EQUALSI
*PERMK *EQUALSI  / 2.22
*END-GRID
*ROCKTYPE 1
*CPOR 7.542063e-06
*PRPOR 14.7
*ROCKCP 104
*THCONR 37
*THCONW 8.3
*THCONO 1.60
*THCONG 0.51
*HLOSSPROP  *OVERBUR 38 59  *UNDERBUR 38 59
```

```
** ================== FLUID DEFINITIONS ==================
*MODEL 2 2 2   ** Components are water and dead oil.  Most water
               ** properties are defaulted (=0).  Dead oil K values
               ** are zero, and no gas properties are needed.
*COMPNAME      "Water"    "OIL"
**                -----          -----
   *CMM           18.02          584
   *PCRIT         3206.2         0       ** These four properties
   *TCRIT         705.4          0       ** are for the gas phase.
   *AVG           1.13e-5        0       ** The dead oil component does
   *BVG           1.075          0       ** not appear in the gas phase.
   *MASSDEN       0              62.0
   *CP            0              5.e-6
   *CT1           0              3.94e-4
   *CPL1          0              1
   *AVISC         0              0.02211
   *BVISC         0              6067
*PRSR 14.7
*TEMR 60
*PSURF 14.7
*TSURF 60

** ============== ROCK-FLUID PROPERTIES ==============
*ROCKFLUID
*SWT   **  Water-oil relative permeabilities
**   Sw        Krw         Krow       Pcow
**  ----    --------     -------    -------
    0.25    0.000000    1.000000   9.438175
    0.30    0.000137    0.670959   7.161045
    0.35    0.001964    0.429810   5.489804
    0.40    0.009323    0.259687   4.326815
    0.45    0.028147    0.145385   3.574438
    0.50    0.066320    0.073393   3.135036
    0.55    0.133587    0.031935   2.910968
    0.60    0.241489    0.011022   2.804598
    0.65    0.403306    0.002518   2.718286
    0.70    0.634020    0.000222   2.554394
    0.75    1.000000    0.000000   2.215283
*SLT   **  Liquid-gas relative permeabilities
**   Sl        Krg         Krog       Pcog
**  ----    --------     -------    -------
    0.25    1.000000    0.000000   1.160117
    0.30    0.754187    0.000038   0.945986
    0.35    0.567366    0.000486   0.772615
    0.40    0.417203    0.002212   0.635640
    0.45    0.298681    0.006539   0.530694
    0.50    0.207121    0.015214   0.453413
    0.55    0.138190    0.030386   0.399431
    0.60    0.087904    0.054597   0.364382
```

```
   0.65     0.052635    0.090767    0.343902
   0.70     0.029117    0.142185    0.333624
   0.75     0.014455    0.212505    0.329183
   0.80     0.006135    0.305732    0.326214
   0.85     0.002032    0.426225    0.320351
   0.90     0.000428    0.578684    0.307230
   0.95     0.000030    0.768150    0.282484
   1.00     0.000000    1.000000    0.241748

** ================  INITIAL CONDITIONS  ================
*INITIAL
** Automatic static vertical equilibrium
*VERTICAL *DEPTH_AVE
*REFPRES 1009
*REFBLOCK 1 1 1
*TEMP *CON 96
*SW *CON 0.38
*SO *CON 0.62

** ================  NUMERICAL CONTROL  ================
*NUMERICAL   ** All these can be defaulted.  The definitions
          ** here match the previous data.
*SDEGREE GAUSS
*DTMAX 90
*NORM     *PRESS 200  *SATUR 0.2   *TEMP 180  *Y 0.2   *X 0.2
*RUN

** ==============  RECURRENT DATA  ======================
*DATE 2017 06 01
  *DTWELL 0.01
    ** INJECTOR:  Constant pressure steam injection type
  *WELL 1 'Injector 1' *VERT 1 1
  *INJECTOR *MOBWEIGHT EXPLICIT 'Injector 1'
  *INCOMP WATER  1.0  0.0
  *TINJW 520
  QUAL 0.76
  *OPERATE *MAX *STW   946  CONT      ** Maximum water rate
  *PERFV 'Injector 1'
            1  1000000.00
            2  1000000.00
            3  1000000.00
            4  1000000.00
            5  1000000.00
  ** PRODUCER:  Constant liquid rate type
  *WELL 2 'Producer 1' *VERT 1 1
  *PRODUCER 'Producer 1'
  *OPERATE *MAX *STL    10000  CONT  ** Starting liquid rate
  **          rad  geofac  wfrac  skin
  GEOMETRY  K  0.25  1.0  1.0  0.0
```

```
      PERF      GEO  'Producer 1'
  **  UBA        ff    Status   Connection
     1 1 1      1     OPEN    FLOW-FROM  'SURFACE'  REFLAYER
     1 1 2      1     OPEN    FLOW-FROM  1
     1 1 3      1     OPEN    FLOW-FROM  2
     1 1 4      1     OPEN    FLOW-FROM  3
     1 1 5      1     OPEN    FLOW-FROM  4
SHUTIN 'Injector 1'
OPEN 'Producer 1'
TIME 365
TIME 760
TIME 1095
TIME 1460
TIME 1825
TIME 2190
TIME 2555
TIME 2920
TIME 3285
TIME 3650
STOP
```

APPENDIX C

MATLAB – ANN TRAINING CODE

```
filename='ANN - eff10.xlsx';
sheet=1;
io_all=xlsread(filename,sheet,'D7:BC5970');

%%%%%%%%%%%%%%%%%%%%%%%%%%%%%%%%%%%%
caseno=5964;
ni=36; %number of input neurons
no=1; %number of outputs neurons

%Number of training, validation, testing
ntrain=4772;
nval=596;
ntest=596;

%Number of hidden neurons
numhid=((ni+no)/2)+sqrt(ntrain);
nh1=30;   nh2=10;   nh=nh1+nh2;   % Two hidden layers
year=2;

%Adjustment of training parameters
goal=0.00001;%Accuracy check
epochs=15000;%# of iterations check
max_fail=6;%# of validation check
memoryReduction=2;%Reduction of memory requirements
%%%%%%%%%%%%%%%%%%%%%%%%%%%%%%%%%%%%

%Normalizing Inputs separately
%Grid & Reservoir Parameters
P(1,:)=(io_all(1:caseno,1))';[Pn(1,:),ps(1,:)]=mapminmax(P(1,:),-1,1); %Area
P(2,:)=(io_all(1:caseno,2))';[Pn(2,:),ps(2,:)]=mapminmax(P(2,:),-1,1); %Total Thickness
P(3,:)=(io_all(1:caseno,3))';[Pn(3,:),ps(3,:)]=mapminmax(P(3,:),-1,1); %Reservoir Depth
P(4,:)=(io_all(1:caseno,4))';[Pn(4,:),ps(4,:)]=mapminmax(P(4,:),-1,1); %kv/kh
P(5,:)=(io_all(1:caseno,5))';[Pn(5,:),ps(5,:)]=mapminmax(P(5,:),-1,1); %Average Porosity
P(6,:)=(io_all(1:caseno,6))';[Pn(6,:),ps(6,:)]=mapminmax(P(6,:),-1,1); %Average Permeability
P(7,:)=(io_all(1:caseno,7))';[Pn(7,:),ps(7,:)]=mapminmax(P(7,:),-1,1); %Rock Compressibility
P(8,:)=(io_all(1:caseno,8))';[Pn(8,:),ps(8,:)]=mapminmax(P(8,:),-1,1); %Heat Capacity of Formation
P(9,:)=(io_all(1:caseno,9))';[Pn(9,:),ps(9,:)]=mapminmax(P(9,:),-1,1); %Thermal Conductivity of Formation
P(10,:)=(io_all(1:caseno,10))';[Pn(10,:),ps(10,:)]=mapminmax(P(10,:),-1,1); %Thermal Conductivity of Oil
P(11,:)=(io_all(1:caseno,11))';[Pn(11,:),ps(11,:)]=mapminmax(P(11,:),-1,1); %Thermal Conductivity of Gas
P(12,:)=(io_all(1:caseno,12))';[Pn(12,:),ps(12,:)]=mapminmax(P(12,:),-1,1); %Heat Capacity of Shale
P(13,:)=(io_all(1:caseno,13))';[Pn(13,:),ps(13,:)]=mapminmax(P(13,:),-1,1); %Thermal Conductivity of Shale
%Fluid Parameters
P(14,:)=(io_all(1:caseno,14))';[Pn(14,:),ps(14,:)]=mapminmax(P(14,:),-1,1); %Oil Molecular Weight
P(15,:)=(io_all(1:caseno,15))';[Pn(15,:),ps(15,:)]=mapminmax(P(15,:),-1,1); %Oil Mass Density
P(16,:)=(io_all(1:caseno,16))';[Pn(16,:),ps(16,:)]=mapminmax(P(16,:),-1,1); %Oil Specific Gravity
```

```
P(17,:)=(io_all(1:caseno,17))';[Pn(17,:),ps(17,:)]=mapminmax(P(17,:),-1,1); %Oil API Gravity
P(18,:)=(io_all(1:caseno,18))';[Pn(18,:),ps(18,:)]=mapminmax(P(18,:),-1,1); %Heat Capacity of Oil
P(19,:)=(io_all(1:caseno,19))';[Pn(19,:),ps(19,:)]=mapminmax(P(19,:),-1,1); %Viscosity Coefficient A
P(20,:)=(io_all(1:caseno,20))';[Pn(20,:),ps(20,:)]=mapminmax(P(20,:),-1,1); %Viscosity Coefficient B
%Rock and Fluid Properties
P(21,:)=(io_all(1:caseno,21))';[Pn(21,:),ps(21,:)]=mapminmax(P(21,:),-1,1); %Residual Oil Saturation
P(22,:)=(io_all(1:caseno,22))';[Pn(22,:),ps(22,:)]=mapminmax(P(22,:),-1,1); %Irreducible Water Saturation
P(23,:)=(io_all(1:caseno,23))';[Pn(23,:),ps(23,:)]=mapminmax(P(23,:),-1,1); %Rel. Perm. Exponent
P(24,:)=(io_all(1:caseno,24))';[Pn(24,:),ps(24,:)]=mapminmax(P(24,:),-1,1); %Cap. Pres. Coefficient for Oil
P(25,:)=(io_all(1:caseno,25))';[Pn(25,:),ps(25,:)]=mapminmax(P(25,:),-1,1); %Cap. Pres. Coefficient for Gas
%Initial Conditions
P(26,:)=(io_all(1:caseno,26))';[Pn(26,:),ps(26,:)]=mapminmax(P(26,:),-1,1); %Reservoir Pressure
P(27,:)=(io_all(1:caseno,27))';[Pn(27,:),ps(27,:)]=mapminmax(P(27,:),-1,1); %Reservoir Temperature
P(28,:)=(io_all(1:caseno,28))';[Pn(28,:),ps(28,:)]=mapminmax(P(28,:),-1,1); %Initial Water Saturation
P(29,:)=(io_all(1:caseno,29))';[Pn(29,:),ps(29,:)]=mapminmax(P(29,:),-1,1); %Initial Oil Saturation
%Steam and Production Parameters
P(30,:)=(io_all(1:caseno,30))';[Pn(30,:),ps(30,:)]=mapminmax(P(30,:),-1,1); %Steam Temperature
P(31,:)=(io_all(1:caseno,31))';[Pn(31,:),ps(31,:)]=mapminmax(P(31,:),-1,1); %Steam Quality
P(32,:)=(io_all(1:caseno,32))';[Pn(32,:),ps(32,:)]=mapminmax(P(32,:),-1,1); %Steam Injection Rate
P(33,:)=(io_all(1:caseno,33))';[Pn(33,:),ps(33,:)]=mapminmax(P(33,:),-1,1); %Injection Time
P(34,:)=(io_all(1:caseno,34))';[Pn(34,:),ps(34,:)]=mapminmax(P(34,:),-1,1); %Soaking Time
P(35,:)=(io_all(1:caseno,35))';[Pn(35,:),ps(35,:)]=mapminmax(P(35,:),-1,1); %Economic Rate Limit
%Lorenz Coefficient (thickness-porosity-permeability)
P(36,:)=(io_all(1:caseno,36))';[Pn(36,:),ps(36,:)]=mapminmax(P(36,:),-1,1);

%Normalizing Outputs
T(1,:)=(io_all(1:caseno,47))';[Tn(1,:),ts(1,:)]=mapminmax(T(1,:),-1,1); %Np/Si-Efficiency - 2

%Fixing weights - trying different # of hidden neurons and train-val-test sets
rand('state',0);

%Creating backpropagation algorithm
net=fitnet([nh1 nh2]); % two hidden layers

%Division of data set for training, validation, testing
net.divideFcn = 'divideind';
net.divideParam.trainInd = 1:ntrain;
net.divideParam.valInd = ntrain+1:ntrain+nval;
net.divideParam.testInd = ntrain+nval+1:ntrain+nval+ntest;

%Adjustment of training parameters
net.trainParam.goal=goal;%Accuracy check
net.trainParam.epochs=epochs;%# of iterations check
net.trainParam.max_fail=max_fail;%# of validation check
net.efficiency.memoryReduction=memoryReduction;%Reduction of memory requirements
net.trainParam.showWindow=true;

%Network Training
[net,tr]=train(net,Pn,Tn);

%Data Set Separation
Pn_train=Pn(1:ni,1:ntrain);
Tn_train=Tn(1:no,1:ntrain);
T_train=T(1:no,1:ntrain);

Pn_val=Pn(1:ni,ntrain+1:ntrain+nval);
Tn_val=Tn(1:no,ntrain+1:ntrain+nval);
T_val=T(1:no,ntrain+1:ntrain+nval);
```

```
Pn_test=Pn(1:ni,ntrain+nval+1:ntrain+nval+ntest);
Tn_test=Tn(1:no,ntrain+nval+1:ntrain+nval+ntest);
T_test=T(1:no,ntrain+nval+1:ntrain+nval+ntest);

%Simulation of the network with the training/validation/testing data
Tn_train_ann=sim(net,Pn_train);
Tn_val_ann=sim(net,Pn_val);
Tn_test_ann=sim(net,Pn_test);
Tn_ann=[Tn_train_ann Tn_val_ann Tn_test_ann];

%Denormalization of the outputs
for i=1:no;
   T_train_ann(i,:)=mapminmax('reverse',Tn_train_ann(i,:),ts(i,:));
   T_val_ann(i,:)=mapminmax('reverse',Tn_val_ann(i,:),ts(i,:));
   T_test_ann(i,:)=mapminmax('reverse',Tn_test_ann(i,:),ts(i,:));
end
T_ann=[T_train_ann T_val_ann T_test_ann];

%Error Calculation
Error_train=abs(T_train-T_train_ann);
Error_val=abs(T_val-T_val_ann);
Error_test=abs(T_test-T_test_ann);
```